UNIVERSITY OF CALIFORNIA, SAN DIEGO

BIOPHYSICAL AND BIOCHEMICAL REGULATION OF THE SHAPE, SIZE, AND MATURITY OF CALF ARTICULAR CARTILAGE

A dissertation submitted in partial satisfaction of the

requirements for the degree Doctor of Philosophy

in

Bioengineering

by

Gregory M. Williams

Committee in charge:

Professor Robert L. Sah, Chair
Professor David Amiel
Professor Stephen M. Klisch
Professor Andrew D. McCulloch
Professor L. Amy Sung
Professor Deborah Watson

2010

ProQuest LLC
789 East Eisenhower Parkway
P.O. Box 1346
Ann Arbor, MI 48106-1346

The dissertation of Gregory M. Williams is approved, and it is acceptable in quality and form for publication on microfilm and electronically:

_____

_____

_____

_____

_____

_____

Chair

University of California, San Diego

2010

TABLE OF CONTENTS

LIST OF FIGURES AND TABLES

ACKNOWLEDGMENTS

First and foremost, I would like to express my sincere gratitude to my graduate research mentor and dissertation committee chair, Dr. Robert Sah, for his shepherding of this work and of my professional development as a bioengineer. I have great respect for his abilities as a scientist and writer, and I know that I have benefited from his advice and example.

I would like to thank the other members of my dissertation committee, Prof. David Amiel, Prof. Stephen Klisch, Prof, Andrew McCulloch, Prof. Amy Sung, and Dr. Deborah Watson for their helpful advice, particularly during the early formulation of this dissertation.

During my graduate studies, I have been very fortunate to collaborate with a number of investigators and their research groups. Prof. Stephen Klisch of Cal Poly has facilitated several summers of exciting collaborative research on the biomechanics and growth of cartilage. I have also enjoyed working with Dr. Deborah Watson and her research team on advancing septal cartilage tissue engineering. Dr. William Bugbee has provided valuable insight into the clinical needs of articular cartilage repair, and I thank him for welcoming me into his OR for observation. Prof. Koichi Masuda, a trusted friend of the CTE lab, never fails to have a helpful suggestion or witty remark. I hope I have been helpful to their research activities just as they have been to mine.

During the course of my graduate studies, I had the privilege to mentor some very bright and energetic students. I thank Jessica, Man, Kevin S., Lauren, Michael,

David, Kristin, Christian, Jen, Kevin Y., and Gerald for all their hard work and wish them the best for the future.

It has been a pleasure working with the folks of the CTE lab. Albert Chen has been the wrangler of numerous, fairly intimidating testing machines critical to my studies. Van Wong has helped keep the disorder of a big lab in check, and the obsessive-compulsive part of me is eternally grateful. Barb Schumacher has been very kind and patient with all my questions and training requests. I thank our many lab assistants for doing what we grad-students would rather not be doing. I am also grateful for the instruction and advice given by the old guard of graduate students, including Won Bae, Michele Temple, Tannin Schmidt, Kyle Jadin, Gayle Derfus, Anya Asanbaeva, and Nancy Hsieh-Bonaserra. Travis Klein helped me get started in the lab, and I hope I wasn't too much of a nuisance as he was finishing up his Ph.D. Ken Gratz not only contributed immensely to the micromechanical analysis, but was also a good friend and lunchtime companion. To my cubicle-mates, Megan Blewis, Ben Wong, and Jen Hwang, I really can't thank you guys enough for making every day in the office just a little better. I wish great success to the new(er) kids on the block: Jen Antonacci, Eun Hee Han, Hoa Nguyen, Andrea Pallante, Bill McCarty, Elaine Chan, and Brad Hansen. I thank you all for providing friendship, useful advice, a helping hand, and even an outlet for venting about the tribulations of graduate school.

I am grateful for the support received outside of UCSD as well. I thank my friends for the opportunities to escape from lab work and recharge my batteries with a day at the beach, a night at the movies or around the poker table, or a weekend of camping. My family has also been tremendously supportive during all of my many, many years in school. I just hope they forgive me for venturing so far from home. I

look forward to conversations at holiday dinners that don't involve the question, "so when are you going to be finished?"

Chapter 2, in full, is reproduced from *Tissue Engineering*, volume 13, issue 12, 2007 with permission from Mary Ann Liebert, Inc. The dissertation author was the primary author of this paper and thanks co-authors Jessica W. Lin and Robert L. Sah. This work was supported in part by grants from the National Institutes of Health (NIH) and the National Science Foundation (NSF), and by a grant to the University of California, San Diego, in support of Robert Sah, from the Howard Hughes Medical Institute (HHMI) through the HHMI Professors Program. Individual support was received through a NSF Graduate Research Fellowship (to the dissertation author, GMW), and a UC LEADS Scholarship (to Jessica Lin).

Chapter 3, in full, is reproduced from *Journal of Biomechanics*, volume 42, number 3, 2009 with permission from Elsevier, Inc. The dissertation author was the primary author and thanks co-authors Kenneth R. Gratz and Robert L. Sah. This work was supported in part by grants from NIH, NSF, and HHMI through the HHMI Professors Program (to UCSD in support of RLS). Individual support was received through a NSF Graduate Research Fellowship (to GMW). The author thanks Dr. Albert Chen and Mr. Man Nguyen for technical assistance during this project.

Chapter 4, in part, has been submitted for publication of the material as it may appear in *Matrix Biology*, 2009. The dissertation author was the primary author and thanks co-author Robert L. Sah. This work was supported in part by grants from NIH, NSF, and HHMI through the HHMI Professors Program (to UCSD in support of RLS). Individual support was received through a NIH Ruth L. Kirchstein Pre-Doctoral Fellowship (to GMW).

Chapter 5, in part, has been submitted for publication of the material as it may appear in *Osteoarthritis and Cartilage*, 2009. The dissertation author was the primary author and thanks co-authors Kristin J. Dills, Christian R. Flores, Michael E. Stender, Kevin M. Stewart, Lauren M. Nelson, Albert C. Chen, Koichi Masuda, Scott J. Hazelwood, Robert L. Sah, and Stephen M. Klisch. This work was supported in part by grants from NIH (SJH, RLS, SMK), NSF (RLS, SMK), HHMI through the HHMI Professors Program (to UCSD in support of RLS), and the Donald E. Bently Center for Engineering Innovation (SMK). Individual support was received through a NSF Graduate Research Fellowship and a NIH Ruth L. Kirchstein Pre-Doctoral Fellowship (to GMW).

Appendix A, in full, is reproduced from *Acta Biomaterialia*, volume 1, number 6, 2005 with permission from Elsevier, Inc. The dissertation author was the primary author and thanks co-authors Travis J. Klein and Robert L. Sah. This work was supported in part by grants from NASA, NIH, and NSF. Individual support was received through a NSF Graduate Research Fellowship (to GMW). The author thanks Dr. Albert Chen and Mr. Van Wong for training and assistance and Dr. Won Bae for generously providing the automated viability analysis code.

The dissertation author was the primary author of Appendix B and thanks co-author Robert L. Sah. This work was supported in part by grants from NIH, NSF, and HHMI through the HHMI Professors Program (to UCSD in support of RLS). Individual support was received through a NSF Graduate Research Fellowship (to GMW).

VITA

2003	B.S.E., Biomedical Engineering Duke University, Durham, North Carolina
2003-2010	Graduate Student Researcher Cartilage Tissue Engineering Laboratory University of California, San Diego, La Jolla, California
2005	M.S., Bioengineering University of California, San Diego, La Jolla, California
2010	Ph.D., Bioengineering University of California, San Diego, La Jolla, California

Journal Articles

Williams GM, and Sah RL. In vitro modulation of cartilage shape plasticity by biochemical regulation of matrix remodeling. *Matrix Biology,* Submitted, 2009.

Williams GM, Dills KJ, Flores CR, Stender ME, Stewart KM, Nelson LM, Chen AC, Masuda K, Hazelwood SJ, Sah RL, and Klisch SM. IGF-1 and TGF-β1 differentially regulate in vitro growth and compressive properties of calf articular cartilage. *Osteoarthritis and Cartilage,* Submitted, 2009.

Williams GM, Chan EF, Temple-Wong MM, Bae WC, Masuda K, Bugbee WD, and Sah RL. Shape, loading, and motion in the bioengineering design, fabrication, and testing of personalized synovial joints. *Journal of Biomechanics,* In Press, 10/08/2009.

Williams GM, Gratz KR, and Sah RL. Asymmetrical strain distributions and neutral axis location of cartilage in flexure. *Journal of Biomechanics* 42:325, 2009.

Williams GM, Klisch SM, and Sah RL. Bioengineering cartilage growth, maturation, and form. *Pediatric Research* 63:527-34, 2008.

Williams GM, Lin JW, and Sah RL. Cartilage reshaping via in vitro mechanical loading. *Tissue Engineering* 13:2903-11, 2007.

Williams GM, Klein TJ, and Sah RL. Cell density alters matrix accumulation in two distinct fractions and the mechanical integrity of alginate-chondrocyte constructs. *Acta Biomaterialia* 1:625-33, 2005.

Alexopoulos LG, Williams GM, Upton ML, Setton LA, and Guilak F. Osteoarthritic changes in the biphasic mechanical properties of the chondrocyte pericellular matrix in articular cartilage. *Journal of Biomechanics* 38:509-17, 2005.

Selected Abstracts

Van Donk J, Dills K, Williams GM, Smith SA, Chen AC, Raub CB, Hazelwood SJ, Klisch SM, Sah RL. Regulation of articular cartilage volume and compressive properties by sequential application of IGF-1 and TGF-beta 1 during in vitro growth. *Annual Fall Meeting of the Biomedical Engineering Society*, 2009.

Pho GN, Yamauchi KA, Williams GM, Raub CB, Smith SA, Hazelwood SJ, Klisch SM, Sah RL. Differential regulation of articular cartilage dimensional growth in vitro by dynamic compression and growth factors in combination. *Annual Fall Meeting of the Biomedical Engineering Society*, 2009.

Stender ME, Flores CR, Dills KJ, Williams GM, Stewart KM, Hazelwood S, Chen AC, Sah RL, Klisch SM. Differential regulation of articular cartilage biomechanical and biochemical properties by IGF-1 and TGF-β1 during in vitro growth. *Proceedings of the ASME Summer Bioengineering Conference*, 2009.

Upasani VV, Farnsworth CL, Chambers RC, Bastrom TP, Williams GM, Sah RL, Newton PO. Disc health preservation after six months of spinal growth modulation: expanding the treatment options for fusionless scoliosis correction. *Annual Meeting of the Pediatric Orthopaedic Society of North America*, e-poster 52, 2009.

Chang AA, Sage AB, Schumacher BL, Williams GM, Sah RL, Watson D. Tissue engineered human septal cartilage in a murine model. *Annual Meeting of the American Academy of Otolaryngology – Head and Neck Surgery*, RF116, 2008.

Williams GM, Gratz KR, and Sah RL. Flexural strains in articular cartilage: effect of non-linear tension compression behavior. *Transactions of the Orthopaedic Research Society* 33:0332, 2008.

Williams GM, Gratz KR, and Sah RL. Asymmetrical strain distribution and neutral axis location of cartilage subjected to bending. *International Symposium on Mechanobiology of Cartilage and Chondrocyte*, 2007.

Williams GM, Lin JW, and Sah RL. Cartilage reshaping via in vitro mechanical loading. *Transactions of the Orthopaedic Research Society* 32:0601 2007.

Williams GM, Lin JW, and Sah RL. Bending loads facilitate cartilage reshaping during short term in vitro culture. *Annual Fall Meeting of the Biomedical Engineering Society*: 1426, 2006

Williams GM, Klein TJ, and Sah RL. Interaction of secreted ECM determines the integrity of engineered cartilage. *Transactions of the Orthopaedic Research Society* 30:1778, 2005.

Alexopoulos LG, Williams GM, Upton ML, Setton LA, and Guilak F. The biomechanical role of the chondrocyte pericellular matrix. *Transactions of the Orthopaedic Research Society* 29:0523, 2004.

Alexopoulos LG, Williams GM, Upton ML, Setton LA, and Guilak F. Biphasic properties of normal and osteoarthritic human chondrons. *Proceedings of the ASME Summer Bioengineering Conference* 883, 2003.

Alexopoulos LG, Haider MA, Vail TP, Williams GM, and Guilak F. Alterations in the mechanical properties of the human chondrocyte pericellular matrix with osteoarthritis. *Transactions of the Orthopaedic Research Society* 28:0107, 2003.

ABSTRACT OF THE DISSERTATION

BIOPHYSICAL AND BIOCHEMICAL REGULATION OF
THE SHAPE, SIZE, AND MATURITY OF
CALF ARTICULAR CARTILAGE

by

Gregory M. Williams

Doctor of Philosophy in Bioengineering
University of California, San Diego, 2010
Professor Robert L. Sah, Chair

Cartilage develops specific forms, sizes, and functional properties under the guidance of naturally present biophysical and biochemical stimuli during *in vivo* growth and maturation. Analogously, controlling the physical and biochemical environment of cartilage during culture may facilitate the *in vitro* manipulation of tissue properties. This dissertation explores flexural deformation as a physical stimulus capable of inducing changes in the free-swelling shape of articular cartilage explants and specific biochemical agents in modulating the shape plasticity, size, and maturity of cartilage through altered matrix metabolism and remodeling. The bulk of

the work described herein was conducted with a model system of immature articular cartilage explants from bovine calves, with consideration of the potential translation of the experimental approaches to other native and engineered chondral tissues.

A system for analyzing mechanically-induced reshaping of cartilage was developed through the creation of a novel bioreactor to apply flexure to cartilage explants and a means of sensitively quantifying specimen shape. Using these tools, static flexure was shown to produce significant changes in the free-swelling shape of cartilage in a duration-dependent manner. The flexural stimulus was characterized with micromechanical strain analysis techniques, and the observed assymetrical strain distributions within the tissue were found to be a result of the pronounced tension-compression nonlinearity of cartilage mechanical properties. Inhibitors of chondrocyte and cartilage extracellular matrix metabolism were used to probe potential mechanisms of cartilage reshaping, and findings indicated that the process of reshaping was largely independent of chondrocyte-mediated matrix synthesis or remodeling. However, a strong temperature-dependent response suggested a possible biophysical mechanism of matrix remodeling. Altering matrix metabolism and remodeling by supplementing cultures with specific biochemical agents or growth factors resulted in changes in tissue composition with respect to the predominant collagen and glycosaminoglycan matrix components. These treatments differentially modulated cartilage volume and functional properties, including shape plasticity and mechanical properties in compression.

These studies further elucidate the regulation of the shape, size, and maturity of cartilage by biophysical and biochemical stimuli. The tools and techniques developed here may be translatable to creating chondral grafts with desired properties for joint repair or craniofacial reconstruction.

CHAPTER 1

INTRODUCTION

1.1 Articular Cartilage Composition, Structure, and Function

Articular cartilage is the load bearing connective tissue which covers the bones in synovial joints and provides a low-friction, wear-resistant surface to facilitate articulation (**Fig. 1.1**). The cells which sparsely populate cartilage are termed chondrocytes, and these are embedded within a highly hydrated extracellular matrix (ECM). The major components of the cartilage ECM are collagens and large aggregating proteoglycans. The chondrocytes build and maintain the ECM through their specialized metabolic activities.

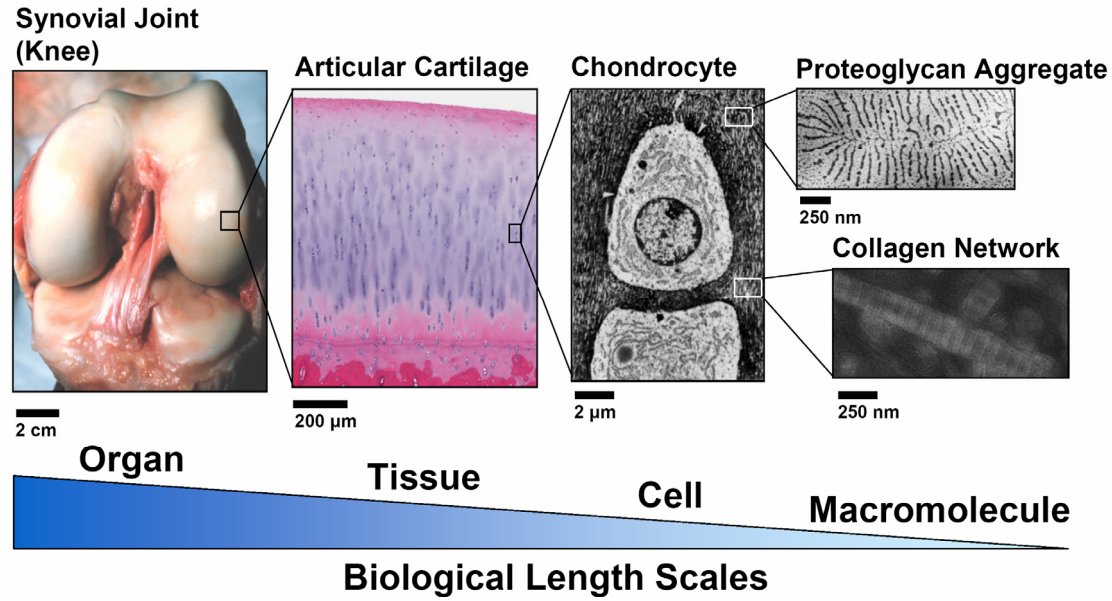

Figure 1.1: Articular cartilage viewed at biological length scales from organ to macromolecular levels. Within synovial joints, articular cartilage covers the ends of bones and provides a low-friction, wear-resistant bearing surface. Articular cartilage consists of chondrocytes embedded within a hydrated extracellular matrix, primarily composed of aggregating proteoglycans and a network of collagens. Joint photo (human) courtesy of Dr. Farshid Guilak. Histological micrograph (caprine, H&E stain) courtesy of Elaine Chan. Electron micrographs adapted from [13, 41, 44].

1.1.a Cartilage ECM Components

The predominant collagen in adult articular cartilage is the fibril forming collagen type II, which can account for >90% of all collagen in the tissue [23]. Other collagens, including types VI, IX, X, and XI, are less abundant in cartilage, but they may still play important roles in the formation or function of the collagen network [23]. Collagen type XI appears to form a template for type II fibril polymerization [10]. Collagen type IX is a fibril-associated collagen with an interrupted triple-helix (FACIT) which binds to the surface of type II fibrils and potentially forms interfibrillar crosslinks [22]. The beaded filament-forming collagen type VI is primarily localized in the chondrocyte pericellular matrix (PCM) and may contribute to the PCM mechanical properties and consequently the local mechanical environment perceived by the chondrocytes [2]. Together these collagens form a network of fibrils which provide stiffness and strength to the tissue in tension and shear [52, 64, 86].

A second major component of the cartilage ECM consists of polyanionic glycosaminoglycans (GAG) covalently attached to aggrecan core protein. These proteoglycans (PG) form large aggregates by non-covalent association with hyaluronan and link protein [34]. The abundant GAG chains impart a highly negative fixed charge density to the tissue and produce an osmotic swelling pressure through their electrostatic interactions [61]. The swelling pressure greatly contributes to the ability of cartilage to resist compression and function as a load-bearing material [62, 64]. A balance arises between the major components of the cartilage ECM as the swelling pressure of the proteoglycans is restrained by the collagen network [59].

The cartilage ECM contains a number of other minor protein and proteoglycan constituents, including cartilage oligomeric matrix protein, fibronectin, biglycan, decorin, fibromodulin, and others [34, 74]. Many of these molecules are postulated to

have roles in the formation or function of the extracellular matrix, including regulating collagen fibril assembly, mediating interactions between matrix molecules, or coupling the chondrocytes to the surrounding matrix.

1.1.b Cartilage Architecture

Mature articular cartilage is described as having a zonal structure varying with depth from the articular surface to the subchondral bone. Zones are typically classified as superficial (S), nearest to and including the articular surface, middle (M), and deep (D). The transition from S to D zones, is characterized by cellular changes including a decrease in density, a shift from flattened to rounded morphology, and an organization of clusters in the middle zone and columns in the deep zone [42, 46]. Matrix composition differs slightly between zones, with aggrecan content increasing with depth [60]. The predominant collagen orientation shifts from tangential to perpendicular to the articular surface with depth [43], and collagen fibril diameters also tend to increase. Mature articular cartilage bears the distinguishing feature of a calcified cartilage interface with the subchondral bone. This feature provides a strong interdigitated bond between uncalcified cartilage and bone through which joint forces are transmitted.

1.1.c Cartilage Mechanical Properties

The load-bearing function of articular cartilage is dependent upon the complex mechanical properties of the tissue which are inhomogeneous, anisotropic, nonlinear, and asymmetric in tension and compression. Mechanical properties vary with depth from the articular surface [51, 70], location within the joint [65], and distance from the chondrocyte [1] and reflect inhomogeneity of matrix composition and structure. Anisotropic tensile moduli and Poisson's ratios in compression vary with the

predominant orientation of collagen fibrils [51, 78]. Cartilage load-bearing also exhibits nonlinear behavior in tension or compression, often appearing as strain-stiffening [17, 57]. Moreover, cartilage is generally stiffer in tension than compression, and the nonlinear transition between these regimes creates a phenomenon referred to as tension-compression nonlinearity [15].

1.2 Articular Cartilage Growth and Maturation

Cartilage growth and maturation occur concurrently during *in vivo* joint development, yet these processes might be independently manipulated *in vitro*. In common usage, terms referring to developmental process have a variety of meanings, but more rigorous definitions may be useful for bioengineering analyses. Clarification is provided through the following definitions. Growth is rather simply defined as the increase in tissue volume resulting from the accumulation of material similar to the original [54, 55]. Growth is also considered distinct from swelling, which is a change in tissue size mediated by a change in the ECM hydration. Remodeling is defined as the modification of tissue properties via biochemical and biophysical changes in composition and structure [54, 55]. Often, remodeling accompanies growth in order to incorporate newly synthesized material into the existing matrix, but remodeling may also occur independently of changes in cartilage size. Maturation is defined as the progressive change of tissue composition and structure to achieve the functional properties of the adult state.

1.2.a Changing Composition, Structure, and Function

The *in vivo* growth and maturation of cartilage can be characterized qualitatively and quantitatively by changes in the tissue's structure, composition, and

functional properties (**Table 1.1**). The bovine stifle joint serves as the model system used throughout the experimental portions of this dissertation and provides a well-studied example of articular cartilage properties at various stages of maturity (third trimester fetal, 1-3 week postnatal calf, and 1-2 year old young adult). Cellularity decreases with maturation from fetus to adult by roughly half or more, with a corresponding increase in the matrix volume fraction [47, 81, 82]. The solid content increases from ~14% in the fetus to ~16% in the calf and ~17% in the adult [82]. The increase in solid content is largely attributable to an increase in collagen concentration, which nearly triples from fetus to adult [81, 82]. The collagen network is also stabilized through the formation of mature, trifunctional pyridinoline crosslinks by reaction of reducible difunctional crosslinks [24]. Pyridinoline concentration increases from the fetal stage by two to four fold in the calf and greater than seven fold in the adult [81]. Throughout maturation, GAG concentration is relatively maintained [81, 82], though the size of individual chondroitin sulfate chains and their abundance relative to keratan sulfate chains typically decrease [76].

Cartilage maturation is also reflected by changes in tissue architecture. Unlike the well-defined zonal architecture of mature cartilage (**§1.1.b**), the thicker immature cartilage contains features of both articular cartilage and epiphyseal growth plate. The bulk of the immature cartilage possesses a fairly isotropic structure with little organization of chondrocytes [42, 46]. However, cell density decreases with depth, particularly near the articular surface [46], while GAG and collagen concentrations and tensile and compressive moduli may increase [7, 53].

The compositional changes from fetus to adult are associated with marked alterations of the cartilage mechanical properties. The compressive aggregate modulus increases by ~180% and the equilibrium tensile modulus increases by ~450% [81, 82].

A large portion of these biochemical and functional changes occurs within the few short weeks between the late fetal and neonatal calf stages of development. These findings support the concept that the functional properties of native or engineered cartilage may be rapidly augmented under specific conditions during brief periods of *in vitro* culture or *in vivo* rehabilitation.

Table 1.1: Summary of the developmental changes in the size, composition, and mechanical properties of bovine articular cartilage from late fetus (third trimester) to calf (1-3 weeks) to young adult (1-2 years). Plus signs (+) indicate relative quantities. GAG = glycosaminoglycan, COL = collagen, and PYR = pyridinoline crosslink concentrations.

	Fetal	Calf	Young Adult
Size	+	++	+++
Cellularity	+++	++	+
GAG	+	+	+
COL	+	++	+++
PYR	+	++	+++
Compressive/ Tensile Stiffness	+	++(+)	+++

1.2.b Mechanisms and Modes of Cartilage Growth

Articular cartilage growth occurs through biological activities of the indwelling chondrocytes that result in increases in the total cellular or matrix volumes. Increased total chondrocyte volume is mediated by proliferation or hypertrophy, whereas increased matrix volume results from the net deposition of accretion of constituent molecules. In studies of immature rats, rabbits, bovines, and possums, a highly proliferative layer of cells near the articular surface has been observed [5, 45, 49, 58]. These findings are consistent with the reported existence of a progenitor cell population at the articular surface [4, 20, 25] and may serve as a means of appositional growth [33]. Chondrocyte hypertrophy and robust production of matrix likely contribute to interstitial growth of cartilage. Chondrocyte hypertrophy accounts for 44-59% of the elongation of rat growth plate, while matrix accretion accounts for another 32-49% [83]. Similar quantification is lacking for epiphyseal cartilage growth mechanisms, but there is evidence that hypertrophy and matrix accretion occur. Hypertrophy is indicated by increasing chondrocyte volume with depth from the articular surface [9]. Chondrocyte density also significantly decreases during development (**§1.2.a**), which, in the absence of appreciable cell death, indicates abundant matrix accretion [47].

1.2.c Regulation of Cartilage Growth, Maturation, and Form

Regulation of chondrocyte cell fates and metabolism by biochemical and mechanical stimuli guide cartilage growth, remodeling, and maturation (**Fig. 1.2**). Transmission of stimuli to the chondrocytes is governed by the physical and chemical properties of the surrounding matrix. Signals perceived within the chondrocyte

microenvironment can alter cell fate and matrix metabolism. In turn, these cellular activities may change the composition, structure, and functional properties of the tissue in ways that promote expansion and maturation of the tissue during development. Contributing to the dynamic regulation of cartilage development, changes in matrix properties may modify the way subsequent stimuli are perceived.

A number of molecular mediators, including growth factors and intracellular transcriptional regulators, have been implicated in the biochemical regulation of joint formation and the growth and maturation of articular cartilage. Members of the insulin-like growth factors (IGF), fibroblast growth factors (FGF), and transforming growth factors beta (TGF-β) families appear to play important roles in these *in vivo* processes as identified through the analysis of genetic mutations leading to abnormal skeletal development in humans and transgenic mice [72]. The culture of chondrocytes or cartilage explants in a controlled *in vitro* environment has yielded additional insight into the biochemical regulation of cartilage growth and maturation. Culturing bovine calf cartilage explants with fetal bovine serum (FBS), IGF-1, or BMP-7 results in an expansive growth phenotype characterized by large increases in size, accumulation of proteoglycan in excess of collagen, and decreases in tensile integrity [6]. Alternatively, culture with TGF-β1 promotes calf cartilage homeostasis with little change in size, composition, or tensile properties [6]. These results support the hypothesis that cartilage expansion can result from a dynamic imbalance of proteoglycan swelling pressure and collagen network restraint [6, 55].

Physical stimuli also serve important functions in the regulation of articular cartilage formation and development. Chondrocytes and cartilage are mechanosensitive, responding to stimuli such as static and dynamic compression, shear, hydrostatic pressure, and fluid shear through altered metabolic activities. Using

a reductionist approach of applying controlled loads, deformations, or fluid flows to cells and explants *in vitro*, the effects of loading on metabolism have been shown to be dependent on the magnitude, rate, and frequency of loading. A general paradigm has emerged from substantial data on aggrecan metabolism, which indicates that static stresses inhibit cartilage matrix synthesis while moderate dynamic stresses promote synthesis [29]. During early joint formation, mechanical stimuli are necessary for proper joint cavitation and morphogenesis. Paralysis of chick embryos can inhibit joint cavitation or result in fusion of cartilage anlagen already separated [21, 63]. During postnatal development, mechanical stimuli contribute to the functional adaptation of joints. In immature canines, different regimes of joint loading, via exercise or limb immobilization, lead to significant differences in articular cartilage structure (e.g. thickness and congruity), composition (e.g. proteoglycan concentration), and functional properties (e.g. indentation stiffness) [36]. Likewise, exercise can produce cartilage thickening and longer, flatter subchondral surfaces in the femoral heads of immature mice [67].

Clinicians frequently use mechanical stimuli to alter the form of developing joints in cases of malformation or deformity. Examples include the use of harnessing to correct hip dysplasia [26] and manipulation and casting to correct club foot [11]. Analogously, mechanical molding is also used as a treatment to alter the shape of non-articular cartilaginous structures, as demonstrated by the use of nasoalveolar molding in the correction of cleft palate [28] and ear splinting for auricular deformities [77]. The mechanisms by which these techniques alter cartilage form are not fully understood. However, they may depend on some maturation-related property of cartilage, since anecdotal evidence for all of these techniques suggests that outcomes are better when performed earlier during postnatal development.

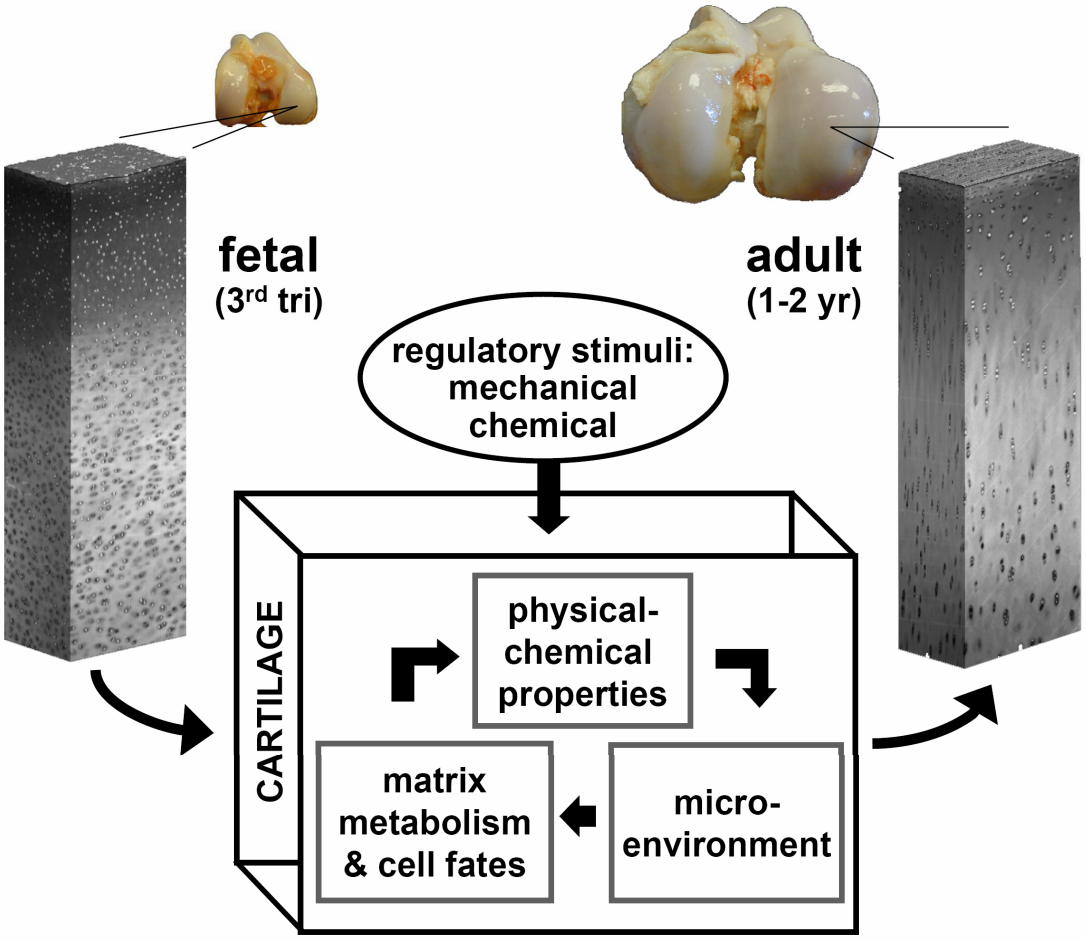

Figure 1.2: Dynamic processes govern the growth and maturation of articular cartilage. Regulatory stimuli are transformed according to the physical and chemical properties of the tissue into signals in the chondrocyte microenvironment to alter matrix metabolism and cell fates. These cellular processes, in turn, contribute to the enlargement of the joint and the evolving tissue composition, structure and functional properties. Some of these changes, particularly the decrease in cell density and attainment of a mature, stratified architecture, are seen in cartilage digital volumetric images (adapted from [47]). Joint photos are courtesy of Dr. Amanda K. Williamson. Adapted from [80].

1.3 Clinical Significance of Cartilage Grafts

1.3.a Treatment of Articular Lesions

The functions of articular cartilage which facilitate efficient and pain-free articulation can be compromised by trauma or diseases such as osteoarthritis and osteochondritis dissecans [19, 37]. With intrinsic regeneration of normal articular cartilage limited and present medical therapies largely palliative in nature, surgical intervention is often used to treat pain and dysfunction. At present, the surgical treatment paradigm for damaged articular surfaces depends on factors such as lesion size and severity (**Fig. 1.3**). For small focal cartilage defects (<2 cm^2), the microfracture technique is commonly used to elicit the formation of fibrocartilage repair tissue by mesenchymal stem cells from subchondral bone [73]. Treatment of slightly larger 2-3 cm^2 defects is often performed by osteochondral autograft transplantation (i.e. mosaicplasty) or autologous chondrocyte implantation (ACI) [12, 31]. Even larger lesions (~4 cm^2) or multiple lesions may be treated by osteochondral allograft transplantation [14]. Finally, joint resurfacing or replacement is typically prescribed for severe degeneration (e.g. end-stage osteoarthritis).

As defect size increases, restoration of the natural joint curvatures and sufficient filling of the defect with mechanically mature tissue become increasingly important parameters for functional recovery. Congruity and filling are achieved in mosaicplasty by careful graft harvest and placement and by the use of variable size grafts [32] and in allograft transplantation by orthotopic matching of the donor tissue to recipient site [18]. Several studies indicate that malpositioned osteochondral grafts can produce altered stresses and strains [56, 85], graft micromotion and instability

[66], and abnormal biological responses including hyperplasia, fibrous growth, and necrosis [39, 66].

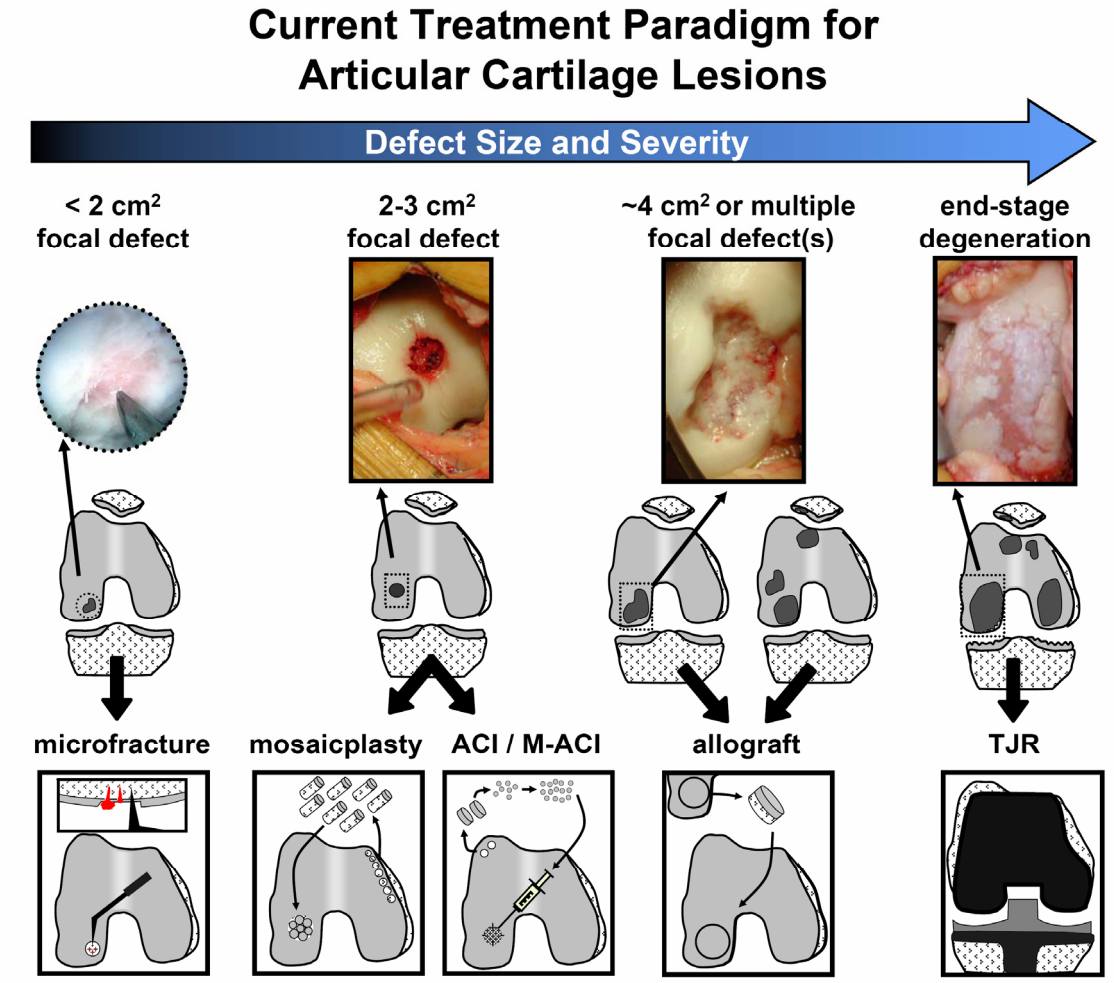

Figure 1.3: The treatment paradigm for articular cartilage lesions of the human knee is often dependent upon the size and severity of the lesion(s). Smaller lesions may be treated by microfracture, osteochondral autografts (mosaicplasty), or (matrix-assisted) autologous chondrocyte implantation (ACI / M-ACI). Larger lesions may be treated with osteochondral allograft transplantation. End-stage degeneration is frequently treated with total joint replacement. Photos are courtesy of Dr. William D. Bugbee. Adapted from [79].

1.3.b Craniofacial Applications for Cartilage Grafts

Cartilage grafts are also frequently used in the surgical reconstruction of the nose, ears, and other craniofacial features following trauma, malformation, tumor resection, etc. Autologous cartilage grafts are generally considered the gold standard material for these procedures [75]. Depending on the therapeutic application, grafts of septal, auricular, and costal cartilage may be sculpted into desired forms using techniques such as carving, scoring and suturing.

1.4 Emerging Technologies in Cartilage Tissue Engineering

As noted in the previous section, cartilage grafts of specified shape, volume, and maturity have important applications in the restoration of damaged joints and the reconstruction of craniofacial structures. However, limitations of current therapies continue to spur improvements in existing procedures as well as the development of new therapies. Emerging technologies in cartilage tissue engineering can potentially provide biologically and mechanically functional tissue for cartilage grafting applications. With respect to joint repair, tissue engineering solutions are progressing from transplantation of cells to transplantation of chondral and osteochondral tissues that have been grown and partially matured *in vitro* (**Fig. 1.4**). The progression of treatments follows a biomimetic strategy of cell proliferation, chondrogenesis, tissue growth, and maturation and may eventually allow for the creation of constructs to repair larger and more severe articular cartilage lesions.

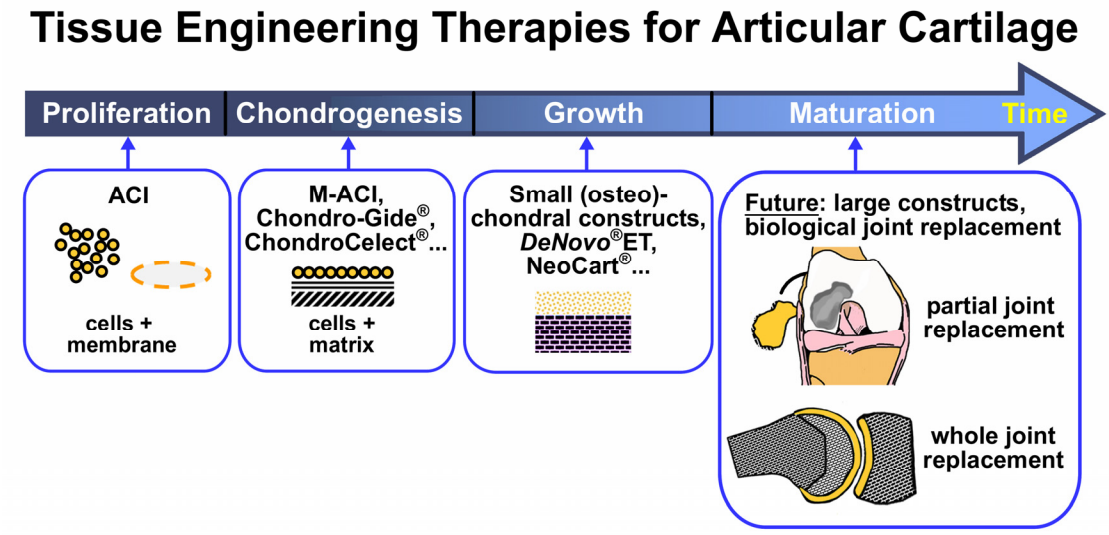

Figure 1.4: Progression of biomimetic tissue engineering therapies for articular cartilage repair. Current therapies of autologous chondrocyte implantation (ACI), matrix-assisted ACI (M-ACI), and small chondral and osteochondral constructs are advancing incrementally towards larger, more phenotypically stable and mature tissues at the time of implantation. Future engineered partial or whole-joint constructs may require or benefit from further *in vitro* shaping, growth, and maturation of tissues. Chondro-Gide®, ChondroCelect®, *DeNovo*®ET, and NeoCart® are products of Geistlich Pharma AG (Wolhusen, Switzerland), TiGenix (Leuven, Belgium), ISTO Technologies, Inc. (St. Louis, Missouri), and Histogenics Corporation (Waltham, Massachusetts), respectively. Adapted from [79].

1.4.b Engineering Shaped Chondral Grafts

Several techniques exist for forming cartilaginous constructs in predetermined shapes. Many scaffold materials used in tissue engineering can be cast, milled, printed, or otherwise formed into anatomical shapes, and thereby serve as templates for cartilage growth [48, 69, 71]. Hydrogel-based constructs can be shaped by injection molding or *in situ* polymerization [3, 16, 40]. Seeding primary or alginate-recovered chondrocytes at high density into molds are scaffold-free approaches to creating anatomical forms [8, 30]. However, the shape fidelity of a construct formed by one of these techniques may diminish with subsequent tissue growth or scaffold degradation.

Thermoforming and electroforming are techniques for permanently altering the shape of cartilage that have been developed for craniofacial applications. Cartilage is mechanically deformed and either heated by laser energy [27, 35] or radiofrequency energy [50] or else subjected to electrical current [38]. Samples retain a large amount of the imposed deformation, but the techniques have certain drawbacks at present. Thermoforming has been shown to reduce chondrocyte viability [50, 68] and may denature collagen in the ECM [84]; whereas electroforming produces tissue discoloration and gas formation that are evidence of electrochemical reactions within the tissue.[38].

1.5 Dissertation Objectives and Overview

The overall motivation of this dissertation was to contribute to understanding how the shape, size, and maturity of cartilage can be prescribed through the *in vitro* application of selected biophysical and biochemical stimuli. Experiments were

conducted primarily using a model system of immature bovine articular cartilage. Advantages of this system include consisting of phenotypically stable chondrocytes within a native matrix, having well characterized composition, structure, and mechanical properties, and being translatable to various tissue engineering and cartilage grafting strategies. The objectives of the dissertation were 1) to establish whether flexural deformations can aid in the contouring of cartilage by inducing changes in tissue shape through matrix remodeling, 2) to characterize more thoroughly the biomechanical behavior of cartilage in flexure, and 3) to determine how biochemical regulation of matrix metabolism and remodeling modulates cartilage shape plasticity, volume, and maturity.

Chapter 2, which was published in *Tissue Engineering*, describes the development of a bioreactor capable of applying flexural deformations to cartilage explants during culture and of a means of quantifying changes in explant shape. Changes in the free-swelling shape of calf cartilage explants were measured at discrete times within the first week of culture and compared across time points and to non-loaded control explant cultures. Potential mechanisms by which flexure results in cartilage matrix remodeling and shape alteration were also investigated through the use of inhibitors of chondrocyte and cartilage matrix metabolism.

Chapter 3, which was published in *Journal of Biomechanics*, provides a detailed look at flexural strains in calf cartilage explants using a novel micromechanical test. The testing configuration mimicked and helped characterize the flexural stimulus used previously in Chapter 2 and subsequently in Chapter 4 for inducing cartilage shape changes. This study examined the role of nonlinear tension-compression behavior of cartilage in producing asymmetrical strain distributions within the tissue. Findings were supported through empirical comparison to alginate

and through theoretical modeling of bimodular materials in pure bending, where material properties served as input parameters.

Chapter 4, which has been submitted to *Matrix Biology* for publication, further explores the shape plasticity of articular cartilage using an assessment built upon the techniques of cartilage reshaping developed in Chapter 2. The shape plasticity of calf and adult bovine cartilage was characterized and found to be consistent with the clinical wisdom of diminishing plasticity with maturation. Moreover, biochemical agents, β-D-xyloside and β-aminopropionitrile, were supplemented to cartilage explant cultures to test whether perturbing proteoglycan and collagen remodeling can modulate the shape plasticity of articular cartilage through changes in matrix composition.

Chapter 5, which has been submitted to *Osteoarthritis and Cartilage* for publication, examines the biochemical regulation of *in vitro* growth and maturation of calf articular cartilage by exogenous IGF-1 and TGF-β1. These two growth factors were examined for their ability to differentially regulate the volumetric growth, matrix composition, and biomechanical properties in compression of cartilage. Regression analysis was also used to further explore composition-function relationships.

Chapter 6 summarizes the major findings of these studies and discusses potential directions for future studies.

Appendix A, which was published in *Acta Biomaterialia*, investigates factors which contribute to the formation of a cohesive extracellular matrix in engineered cartilaginous tissues. Rather than using a model system of explants of immature bovine articular cartilage as in the previous chapters, this study examined isolated chondrocytes from this tissue embedded in alginate hydrogel. The effects of initial cell density on the *de novo* synthesis and distribution of proteoglycan and collagen and on

the construct equilibrium tensile modulus were examined. In addition, regression analysis was used to evaluate composition-structure-function relationships with a particular focus on how distribution of matrix within the construct affects the strength of these relationships.

Appendix B supplements the findings of Chapter 2 by extending the study of potential mechanisms of cartilage reshaping. An inhibitor of matrix metalloproteinases and a more broadly acting protease inhibitor cocktail are used to investigate the potential role of matrix catabolism during mechanically-induced cartilage reshaping.

1.6 References

1. Alexopoulos LG, Setton LA, Guilak F: The biomechanical role of the chondrocyte pericellular matrix in articular cartilage. *Acta Biomater* 1:317-25, 2005.

2. Alexopoulos LG, Youn I, Bonaldo P, Guilak F: Developmental and osteoarthritic changes in Col6a1-knockout mice: biomechanics of type VI collagen in the cartilage pericellular matrix. *Arthritis Rheum* 60:771-9, 2009.

3. Alhadlaq A, Elisseeff JH, Hong L, Williams CG, Caplan AI, Sharma B, Kopher RA, Tomkoria S, Lennon DP, Lopez A, Mao JJ: Adult stem cell driven genesis of human-shaped articular condyle. *Ann Biomed Eng* 32:911-23, 2004.

4. Alsalameh S, Amin R, Gemba T, Lotz M: Identification of mesenchymal progenitor cells in normal and osteoarthritic human articular cartilage. *Arthritis Rheum* 50:1522-32, 2004.

5. Apte SS: Validation of bromodeoxyuridine immunohistochemistry for localization of S-phase cells in decalcified tissues. A comparative study with tritiated thymidine autoradiography. *Histochem J* 22:401-8, 1990.

6. Asanbaeva A, Masuda K, Thonar EJ-MA, Klisch SM, Sah RL: Regulation of immature cartilage growth by IGF-I, TGF-beta1, BMP-7, and PDGF-AB: role of metabolic balance between fixed charge and collagen network. *Biomech Model Mechanobiol* 7:263-76, 2008.

7. Asanbaeva A, Masuda K, Thonar EJ, Klisch SM, Sah RL: Mechanisms of cartilage growth: modulation of balance between proteoglycan and collagen in vitro using chondroitinase ABC. *Arthritis Rheum* 56:188-98, 2007.

8. Aufderheide AC, Athanasiou KA: Assessment of a bovine co-culture, scaffold-free method for growing meniscus-shaped constructs. *Tissue Eng* 13:2195-205, 2007.

9. Aydelotte MB, Kuettner KE: Differences between sub-populations of cultured bovine articular chondrocytes. I. morphology and cartilage matrix production. *Connect Tissue Res* 18:205-22, 1988.

10. Blaschke UK, Eikenberry EF, Hulmes DJ, Galla HJ, Bruckner P: Collagen XI nucleates self-assembly and limits lateral growth of cartilage fibrils. *J Biol Chem* 275:10370-8, 2000.

11. Brand RA, Siegler S, Pirani S, Morrison WB, Udupa JK: Cartilage anlagen adapt in response to static deformation. *Med Hypotheses* 66:653-9, 2006.

12. Brittberg M: Autologous chondrocyte transplantation. *Clin Orthop Rel Res* 367S:147-55, 1999.

13. Buckwalter JA, Roughley PJ, Rosenberg LC: Age-related changes in cartilage proteoglycans: quantitative electron microscopic studies. *Micros Res Tech* 28:398-408, 1994.

14. Bugbee WD: Osteochondral allograft transplantation. In: *Articular Cartilage Lesions: A Practical Guide to Assessment and Treatment,* ed. by BJ Cole, Malek MM, Springer, New York, 2004, 82-94.

15. Chahine NO, Wang CC, Hung CT, Ateshian GA: Anisotropic strain-dependent material properties of bovine articular cartilage in the transitional range from tension to compression. *J Biomech* 37:1251-61, 2004.

16. Chang SC, Rowley JA, Tobias G, Genes NG, Roy AK, Mooney DJ, Vacanti CA, Bonassar LJ: Injection molding of chondrocyte/alginate constructs in the shape of facial implants. *J Biomed Mater Res* 55:503-11, 2001.

17. Charlebois M, McKee MD, Buschmann MD: Nonlinear tensile properties of bovine articular cartilage and their variation with age and depth. *J Biomech Eng* 126:129-37, 2004.

18. Convery FR, Meyers MH, Akeson WH: Fresh osteochondral allografting of the femoral condyle. *Clin Orthop Rel Res* 273:139-45, 1991.

19. Curl WW, Krome J, Gordon ES, Rushing J, Smith BP, Poehling GG: Cartilage injuries: a review of 31,516 knee arthroscopies. *Arthroscopy* 13:456-60, 1997.

20. Dowthwaite GP, Bishop JC, Redman SN, Khan IM, Rooney P, Evans DJ, Haughton L, Bayram Z, Boyer S, Thompson B, Wolfe MS, Archer CW: The surface of articular cartilage contains a progenitor cell population. *J Cell Sci* 117:889-997, 2004.

21. Drachman D, Sokoloff L: The role of movement in embryonic joint development. *Dev Biol* 14:401-20, 1966.

22. Eyre DR: Collagens and cartilage matrix homeostasis. *Clin Orthop Rel Res Relat Res*:S118-22, 2004.

23. Eyre DR, Dickson IR, van Ness K: The collagens of articular cartilage. *Sem Arthritis Rheum* 21,S2:2-11, 1991.

24. Eyre DR, Grypnas MD, Shapiro FD, Creasman CM: Mature crosslink formation and molecular packing in articular cartilage collagen. *Sem Arthritis Rheum* 11:46-7, 1981.

25. Fickert SF, J. Brenner, RE.: Identification of subpopulations with characterisitics of mesenchymal progenitor cells from human osteoarthritic cartilage using triple staining for cell surface markers. *Arthritis Research and Therapy* 6:R422-R32, 2004.

26. Gabuzda GM, Renshaw TS: Reduction of congenital dislocation of the hip. *J Bone Joint Surg Am* 74:624-31, 1992.

27. Gray DS, Kimball JA, Wong BJ: Shape retention in porcine-septal cartilage following Nd:YAG (lambda = 1.32 microm) laser-mediated reshaping. *Lasers Surg Med* 29:160-4, 2001.

28. Grayson BH, Maull D: Nasoalveolar molding for infants born with clefts of the lip, alveolus, and palate. *Clin Plast Surg* 31:149-58, vii, 2004.

29. Guilak F, Sah RL, Setton LA: Physical regulation of cartilage metabolism. In: *Basic Orthopaedic Biomechanics,* ed. by VC Mow, Hayes WC, Raven Press, New York, 1997, 179-207.

30. Han E, Bae WC, Hsieh-Bonassera ND, Wong VW, Schumacher BL, Gortz S, Masuda K, Bugbee WD, Sah RL: Shaped, stratified, scaffold-free grafts for articular cartilage defects. *Clin Orthop Relat Res* 466:1912-20, 2008.

31. Hangody L, Feczko P, Bartha L, Bodo G, Kish G: Mosaicplasty for the treatment of articular defects of the knee and ankle. *Clin Orthop Rel Res*:328-36, 2001.

32. Hangody L, Rathonyi GK, Duska Z, Vasarhelyi G, Fules P, Modis L: Autologous osteochondral mosaicplasty. *J Bone Joint Surg* 86-A, Supplement 1:65-72, 2004.

33. Hayes AJ, MacPherson S, Morrison H, Dowthwaite G, Archer CW: The development of articular cartilage: evidence for an appositional growth mechanism. *Anat Embryol (Berl)* 203:469-79, 2001.

34. Heinegard D, Oldberg A: Structure and biology of cartilage and bone matrix noncollageneous macromolecules. *FASEB J* 3:2042-51, 1989.

35. Helidonis E, Sobol E, Kavvalos G, Bizakis J, Christodoulou P, Velegrakis G, Segas J, Bagratashvili V: Laser shaping of composite cartilage grafts. *Am J Otolaryngol* 14:410-2, 1993.

36. Helminen HJ, Hyttinen MM, Lammi MJ, Arokoski JP, Lapvetelainen T, Jurvelin J, Kiviranta I, Tammi MI: Regular joint loading in youth assists in the establishment and strengthening of the collagen network of articular cartilage and contributes to the prevention of osteoarthrosis later in life: a hypothesis. *J Bone Miner Metab* 18:245-57, 2000.

37. Hjelle K, Solheim E, Strand T, Muri R, Brittberg M: Articular cartilage defects in 1,000 knee arthroscopies. *Arthroscopy* 18:730-4, 2002.

38. Ho KH, Diaz Valdes SH, Protsenko DE, Aguilar G, Wong BJ: Electromechanical reshaping of septal cartilage. *Laryngoscope* 113:1916-21, 2003.

39. Huang FS, Simonian PT, Norman AG, Clark JM: Effects of small incongruities in a sheep model of osteochondral autografting. *Am J Sports Med* 32:1842-8, 2004.

40. Hung CT, Lima EG, Mauck RL, Taki E, LeRoux MA, Lu HH, Stark RG, Guo XE, Ateshian GA: Anatomically shaped osteochondral constructs for articular cartilage repair. *J Biomech* 36:1853-64, 2003.

41. Hunziker EB: Articular cartilage structure in humans and experimental animals. In: *Articular Cartilage and Osteoarthritis,* ed. by KE Kuettner, Schleyerbach R, Peyron JG, Hascall VC, Raven Press, New York, 1992, 183-99.

42. Hunziker EB, Kapfinger E, Geiss J: The structural architecture of adult mammalian articular cartilage evolves by a synchronized process of tissue resorption and neoformation during postnatal development. *Osteoarthritis Cartilage* 15:403-13, 2007.

43. Hunziker EB, Michel M, Studer D: Ultrastructure of adult human articular cartilage matrix after cryotechnical processing. *Microsc Res Tech* 37:271-84, 1997.

44. Hunziker EB, Wagner J, Studer D: Vitrified articular cartilage reveals novel ultra-structural features respecting extracellular matrix architecture. *Histochem Cell Biol* 106:375-82, 1996.

45. Jadin KD. Mechanisms of growth of articular cartilage: cell organization and fates. PhD Thesis. La Jolla: University of California, San Diego; 2006.

46. Jadin KD, Bae WC, Schumacher BL, Sah RL: Three-dimensional (3-D) imaging of chondrocytes in articular cartilage: growth-associated changes in cell organization. *Biomaterials* 28:230-9, 2007.

47. Jadin KD, Wong BL, Bae WC, Li KW, Williamson AK, Schumacher BL, Price JH, Sah RL: Depth-varying density and organization of chondrocyte in immature and mature bovine articular cartilage assessed by 3-D imaging and analysis. *J Histochem Cytochem* 53:1109-19, 2005.

48. Kamil SH, Kojima K, Vacanti MP, Bonassar LJ, Vacanti CA, Eavey RD: In vitro tissue engineering to generate a human-sized auricle and nasal tip. *Laryngoscope* 113:90-4, 2003.

49. Kavanagh E: Division and death of cells in developing synovial joints and long bones. *Cell Biology International* 26:679-88, 2002.

50. Keefe MW, Rasouli A, Telenkov SA, Karamzadeh AM, Milner TE, Crumley RL, Wong BJ: Radiofrequency cartilage reshaping: efficacy, biophysical measurements, and tissue viability. *Arch Facial Plast Surg* 5:46-52, 2003.

51. Kempson GE, Freeman MAR, Swanson SAV: Tensile properties of articular cartilage. *Nature* 220:1127-8, 1968.

52. Kempson GE, Muir H, Pollard C, Tuke M: The tensile properties of the cartilage of human femoral condyles related to the content of collagen and glycosaminoglycans. *Biochim Biophys Acta* 297:456-72, 1973.

53. Klein TJ, Chaudhry M, Bae WC, Sah RL: Depth-dependent biomechanical and biochemical properties of fetal, newborn, and tissue-engineered articular cartilage. *J Biomech* 40:182-90, 2007.

54. Klisch SM, Asanbaeva A, Oungoulian SR, Masuda K, Thonar EJ-MA, Davol A, Sah RL: A cartilage growth mixture model with collagen remodeling: validation protocols. *J Biomech Eng* 130:031006, 2008.

55. Klisch SM, Chen SS, Sah RL, Hoger A: A growth mixture theory for cartilage with applications to growth-related experiments on cartilage explants. *J Biomech Eng* 125:169-79, 2003.

56. Koh JL, Wirsing K, Lautenschlager E, Zhang LO: The effect of graft height mismatch on contact pressure following osteochondral grafting. A biomechanical study. *Am J Sports Med* 32:317-20, 2004.

57. Kwan MK, Lai WM, Mow VC: A finite deformation theory for cartilage and other soft hydrated connective tissues--I. equilibrium results. *J Biomech* 23:145-55, 1990.

58. Mankin HJ: Localization of tritiated thymidine in articular cartilage of rabbits. I. growth in immature cartilage. *J Bone Joint Surg Am* 44-A:682-98, 1962.

59. Maroudas A: Balance between swelling pressure and collagen tension in normal and degenerate cartilage. *Nature* 260:808-9, 1976.

60. Maroudas A: Physico-chemical properties of articular cartilage. In: *Adult Articular Cartilage,* ed. by MAR Freeman, Pitman Medical, Tunbridge Wells, England, 1979, 215-90.

61. Maroudas A, Bannon C: Measurement of swelling pressure in cartilage and comparison with the osmotic pressure of constituent proteoglycans. *Biorheology* 18:619-32, 1981.

62. Maroudas A, Katz EP, Wachtel EJ, Mizrahi J, Soudry M: Physico-chemical properties and functional behavior of normal and osteoarthritic human cartilage. In: *Articular Cartilage Biochemistry,* ed. by K Kuettner, Schleyerbach R, Hascall VC, Raven Press, New York, 1986.

63. Mitrovic D: Development of the articular cavity in paralyzed chick embryos and in chick embryo limb buds cultured on chorioallantoic membranes. *Acta Anat (Basel)* 113:313-24, 1982.

64. Mow VC, Gu WY, Chen FH: Structure and Function of Articular Cartilage and Meniscus. In: *Basic Orthopaedic Biomechanics and Mechano-Biology,* ed. by VC Mow, Huiskes R, Lippincott Williams & Wilkins, Philadelphia, 2005, 720.

65. Nugent GE, Law AW, Wong EG, Temple MM, Bae WC, Chen AC, Kawcak CE, Sah RL: Site- and exercise-related variation in structure and function of cartilage from equine distal metacarpal condyle. *Osteoarthritis Cartilage* 12:826-33, 2004.

66. Pearce SG, Hurtig MB, Clarnette R, Kalra M, Cowan B, Miniaci A: An investigation of 2 techniques for optimizing joint surface congruency using multiple cylindrical osteochondral autografts. *Arthroscopy* 17:50-5, 2001.

67. Plochocki JH, Riscigno CJ, Garcia M: Functional adaptation of the femoral head to voluntary exercise. *Anat Rec A Discov Mol Cell Evol Biol* 288:776-81, 2006.

68. Rasouli A, Sun CH, Basu R, Wong BJ: Quantitative assessment of chondrocyte viability after laser mediated reshaping: a novel application of flow cytometry. *Lasers Surg Med* 32:3-9, 2003.

69. Schek RM, Taboas JM, Hollister SJ, Krebsbach PH: Tissue engineering osteochondral implants for temporomandibular joint repair. *Orthod Craniofac Res* 8:313-9, 2005.

70. Schinagl RM, Gurskis D, Chen AC, Sah RL: Depth-dependent confined compression modulus of full-thickness bovine articular cartilage. *J Orthop Res* 15:499-506, 1997.

71. Sedrakyan S, Zhou ZY, Perin L, Leach K, Mooney D, Kim TH: Tissue engineering of a small hand phalanx with a porously casted polylactic acid-polyglycolic acid copolymer. *Tissue Eng* 12:2675-83, 2006.

72. Shum L, Coleman CM, Hatakeyama Y, Tuan RS: Morphogenesis and dysmorphogenesis of the appendicular skeleton. *Birth Defects Res C Embryo Today* 69:102-22, 2003.

73. Steadman JR, Rodkey WG, Briggs KK: Microfracture to treat full-thickness chondral defects: surgical technique, rehabilitation, and outcomes. *J Knee Surg* 15:170-6, 2002.

74. Svensson L, Oldberg A, Heinegard D: Collagen binding proteins. *Osteoarthritis Cartilage* 9 Suppl A:S23-8, 2001.

75. Tardy ME, Denneny J, 3rd, Fritsch MH: The versatile cartilage autograft in reconstruction of the nose and face. *Laryngoscope* 95:523-33, 1985.

76. Thonar EJ, Buckwalter JA, Kuettner KE: Maturation-related differences in the structure and composition of proteoglycans synthesized by chondrocytes from bovine articular cartilage. *J Biol Chem* 261:2467-74, 1986.

77. van Wijk MP, Breugem CC, Kon M: Non-surgical correction of congenital deformities of the auricle: a systematic review of the literature. *J Plast Reconstr Aesthet Surg* 62:727-36, 2009.

78. Wang CC, Chahine NO, Hung CT, Ateshian GA: Optical determination of anisotropic material properties of bovine articular cartilage in compression. *J Biomech* 36:339-53, 2003.

79. Williams GM, Chan EF, Temple-Wong MM, Bae WC, Masuda K, Bugbee WD, Sah RL: Shape, loading, and motion in the bioengineering design, fabrication, and testing of personalized synovial joints. *J Biomech* ePub, 10/6/2009, 2009.

80. Williams GM, Klisch SM, Sah RL: Bioengineering cartilage growth, maturation, and form. *Pediatr Res* 63:527-34, 2008.

81. Williamson AK, Chen AC, Masuda K, Thonar EJ-MA, Sah RL: Tensile mechanical properties of bovine articular cartilage: variations with growth and relationships to collagen network components. *J Orthop Res* 21:872-80, 2003.

82. Williamson AK, Chen AC, Sah RL: Compressive properties and function-composition relationships of developing bovine articular cartilage. *J Orthop Res* 19:1113-21, 2001.

83. Wilsman NJ, Farnum CE, Leiferman EM, Fry M, Barreto C: Differential growth by growth plates as a function of multiple parameters of chondrocytic kinetics. *J Orthop Res* 14:927-36, 1996.

84. Wong BJ, Milner TE, Kim HH, Nelson JS, Sobol EN: Stress relaxation of porcine septal cartilage during Nd:YAG (λ=1.32 μm) laser irradiation: mechanical, optical, and thermal responses. *J Biomed Optics* 3:409-14, 1998.

85. Wu JZ, Herzog W, Hasler EM: Inadequate placement of osteochondral plugs may induce abnormal stress-strain distributions in articular cartilage --finite element simulations. *Med Eng Phys* 24:85-97, 2002.

86. Zhu W, Mow VC, Koob TJ, Eyre DR: Viscoelastic shear properties of articular cartilage and the effects of glycosidase treatment. *J Orthop Res* 11:771-81, 1993.

CHAPTER 2

CARTILAGE RESHAPING
VIA IN VITRO MECHANICAL LOADING

2.1 Abstract

Shaped cartilage grafts can be used in the restoration of injured joints and reconstruction of deformities of the head and neck. This study describes a novel method for altering cartilage shape, based on the hypothesis that mechanical loading coupled with *in vitro* tissue growth and remodeling facilitates tissue reshaping. Static bending deformations were imposed on strips of immature articular cartilage, and retention of the imposed shape and structural and biochemical measures of growth were assessed following 2, 4, and 6 days of incubation. The results show that mechanical reshaping of tissue is feasible, as shape retention was greater than 86% after 6 days of culture. The imposed mechanical deformations had little effect on measures of tissue viability or growth within the 6 day culture period. The addition of cycloheximide to the culture media only slightly reduced the ability to reshape these tissues, but cycloheximide plus a lower culture temperature of 4°C markedly inhibited the reshaping response. These results suggest a limited role for chondrocyte biosynthesis but a potentially important role for metabolic reactions in the cartilage

matrix in the reshaping process. The ability to modulate cartilage shape *in vitro* may prove useful for tissue engineering of shaped cartilage grafts.

2.2 Introduction

Cartilage grafts of pre-determined shapes and sizes have important therapeutic applications in the restoration of damaged joints and the reconstruction of head and neck deformities. Focal defects in articular cartilage are common injuries of the knee which can cause pain and disability [9, 20]. Because these injuries have a minimal capacity to heal, surgical interventions such as microfracturing, autologous chondrocyte implantation (ACI), and osteochondral auto- and allografting are often required [7]. As defect size increases, restoration of the natural joint curvatures may become an increasingly important parameter for functional recovery. Careful orthotopic matching of osteochondral allograft tissue currently meets this requirement [8], but clinical reports of successful reattachments of loose chondral fragments [24, 32] provide evidence that anatomically-shaped chondral grafts may be a feasible therapeutic alternative.

Shaped cartilage grafts are also frequently used in reconstructive procedures of the nose, ears, and other features of the head and neck. Autologous septal, auricular, and costal cartilage grafts are often sculpted into desired forms using techniques such as carving, scoring and suturing [42]. Because these methods can adversely affect the viability of the graft tissue and generate excessive tissue waste, there has been interest in developing an effective means to reshape natural or engineered cartilage into useful forms for grafting.

Methods of cartilage reshaping currently in development include thermoforming and electroforming. These techniques consist of mechanically deforming cartilage, and subsequently applying either laser [14, 18] or radiofrequency heating [25] (in thermoforming) or electrical current [21] (in electroforming). After these treatments, cartilage samples retain a large amount of the imposed deformation

[14, 21, 25]. The heat generated within the tissue during thermoforming has been shown to reduce chondrocyte viability [25, 36] and may also denature matrix proteins such as collagen [45]. In electroforming experiments, observations of tissue discoloration and gas formation provide evidence for electrochemical reactions within the tissue [21]. It is largely unknown how alterations in cartilage graft viability and structure resulting from these reshaping methods would affect their therapeutic success.

Tissue engineering approaches for creating shaped chondral tissues have also been explored, and encouraging results have been achieved. In general, these studies usually follow one of two strategies: 1) seeding cells with a scaffold, typically a polymerizable hydrogel, into a negative mold [1, 6, 22], or 2) seeding cells into a shaped scaffold created by milling, casting, solid freeform fabrication or other techniques [23, 38, 39]. One challenge to such approaches is that the initial, engineered shape of a construct may change during *in vitro* culture because of tissue growth or scaffold degradation. Consequently, there may be a need for reshaping methods to alter the final shape of these engineered tissues. Techniques that provide an initial form and alter the final contours may serve a complementary approach to engineering shaped chondral tissues.

Cartilage is a mechanosensitive tissue, and its responses to physical forces have been studied *in vivo* and *in vitro*. Mechanical stimuli play an important role in the development and growth of cartilage *in vivo*, from early joint cavitation and morphogenesis [10], to the functional adaptation of the tissue nearing maturation [28, 35]. The metabolic responses of chondrocytes and cartilage explants to controlled mechanical stimuli *in vitro* have also been extensively studied and reviewed [15, 17]. A better understanding of these metabolic responses has encouraged the use of

mechanical loading in what have been termed functional tissue engineering studies to enhance the biochemical and mechanical properties of engineered cartilage [16]. However, the effects of mechanical loading on the *in vitro* growth and remodeling of cartilage as they relate to tissue shape have not been thoroughly explored.

To address the need for shaped cartilage grafts, a technique which reshapes natural or engineered cartilage while preserving tissue integrity and viability may be useful. This study investigated the hypothesis that the application of mechanical loads to immature cartilage *in vitro* will facilitate tissue reshaping through the metabolic processes of the chondrocytes and cartilage matrix. Specifically, cartilage explants were subjected to bending deformations, and changes in sample shape were quantified after *in vitro* growth and remodeling of the tissue (**Fig. 2.1, A**).

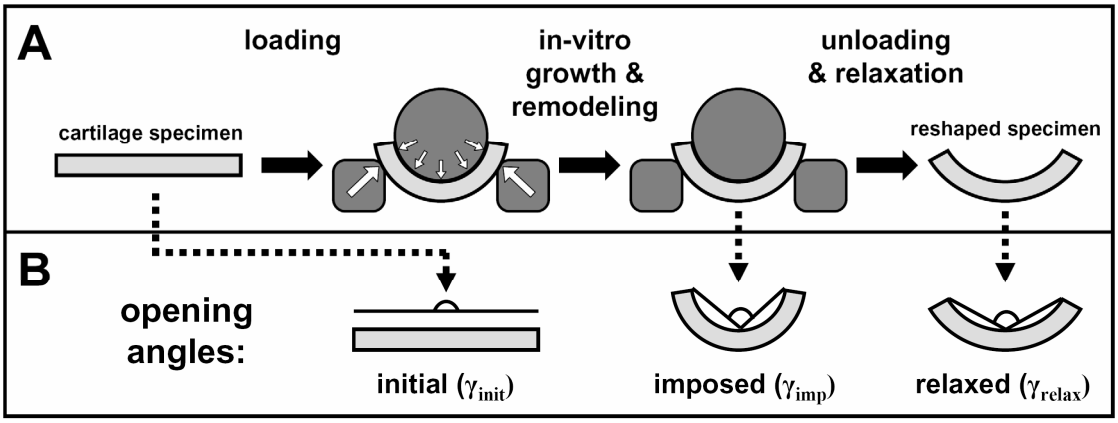

Figure 2.1: (**A**) Hypothesized method and experimental configuration for reshaping immature cartilage via the application of mechanical loads to direct tissue growth and remodeling. (**B**) Illustration of the opening angles used in this study as quantitative measures of specimen shape.

2.3 Materials and Methods

Cartilage Explant Preparation and Incubation

Articular cartilage blocks were harvested from the patellofemoral grooves of 1-3 week old bovine calves (5 animals) and kept hydrated throughout preparation with cold (~4°C) phosphate-buffered saline (PBS). The superficial ~0.5 mm of tissue was removed with a vibrating microtome (Vibratome, St. Louis, MO) and discarded. The underlying ~1 mm of middle zone cartilage was obtained and trimmed into strips measuring 1x2x10 mm^3 (HxWxL), with the length parallel to the patellofemoral groove. Samples were incubated overnight free-swelling in medium consisting of Dulbecco's Modified Eagle's Medium (DMEM) with 20% fetal bovine serum (FBS), ascorbic acid (100 μg/ml), antimicrobials (100 U/ml penicillin, 100 μg/ml streptomycin, 0.25 μg/ml Fungizone), amino acids (0.1 mM MEM non-essential amino acids, 0.4 mM L-proline, 2 mM L-glutamine), and HEPES (10 mM) at 37°C. On the day after harvest, samples were weighed wet and their thickness was measured using a non-contact laser measuring sensor (Acuity AR200, Schmitt Industries, Portland, OR), a process validated by using calibration objects of known thickness.

In the initial experiment, the effects of load and incubation time on shape change and shape retention were examined. Cartilage strips in the loaded group were placed over spans of ~7 mm in length in custom-built loading devices. A controlled, static bending deformation was applied to the cartilage strips using spring-loaded, cylindrical stainless steel posts (4.75 mm dia.) as illustrated (**Fig. 2.1, A**). Each loading device was enclosed in a sterile 50 ml centrifuge tube with medium and placed in an incubator. Other samples were cultured free-swelling as a control. Loaded and free-swelling samples were incubated in 3.5 ml of medium for an additional 2, 4, or 6

days and the medium was changed every other day. At the end of these incubation periods, samples were subjected to the following analyses.

Shape Analysis

Specimen shape was quantified as an "opening angle" (γ) [29] defined here as the angle with a vertex at the midpoint of a specimen and endpoints at the two internal corners (**Fig. 2.1, B**). Digital images of specimens and subsequent analysis with ImageJ software (NIH, Bethesda, MD) were used to calculate opening angles. The initial, straight sample shape (γ_{init}) was found to deviate less than 1° from 180° in each specimen of a control group (n=8) and thus was assumed to be 180° for all samples. For loaded samples, the opening angle was determined from images taken while the sample was still loaded (imposed shape, γ_{imp}) and following 2 hours of free-swelling relaxation in PBS at 4°C (relaxed shape, γ_{relax}). Pilot studies showed that ~2 days was sufficient for shape recovery to reach equilibrium, defined as γ_{relax} changing less than 0.1°/hr, and ~50% of the response occurred during the initial 2 hours of relaxation. Because it was necessary to perform additional biochemical and viability tests on these tissues, the 2 hour relaxation period was chosen to obtain a measure of the total response. The percentage of the imposed change in shape which was retained following this relaxation period was calculated as

$$\text{shape retention (\%)} = \frac{\gamma_{init} - \gamma_{relax}}{\gamma_{init} - \gamma_{imp}} \text{x}100 \qquad (1)$$

Biochemical Analyses and Viability

After the shape analysis, post-culture sample wet weights and thicknesses were determined, and the changes in these structural properties as a percent of the pre-

culture values were calculated. A central segment of the sample, ~2 mm in length, was then cut with a scalpel from each sample, weighed wet, and digested with proteinase K (Roche Diagnostics, Indianapolis, IN) for biochemical analyses. Tissue digests were assessed for DNA with PicoGreen® (Invitrogen) [31], glycosaminoglycans with dimethylmethylene blue [12], and hydroxyproline with dimethylaminobenzaldehyde [44]. Subsequently, cell and collagen contents were determined using ratios of 7.7 pg DNA/cell [26] and 7.25 g COL/g hydroxyproline [19, 34].

To ascertain whether chondrocyte viability was maintained during sample preparation and culture, pieces of tissue adjacent to the removed biochemical portions and samples on the day of harvest were assessed using the the Live/Dead® Viability/Cytotoxicity Kit (Invitrogen, Carlsbad, CA) [43]. These samples were placed in 200 μl PBS containing 40 μM calcein AM and 20 μM ethidium homodimer-1 for 20 minutes at room temperature. Samples were then washed twice in PBS for 10 minutes each and imaged in cross-section using fluorescent microscopy. Quantitative viability analyses were performed using Matlab (Mathworks, Natick, MA) image processing tools as described previously [3]. No fewer than 93% of chondrocytes in the examined tissues were viable, and no differences were apparent between bent and free-swelling samples or between freshly prepared and cultured samples. The limited amount of cell death was mostly localized within ~100 μm of sample edges, where the cartilage had been cut.

Inhibition of Chondrocyte and Cartilage Matrix Metabolism

In a subsequent experiment, several treatments were used to inhibit chondrocyte and cartilage matrix metabolism and examined for their effects on cartilage reshaping. Samples were prepared as before from 6 additional animals and

divided into four experimental groups. Samples in the first group were pre-treated for 1 hour and cultured at 37°C in medium with 100 μg/ml cycloheximide (CHX) [27, 37], an inhibitor of protein synthesis. Samples in the second group were also treated with CHX, but were maintained at 4°C to reduce the rate of biochemical reactions within the tissue. Since the reduction of temperature slows both cell biosynthesis and overall metabolic activity, CHX was included in these cultures to ensure thorough and specific inhibition of cell biosynthesis. Cellular activities were inhibited in a third group of samples by rendering the tissue non-viable (NV) by freezing at -70°C followed by thawing and incubation at 37°C. The lack of viable cells was confirmed using the Live/Dead® Kit. Still other samples were left untreated and incubated as before to serve as a control. All samples were placed in loading devices, deformed, and cultured for an additional 6 days. Samples kept at 4°C were sealed in sterile tubes to maintain pH and placed in a refrigerator. Medium was changed every other day with fresh media pre-equilibrated at either 37°C or 4°C. At the termination of culture, shape analysis was performed as previously described.

A control study was also performed to confirm the inhibitory effects of these treatments on radiolabeled proline incorporation, a marker of protein synthesis. Cartilage samples were prepared as before, but trimmed into shorter 1x2x3 mm^3 explants. CHX-treated, NV, and control samples were incubated free-swelling for three days in media supplemented with 20 μCi/ml [^{3}H]proline and 100 μg/ml CHX where appropriate. To remove unincorporated isotope, samples were thoroughly washed with 0.4 ml of medium 6 times over 2 hours, moved to a new culture plate, and incubated for an additional 24 hours in medium without radiolabel. At the termination of culture, tissue was weighed wet and digested with proteinase K. The

tissue digests and chase medium were analyzed for incorporated radioactivity, which is reported as the sum of the two.

Statistics

Data are presented as means ± standard errors of the mean, unless otherwise noted. In the first experiment, ANOVA ($\alpha = 0.05$) was used to determine the effects of loading (+/-) and culture time (2, 4, 6 days) on sample shape retention, structural changes, and biochemical composition. In the second experiment, ANOVA was used to determine the effect of treatment (CHX 37°C, CHX 4°C, NV 37°C) on sample shape retention and radiolabeled proline incorporation. For each analysis, the source animal was also treated as a random factor, and appropriate post hoc comparisons were made using a Tukey test. In addition, the percentage shape retention data was arcsine transformed before analysis [41]. Statistical analyses were performed using Systat 10.2.05 (Systat Software, Richmond, CA).

2.4 Results

Effects of Bending and Culture Time on Tissue Properties

To ensure similar mechanics in specimens undergoing mechanical loading, samples were prepared uniformly with an average pre-culture thickness of 1.07 ± 0.11 mm (mean ± SD). The loading devices could impose a consistent bending deformation to the samples throughout culture, and this was measured as an 89 ± 4° (mean ± SD) imposed change in the opening angle (γ_{init}-γ_{imp}). In a separate experiment, the peak force required to produce these bending deformations was found to be 0.66 ± 0.11 N, and the force relaxed to 17% and 15% of this peak 2 and 4 hours, respectively, after

the application of load. Following unloading and 2 hours of stress relaxation, the samples cultured under load were markedly different in shape compared to the free-swelling controls (**Fig. 2.2, A-F**). The free-swelling controls showed little change in shape relative to the initial, straight configuration, and their average change in opening angle for all culture times was only 2 ± 1°. The loaded samples exhibited smooth two-dimensional curvatures which reflected varying degrees of shape retention after the different culture periods. The calculated shape retention for the loaded samples was high at all culture times but increased with time (**Fig. 2.3**). Shape retention was 65 ± 3% after only 2 days of culture, but this was significantly less than the 81 ± 3% ($p<0.05$) and 86 ± 3% ($p<0.01$) retention after 4 and 6 days, respectively.

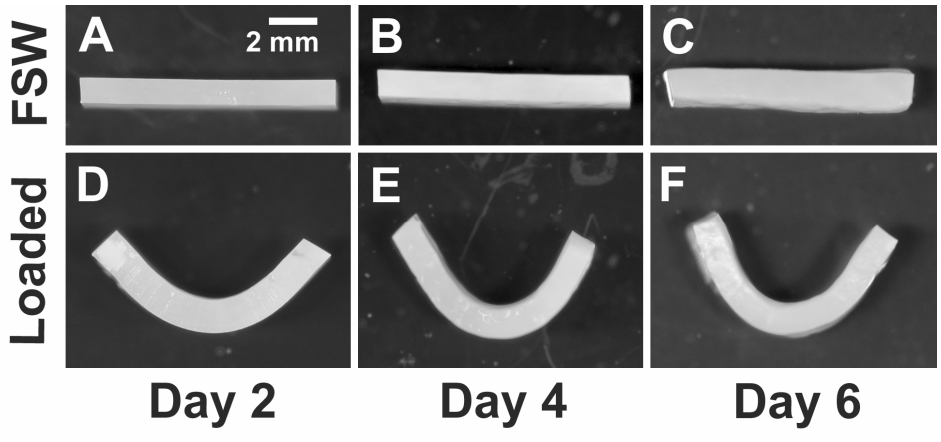

Figure 2.2: (**A-C**) Free-swelling (FSW) and (**D-F**) loaded specimens cultured for (**A,D**) 2, (**B,E**) 4, and (**C,F**) 6 days, shown after 2 hours of free-swelling stress relaxation in phosphate buffered saline.

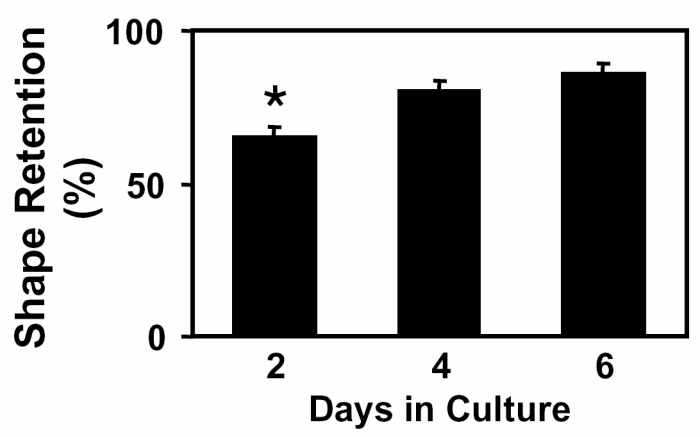

Figure 2.3: The percentage of the imposed shape retained for loaded specimens cultured for 2, 4, and 6 days, quantified following a 2 hour stress relaxation. ✶ $p<0.05$ compared to other culture times. Data are means + SEM and n = 7-9.

The application of bending loads had no significant effects on the change in sample thickness or wet weight through six days of culture (**Fig. 2.4**). However, these structural properties increased with time in culture ($p<0.05$). Glycosaminoglycan, collagen, and cell contents of the explants were also measured and normalized to the final tissue wet weight (**Fig. 2.5, A-C**) and, to facilitate comparisons, the initial wet weight (**Fig. 2.5, D-F**), using the ratio of pre- and post-culture sample weights. Again, no significant differences were detected between the loaded and free-swelling samples for any of these measures. Culture time was a significant factor for collagen and cell contents normalized to the final wet weight ($p<0.05$; **Fig. 2.5, B,C**), presumably reflecting the significant effect of time on increasing wet weight.

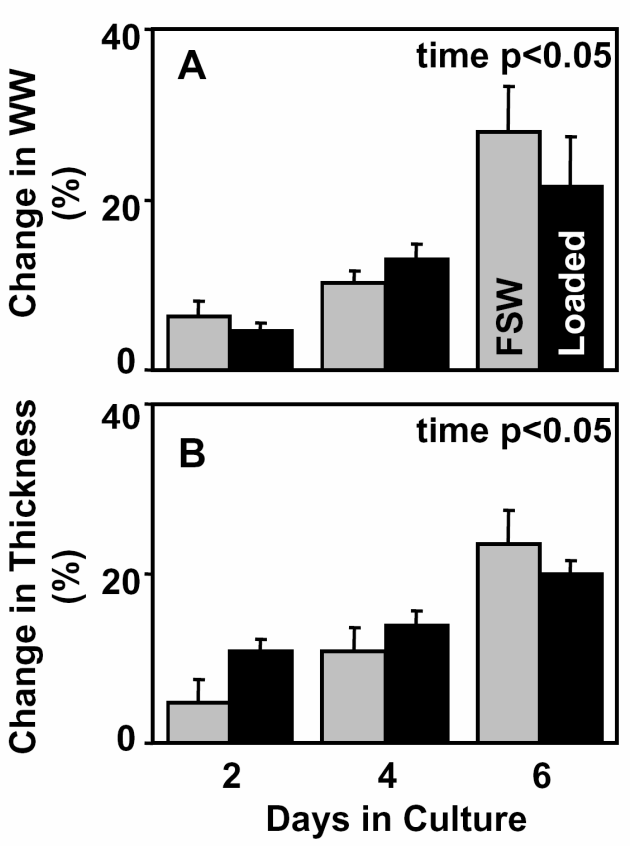

Figure 2.4: Changes in specimen (**A**) wet weights (WW) and (**B**) thicknesses for free-swelling (FSW, gray bars) and loaded (black bars) conditions following various times in culture. Data are means + SEM and n = 7-9.

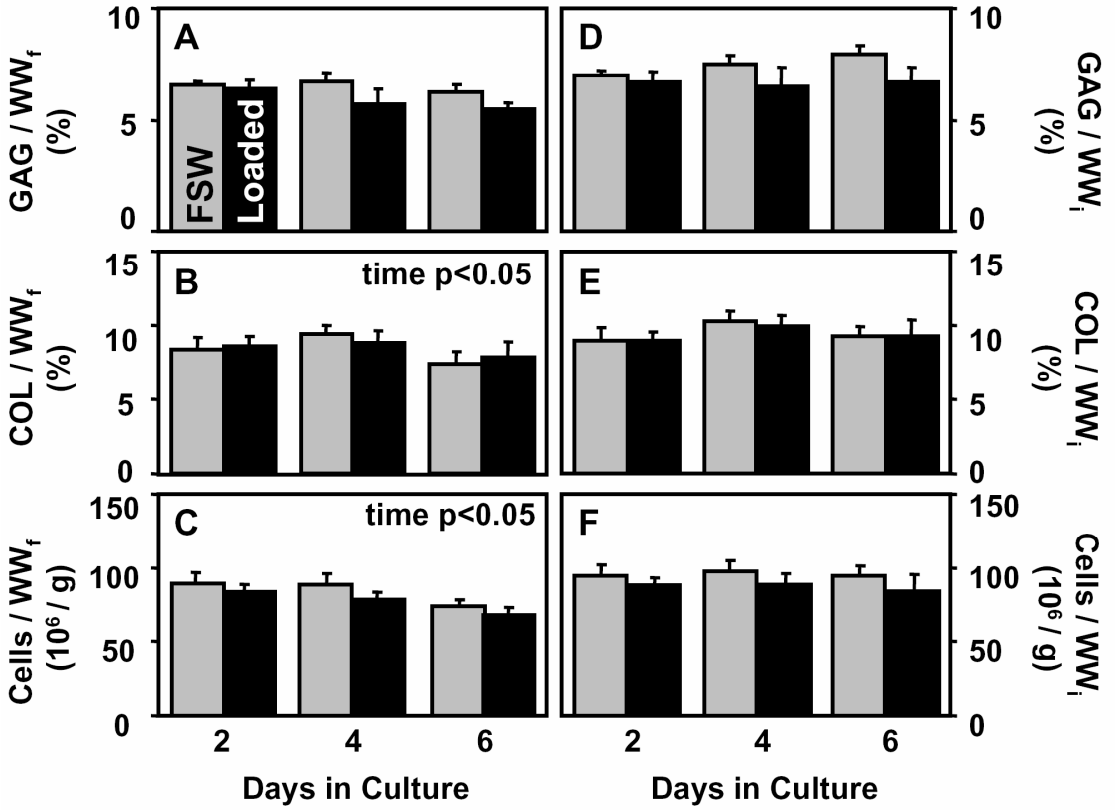

Figure 2.5: (**A,D**) Glycosaminoglycan (GAG), (**B,E**) collagen (COL), and (**C,D**) cell content of free-swelling (FSW, gray bars) and loaded (black bars) specimens following various times in culture. Data are normalized to the (**A-C**) final wet weights (WW_f) and the (**D-F**) initial wet weights (WW_i) of the specimens. Data are means + SEM and n = 7-9.

Effects of Chondrocyte and Cartilage Matrix Metabolism Inhibition on Reshaping

In the second experiment, treatments including culturing samples in the presence of cycloheximide (CHX 37°C) and rendering samples non-viable prior to culture (NV 37°C) were used to inhibit chondrocyte metabolism. Another treatment consisting of culturing samples with CHX at a reduced temperature (CHX 4°C) was used to inhibit both chondrocyte and cartilage matrix metabolism. The efficacy of these various treatments with regards to their ability to inhibit chondrocyte biosynthesis was tested in a control study in which radiolabeled proline incorporation into cartilage explants was used as a measure of chondrocyte protein synthesis. The results of this control study confirmed that the treatments resulted in significantly less [^{3}H] proline incorporation than in untreated controls ($p<0.001$; **Fig. 2.6, A**). The two treatments with CHX (CHX 37°C and CHX 4°C) each resulted in approximately 92% lower incorporation, and the non-viable samples resulted in approximately 98% lower incorporation than in controls.

These treatments imposed varying degrees of inhibition on the process of cartilage reshaping (**Fig. 2.6, B**) in a manner not entirely consistent with their reduction of biosynthesis. After unloading and relaxation at the termination of the 6-day culture, samples which had been incubated in medium containing CHX at 37°C (CHX 37°C) showed only slightly less shape retention than untreated controls (78 ± 3% vs. 90 ± 1%; $p<0.05$). However, samples cultured in the same medium at 4°C (CHX 4°C) had dramatically less ability to retain the imposed shape (22 ± 2%, $p<0.001$). Samples that had been rendered non-viable before incubation (NV 37°C) had a level of shape retention (52 ± 6%) between that of the other treatments.

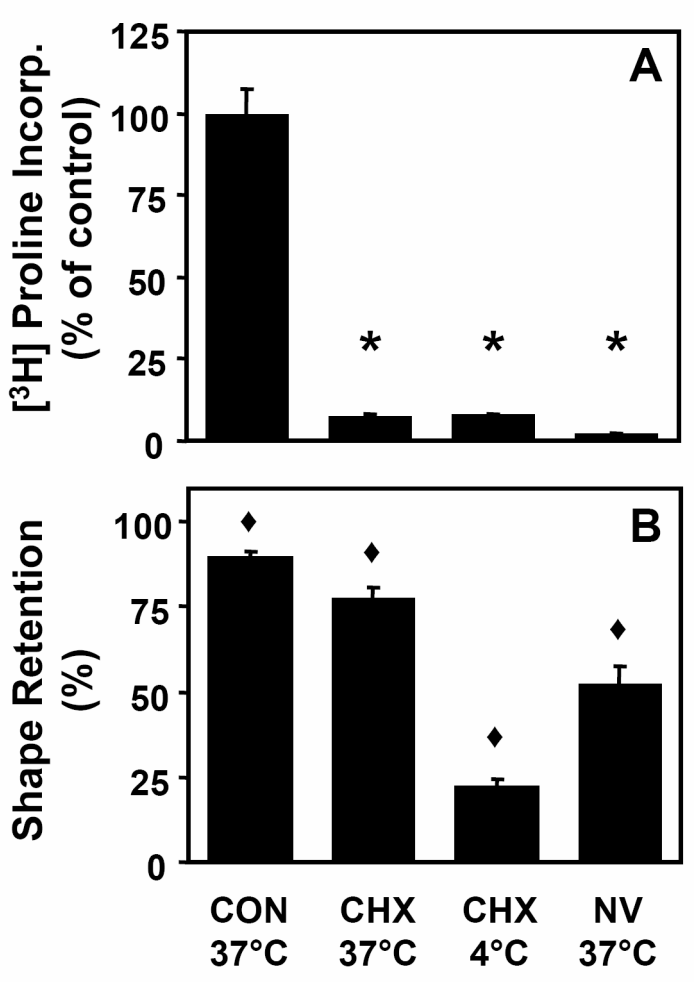

Figure 2.6: (**A**) Metabolic inhibition treatments (cycloheximide [CHX], non-viable [NV], 4°C) result in significantly less radiolabeled proline incorporation in free-swelling explants compared to control. (**B**) Treatments have varied effects on the shape retention of samples loaded for 6 days. ✶ $p<0.001$ compared to control. ♦ $p<0.05$ compared to all groups. Data are means + SEM, and n = (**A**) 7-8 and (**B**) 9-11.

2.5 Discussion

In this study, a technique was successfully developed to reshape immature cartilage through the application of bending mechanical loads during *in vitro* culture. With this technique, a large percentage of the shape imposed during culture was retained by the specimens after unloading and relaxation (**Fig. 2.2 & 2.3**), although it remains to be shown how additional culture without a mechanical stimulus would further affect specimen shape. Moreover, several treatments were used to inhibit chondrocyte and cartilage matrix metabolism, and these provided insight into the potential mechanisms of the demonstrated reshaping process.

The efficacy of this method of reshaping compares favorably with other techniques described previously. In this study, incubation under load for 6 days resulted in specimens retaining 86-90% of the imposed shape after a 2 hour relaxation (**Fig. 2.3 & 2.6, B**). Similarly, shape retentions have been reported in the ranges of 58-75% using laser-mediated reshaping [14] and 80-90% using electroforming [21]. However, conclusions drawn from these comparisons should be tempered in consideration of differences in the tissue sources, the sample geometries, and the methods used to quantify specimen shape.

Although the thermoforming techniques offer a nearly instantaneous method for cartilage reshaping, tissue viability has been reduced by as much as 80-85% immediately following laser or RF heating, with further loss of viability during subsequent culture [25, 36]. Since chondrocyte viability may be an important parameter for success in various cartilage graft therapies, the molding technique developed here was designed to maintain viability. Preservation of chondrocyte viability was achievable (>93%) in cartilage subjected to the bending deformations used in this study.

The effects of the applied bending deformations on the growth and remodeling of the tissue were also of interest, because these might serve as possible mechanisms of reshaping. Physical forces are potent regulators of cartilage metabolism, and studies investigating the mechanobiology of cartilage explants in vitro have typically used static or dynamic applications of mechanical compression or shear, osmotic loading, or hydrostatic pressure [15, 17]. For comparison, the deformations of the cartilage samples in this study can be best understood in terms of static beam bending analysis from engineering mechanics. A beam or strip of tissue at equilibrium under a bending deformation would be expected to have a neutral axis along its length with gradients of tensile and compressive strains extending in opposite directions [33, 46], but the nonlinear behavior of cartilage in the tension-compression transition complicates a more thorough analysis of this loading configuration [5].

In this study, structural properties and biochemical composition (**Fig. 2.4 & 2.5**) served as bulk measures of tissue growth and remodeling. In general, changes with time in the structural and biochemical properties of free-swelling explants followed previously reported trends [2], but there was no significant effect of loading on any of these metrics. However, the potential effects of loading on chondrocyte biosynthetic rates may not have appeared in bulk measures of matrix content during such short culture durations. The use of radiolabeled precursors [4, 30, 37] might provide further insight into the effects of bending on chondrocyte metabolism in different regions of the tissue. In terms of metabolism of matrix components, moderate dynamic loading is generally more anabolic than static loading [15, 17]. Although static bending was effective for tissue reshaping in this study, dynamic applications of bending may also prove efficient at reshaping while concurrently promoting in vitro growth.

In the second experiment, treatments which inhibited chondrocyte and cartilage matrix metabolism were used to further elucidate the possible mechanisms of the reshaping process (**Fig. 2.6**). The finding that CHX, an inhibitor of protein synthesis [27], slightly reduced shape retention suggests only a minor role for chondrocyte protein biosynthesis in the reshaping process, although cells may alter their matrix environment through other means. Samples which were rendered non-viable prior to incubation at 37°C showed even less shape retention, but the freezing of these samples may have had effects on the tissue not specific to reducing biosynthesis. The samples cultured in medium with CHX and maintained at 4°C had markedly poorer shape retention than all other groups. Because temperature reduction slows biochemical reaction rates in the whole tissue, this result potentially identifies an important role of metabolic reactions in the cartilage extracellular matrix. These processes could be catabolic, such as enzymatic cleavage of matrix (e.g. by matrix metalloproteinases) which relieves residual stresses [13], or anabolic, such as the formation of stabilizing cross-links within the collagen network [11]. Lastly, mechanical phenomena that result in the disruption or rearrangement of matrix components are another possible mechanism of cartilage reshaping, that could conceivably be temperature dependent. Further experiments are needed to elaborate on the possible roles of specific mechanisms, but these studies may provide a basis for novel enhancements or manipulations of cartilage reshaping.

The explants used in this study consisted of middle zone articular cartilage taken from immature animals. Middle zone tissue was chosen because it facilitated consistent sample preparation and minimized depth-dependent swelling and growth behaviors. Eliminating the subtle anatomical curvatures at the articular surface allowed easier and more consistent preparation of flat cartilage strips. This method of

preparation decreased the variability in both the initial shape (γ_{init}) and the pre-culture thickness, ensuring more uniform mechanical loading of the specimens. In addition, removing the superficial-most tissue was expected to decrease any gradients in swelling and growth behaviors, which could potentially cause shape changes even in the free-swelling controls. Depth-varying matrix content and architecture in mature articular cartilage provide the basis for non-uniform swelling behaviors which can result in curling of cartilage when released from the subchondral bone [40]. Additionally, immature cartilage explants from superficial and middle zones have exhibited different volumetric growth rates *in vitro* [2]. The free-swelling samples of middle zone cartilage in this study developed minimal changes in shape and thus served as a sufficient control for those samples being reshaped through mechanical loading. In consideration of possible therapeutic applications, it could be advantageous for shaped chondral grafts to include the superficial zone for its mechanical and tribological functions, and these grafts might be required to have concave or convex geometries. Since articular cartilage has a tendency to curl around its superficial surface, it might be expected that a convex geometry would be more difficult to attain. Future studies of mechanical reshaping will need to consider the effects of retaining the superficial zone and the orientation of the tissue with regard to the final geometry.

This study provided "proof of concept" for using mechanical loading during *in vitro* culture to modulate the shape of cartilaginous tissues. Although tissue reshaping was shown in a simplified two-dimensional bending configuration, expanding this technique to more-complex three-dimensional geometries could enhance its potential for clinical utility. Successful creation of these more-complex geometries will likely require detailed analyses of the desired shapes and careful selection of the initial tissue

with regard to size and structure. Because shaped cartilage grafts have applications in the reconstruction of damaged joints and deformities of the head and neck, it would be of interest to investigate the efficacy of mechanical reshaping on articular and non-articular cartilages. This method may also have potential for shaping engineered cartilaginous tissues and could supplement the *in vitro* growth and maturation of these tissues. Additional studies will be needed to examine the ability to form more-complex geometries and to reshape cartilaginous tissues from various sources using the mechanical molding technique.

2.6 Acknowledgments

Chapter 2, in full, is reproduced from *Tissue Engineering*, volume 13, issue 12, 2007 with permission from Mary Ann Liebert, Inc. The dissertation author was the primary author of this paper and thanks co-authors Jessica W. Lin and Robert L. Sah. This work was supported in part by grants from the National Institutes of Health (NIH) and the National Science Foundation (NSF), and by a grant to the University of California, San Diego, in support of Robert Sah, from the Howard Hughes Medical Institute (HHMI) through the HHMI Professors Program. Individual support was received through a NSF Graduate Research Fellowship (to the dissertation author, GMW), and a UC LEADS Scholarship (to Jessica Lin).

2.7 References

1. Alhadlaq A, Elisseeff JH, Hong L, Williams CG, Caplan AI, Sharma B, Kopher RA, Tomkoria S, Lennon DP, Lopez A, Mao JJ: Adult stem cell driven genesis of human-shaped articular condyle. *Ann Biomed Eng* 32:911-23, 2004.

2. Asanbaeva A, Masuda K, Thonar EJ-MA, Klisch SM, Sah RL: Regulation of immature cartilage growth by IGF-I, TGF-alpha 1, BMP-7, and PDGF-AB: role of metabolic balance between fixed charge and collagen network. *Biomech Model Mechanobiol* 7:263-76, 2007.

3. Bae WC, Schumacher BL, Sah RL: Indentation probing of human articular cartilage: effect on chondrocyte viability. *Osteoarthritis Cartilage* 15:9-18, 2007.

4. Buschmann MD, Maurer AM, Berger E, Hunziker EB: A method of quantitative autoradiography for the spatial localization of proteoglycan synthesis rates in cartilage. *J Histochem Cytochem* 44:423-31, 1996.

5. Chahine NO, Wang CC, Hung CT, Ateshian GA: Anisotropic strain-dependent material properties of bovine articular cartilage in the transitional range from tension to compression. *J Biomech* 37:1251-61, 2004.

6. Chang SC, Rowley JA, Tobias G, Genes NG, Roy AK, Mooney DJ, Vacanti CA, Bonassar LJ: Injection molding of chondrocyte/alginate constructs in the shape of facial implants. *J Biomed Mater Res* 55:503-11, 2001.

7. Cole BJ, Malek MM. Articular Cartilage Lesions: A Practical Guide to Assessment and Treatment. New York: Springer; 2004.

8. Convery FR, Meyers MH, Akeson WH: Fresh osteochondral allografting of the femoral condyle. *Clin Orthop Rel Res* 273:139-45, 1991.

9. Curl WW, Krome J, Gordon ES, Rushing J, Smith BP, Poehling GG: Cartilage injuries: a review of 31,516 knee arthroscopies. *Arthroscopy* 13:456-60, 1997.

10. Drachman D, Sokoloff L: The role of movement in embryonic joint development. *Dev Biol* 14:401-20, 1966.

11. Eyre DR, Paz MA, Gallop PM: Cross-linking in collagen and elastin. *Ann Rev Biochem* 53:717-48, 1984.

12. Farndale RW, Buttle DJ, Barrett AJ: Improved quantitation and discrimination of sulphated glycosaminoglycans by use of dimethylmethylene blue. *Biochim Biophys Acta* 883:173-7, 1986.

13. Fry H, Robertson WV: Interlocked stresses in cartilage. *Nature* 215:53-4, 1967.

14. Gray DS, Kimball JA, Wong BJ: Shape retention in porcine-septal cartilage following Nd:YAG (lambda = 1.32 microm) laser-mediated reshaping. *Lasers Surg Med* 29:160-4, 2001.

15. Grodzinsky AJ, Levenston ME, Jin M, Frank EH: Cartilage tissue remodeling in response to mechanical forces. *Annu Rev Biomed Eng* 2:691-713, 2000.

16. Guilak F, Butler DL, Goldstein SA: Functional tissue engineering: the role of biomechanics in articular cartilage repair. *Clin Orthop Rel Res*:S295-305., 2001.

17. Guilak F, Sah RL, Setton LA: Physical regulation of cartilage metabolism. In: *Basic Orthopaedic Biomechanics,* ed. by VC Mow, Hayes WC, Raven Press, New York, 1997, 179-207.

18. Helidonis E, Sobol E, Kavvalos G, Bizakis J, Christodoulou P, Velegrakis G, Segas J, Bagratashvili V: Laser shaping of composite cartilage grafts. *Am J Otolaryngol* 14:410-2, 1993.

19. Herbage D, Bouillet J, Bernengo J-C: Biochemical and physicochemical characterization of pepsin-solubilized type-II collagen from bovine articular cartilage. *Biochem J* 161:303-12, 1977.

20. Hjelle K, Solheim E, Strand T, Muri R, Brittberg M: Articular cartilage defects in 1,000 knee arthroscopies. *Arthroscopy* 18:730-4, 2002.

21. Ho KH, Diaz Valdes SH, Protsenko DE, Aguilar G, Wong BJ: Electromechanical reshaping of septal cartilage. *Laryngoscope* 113:1916-21, 2003.

22. Hung CT, Lima EG, Mauck RL, Taki E, LeRoux MA, Lu HH, Stark RG, Guo XE, Ateshian GA: Anatomically shaped osteochondral constructs for articular cartilage repair. *J Biomech* 36:1853-64, 2003.

23. Kamil SH, Kojima K, Vacanti MP, Bonassar LJ, Vacanti CA, Eavey RD: In vitro tissue engineering to generate a human-sized auricle and nasal tip. *Laryngoscope* 113:90-4, 2003.

24. Kaplonyi G, Zimmerman I, Frenyo AD, Farkas T, Nemes G: The use of fibrin adhesive in the repair of chondral and osteochondral injuries. *Injury* 19:267-72, 1988.

25. Keefe MW, Rasouli A, Telenkov SA, Karamzadeh AM, Milner TE, Crumley RL, Wong BJ: Radiofrequency cartilage reshaping: efficacy, biophysical measurements, and tissue viability. *Arch Facial Plast Surg* 5:46-52, 2003.

26. Kim YJ, Sah RLY, Doong JYH, Grodzinsky AJ: Fluorometric assay of DNA in cartilage explants using Hoechst 33258. *Anal Biochem* 174:168-76, 1988.

27. Kimura JH, Caputo CB, Hascall VC: The effect of cycloheximide on synthesis of proteoglycans by cultured chondrocytes from the Swarm rat chondrosarcoma. *J Biol Chem* 256:4368-76, 1981.

28. Kiviranta I, Tammi M, Jurvelin J, Saamanen AM, Helminen HJ: Moderate running exercise augments glycosaminoglycans and thickness of articular cartilage in the knee joint of young beagle dogs. *J Orthop Res* 6:188-95, 1988.

29. Liu SQ, Fung YC: Zero-stress states of arteries. *J Biomech Eng* 110:82-4, 1988.

30. Maroudas A: Determination of the rate of glycosaminoglycan synthesis *in vivo* using radioactive sulfate as tracer: comparison with *in vitro* results. In: *Methods in Cartilage Research,* ed. by A Maroudas, Kuettner KE, Academic Press, New York, 1990, 143-8.

31. McGowan KB, Kurtis MS, Lottman LM, Watson D, Sah RL: Biochemical quantification of DNA in human articular and septal cartilage using PicoGreen and Hoechst 33258. *Osteoarthritis Cartilage* 10:580-7, 2002.

32. Nakamura N, Horibe S, Iwahashi T, Kawano K, Shino K, Yoshikawa H: Healing of a chondral fragment of the knee in an adolescent after internal fixation. A case report. *J Bone Joint Surg Am* 86-A:2741-6, 2004.

33. Nicosia MA: A theoretical framework to analyze bend testing of soft tissue. *J Biomech Eng* 129:117-20, 2007.

34. Pal S, Tang L-H, Choi H, Habermann E, Rosenberg L, Roughley P, Poole AR: Structural changes during development in bovine fetal epiphyseal cartilage. *Collagen Rel Res* 1:151-76, 1981.

35. Plochocki JH, Riscigno CJ, Garcia M: Functional adaptation of the femoral head to voluntary exercise. *Anat Rec A Discov Mol Cell Evol Biol* 288:776-81, 2006.

36. Rasouli A, Sun CH, Basu R, Wong BJ: Quantitative assessment of chondrocyte viability after laser mediated reshaping: a novel application of flow cytometry. *Lasers Surg Med* 32:3-9, 2003.

37. Sah RL, Kim YJ, Doong JH, Grodzinsky AJ, Plaas AHK, Sandy JD: Biosynthetic response of cartilage explants to dynamic compression. *J Orthop Res* 7:619-36, 1989.

38. Schek RM, Taboas JM, Hollister SJ, Krebsbach PH: Tissue engineering osteochondral implants for temporomandibular joint repair. *Orthod Craniofac Res* 8:313-9, 2005.

39. Sedrakyan S, Zhou ZY, Perin L, Leach K, Mooney D, Kim TH: Tissue engineering of a small hand phalanx with a porously casted polylactic acid-polyglycolic acid copolymer. *Tissue Eng* 12:2675-83, 2006.

40. Setton LA, Toyama H, Mow VC: Swelling and curling behaviors of articular cartilage. *J Biomech Eng* 120:355-61, 1998.

41. Sokal RR, Rohlf FJ. Biometry. 3rd ed. New York: WH Freeman and Co.; 1995.

42. Tardy ME, Denneny J, 3rd, Fritsch MH: The versatile cartilage autograft in reconstruction of the nose and face. *Laryngoscope* 95:523-33, 1985.

43. Williams GM, Klein TJ, Sah RL: Cell density alters matrix accumulation in two distinct fractions and the mechanical integrity of alginate-chondrocyte constructs. *Acta Biomaterialia* 1:625-33, 2005.

44. Woessner JF: The determination of hydroxyproline in tissue and protein samples containing small proportions of this imino acid. *Arch Biochem Biophys* 93:440-7, 1961.

45. Wong BJ, Milner TE, Kim HH, Nelson JS, Sobol EN: Stress relaxation of porcine septal cartilage during Nd:YAG (λ=1.32 μm) laser irradiation: mechanical, optical, and thermal responses. *J Biomed Optics* 3:409-14, 1998.

46. Yu Q, Zhou J, Fung YC: Neutral axis location in bending and Young's modulus of different layers of arterial wall. *Am J Physiol* 265:H52-60, 1993.

CHAPTER 3

ASYMMETRICAL STRAIN DISTRIBUTIONS AND NEUTRAL AXIS LOCATION OF CARTILAGE IN FLEXURE

3.1 Abstract

Flexural deformation has been used for the biomechanical characterization of native and engineered cartilage and as a mechanical stimulus to induce alteration of cartilage shape during *in vitro* culture. Flexure is also a physiologically relevant mode of deformation for various cartilaginous structures such as the ears and nose, but a kinematic description of cartilage in flexure is lacking even for simple deformations. The hypothesis of this study was that tension-compression (T-C) nonlinearity of cartilage will result in asymmetrical strain distributions during bending, while a material with similar behavior in tension and compression, such as alginate, will have a more symmetrical distribution of strains. Strips of calf articular cartilage and alginate were tested under uniform circular bending, and strains were determined by a micromechanical analysis of images acquired by epifluorescence microscopy. This experimental analysis was interpreted in the context of a model of small-deflection, pure bending of thin, homogeneous beams of a bimodular elastic material. The results supported the hypothesis and showed that marked asymmetry existed in cartilage

flexural strains where the location of the neutral axis was significantly different than the midline and closer to the tensile surface. In contrast, alginate samples had a centrally located neutral axis. These experimental results were supported by the model indicating that the bimodular simplification of cartilage properties is a useful first approximation of T-C nonlinearity in these tests. The neutral axis location in cartilage samples was not influenced by testing orientation (towards or away from the superficial-most tissue) or magnitude of flexure. These findings characterize the kinematics of cartilage at equilibrium during simple bending and indicate that T-C nonlinearity is an important determinant of the flexural strain distributions in the tested tissue.

3.2 Introduction

Mechanical loading of cartilage explants can regulate chondrocyte metabolism and direct growth and remodeling [15]. Specific mechanical stimuli may be used to manipulate cartilage properties including matrix composition, mechanical properties, and shape. For instance, bending of immature articular cartilage during *in vitro* culture can induce marked changes in tissue shape [31]. Identification of the mechanobiological processes underlying these shape changes may be facilitated by a biomechanical characterization of cartilage subjected to such flexure. This technique of shaping cartilaginous tissues may have applications towards creating grafts of specific shapes for joint repair or craniofacial reconstruction and towards understanding the effects of physical forces on the developing morphologies of cartilage structures.

Flexure is a physiologically relevant mode of deformation for many types of cartilage including those located within the nose, ears, and ribs. To better understand the biomechanical functions of these tissues, tests such as three-point or curved-beam bending have been used to characterize nasal septal, auricular, costal, and tracheal cartilages, with moduli reported in the range of 4-9 MPa [11, 14, 21, 24]. These properties may also serve as useful benchmarks for assessing engineered cartilage being developed for therapeutic purposes [11, 24]. While bending may produce tensile, compressive, and shear deformations, previous studies of cartilage flexural properties have not experimentally quantified strain distributions within the tissue during bending.

The complex mechanical properties of cartilage increase the difficulty of predicting deformation behavior when the tissue is subjected to bending. In particular, articular cartilage has a well-characterized, nonlinear, equilibrium stress-strain

response that is stiffer in tension [1, 32] than in compression [23, 33]. The transition between these two regimes occurs smoothly, and this behavior of cartilage has been termed as tension-compression (T-C) nonlinearity [6, 20, 26]. Additional reports of nonlinear behavior include slight softening with increasing compressive strain (15-30%) in immature bovine cartilage and stiffening with increasing tensile strain (2-10%) in more mature bovine cartilage [8, 12]. These properties may result in stress and strain distributions within cartilage during flexure that significantly deviate from those predicted by fundamental, linearly elastic beam theory. An experimental approach for measuring intra-cartilage strains may provide insight into the biomechanics of cartilage in flexure.

Methods for measuring intra-cartilage strains have combined microscopy with point-tracking of fluorescently labeled chondrocyte nuclei [25] or digital image correlation [29]. These techniques have been useful for determining spatially varying strain distributions arising from depth-dependent inhomogeneity of material properties in articular cartilage under compression [25, 29]. Complex strain patterns within cartilage near an indentation probe or an articular defect have been assessed through similar methods [4, 13]. The application of these techniques to cartilage in flexure could produce a detailed depiction of the intra-tissue mechanical environment in this deformation state.

The hypothesis of this study was that T-C nonlinearity, such as that attributed to cartilage, will result in asymmetrical strain distributions during bending, while a material with similar behavior in tension and compression, such as alginate, will have reduced asymmetry. In addition, effects of potential cartilage inhomogeneity and magnitude of flexure were examined by varying the tissue orientation and bending radius of curvature.

3.3 Materials and Methods

Cartilage Sample Preparation

Cartilage blocks were harvested from the patellofemoral grooves of 1-3 week-old bovines obtained fresh from an abattoir. Slices of middle zone cartilage (~0.5-1.5 mm from the articular surface) were obtained using a vibrating microtome (Vibratome, St. Louis, MO) and were cut into strips measuring ~1×2×10 mm^3 (H×W×L). As a critical dimension in determining flexural strains, the thickness was measured at three locations along the span of each cartilage sample and averaged. Each sample was found to be uniformly thick (±0.02 mm), and the average thickness of all samples was 1.00±0.04 mm (mean ± SD). Cartilage strips were stored for up to 48 hours in Dulbecco's Modified Eagle's Medium at 4°C. Prior to mechanical testing, cartilage was immersed for 20 min in 1 ml of phosphate buffered saline (PBS) containing 20 μg/ml propidium iodide to stain chondrocyte nuclei and then washed twice for 10 min each in PBS.

The effect of cartilage orientation relative to the direction of bending (towards or away from the superficial-most side) was assessed in four pairs of adjacent cartilage strips (n=8) from two animals. Upon finding no significant effect of orientation as indicated in the results, these data were pooled with those from an additional animal (n=12 strips total). The effect of the bending radius of curvature was investigated using cartilage strips (n=7) from two animals.

Alginate Sample Preparation

For comparative analysis, alginate was primarily chosen for having similar tensile and compressive moduli, homogeneity at a microscale, and the ability to include fluorescent fiducial markers. A 2% solution of alginate (Keltone LVCR, Kelco, Chicago, IL) was prepared in 0.9% saline and passed through a 0.22 μm polyethersulfone filter (Millipore, Billerica, MA). Fluorescent microspheres (Bangs Laboratories, Fishers, IN) with 7.32 μm mean diameter were suspended in the solution at 4×10^6 beads/ml. Alginate was gelled into slabs using a custom mold that allowed Ca^{++} diffusion, as described previously [30], and cut into strips (~1×2×10 mm^3, H×W×L) for flexure or disks (Ø 5 by 1 mm H) for unconfined compression. Each alginate strip was uniformly thick (±0.04 mm), and the average of all strips was 1.05±0.09 mm (mean ± SD). Alginate samples were equilibrated in Dulbecco's PBS (D-PBS) containing calcium and magnesium (Invitrogen, Carlsbad, CA) for at least 24 hours prior to mechanical testing to stabilize the mechanical properties of the polymerized hydrogel [22].

Mechanical Test in Flexure

In the first set of experiments, bending deformations were applied to cartilage and alginate strips in a configuration consistent with that used previously for the *in vitro* reshaping of cartilage [31]. A custom, microscope-mounted testing device consisted of a chamber containing a cylindrical, self-aligning loading post and a sample support, which were displaced relative to one another by a hand-controlled micrometer. Displacement rates were similar among tests (~0.25 mm/s) but not explicitly controlled, since only equilibrium states were being studied. Specimens were supported over a 7 mm span and bent flush around the loading post (Ø 4.75 mm)

to achieve a uniform circular deformation (**Fig. 3.1, A**). The chamber allowed visualization by epifluorescence microscopy of the sample surface in the plane of bending relative to the x and z axes (length and depth; also anterior-posterior and superficial-deep in cartilage samples). Digital images were acquired in the unloaded reference state and the equilibrium deformed state following stress relaxation (1 hr for alginate; 2 hrs for cartilage; based on pilot studies) (**Fig. 3.1, B**). Throughout the test, cartilage and alginate samples were immersed in PBS and D-PBS, respectively, at room temperature (22-24°C).

In the second set of experiments, cartilage strips were bent around a series of loading posts of decreasing diameter, Ø 15.53 mm (large), 7.92 mm (medium), and 4.75 mm (small). Following each stress relaxation and imaging step, samples were briefly unloaded to switch loading posts and then deformed around the next smaller post.

Micromechanical Strain Analysis

Strain analysis was performed with a custom-written Matlab algorithm (The Mathworks, Natick, MA) using a combination of discrete point-tracking and digital image correlation as described in detail elsewhere [13]. Briefly, a region of interest (ROI) was manually chosen in the center of each sample, spanning the full thickness and ~0.67 mm in length (**Fig. 3.1, B**). Fluorescent nuclei and beads were localized, and a subset of these, spaced at ~46 μm, was tracked between the reference and deformed states by maximizing the normalized cross-correlation. A uniform square mesh of points, also with 46 μm spacing in the reference state, was selected in the ROI starting one unit mesh length from the concave surface (z=0). Spacing parameters were chosen to provide sufficient resolution of data points within the ROI and to help

maximize correlation. The location of each mesh point in the deformed state was determined by a local affine mapping of tracked nuclei or beads within 93 μm. Displacements of mesh points were used to calculate displacement gradients and Lagrangian strains. For each test, strain profiles (E_{xx}, E_{zz}, and E_{xz}) through the thickness of the sample were determined at an x-coordinate where $\Sigma|E_{xz}|$ was a minimum.

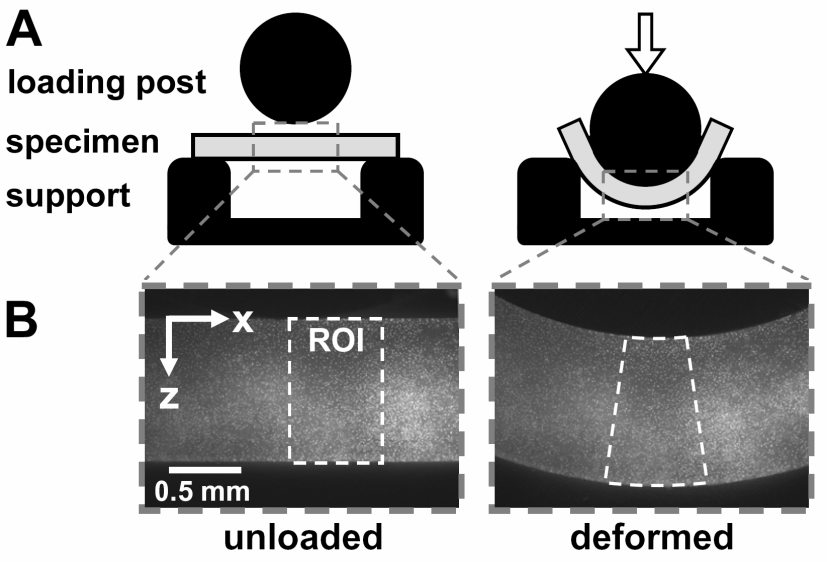

Figure 3.1: (A) Illustration of the mechanical testing setup for applying bending deformations of uniform curvature and **(B)** experimental images of cartilage in unloaded and deformed configurations. Central region of interest (ROI) is indicated by white dashed boxes.

Model of Pure Beam Bending of a Bimodular Material

According to Euler-Bernoulli beam theory, small-deflection, pure bending (i.e. uniform bending moment) of a thin, homogeneous beam results in a uniform circular deformation, a uniaxial state of stress in the longitudinal direction (x-axis), and a linear profile of longitudinal normal strain (E_{xx}) from compression to tension [5]. The flexure test used here imposed a uniform circular deformation on samples to approximate pure beam bending. A simple analytical model of pure bending was employed to illustrate the consequences of material T-C nonlinearity on the neutral axis location (depth where $E_{xx}=0$) and to predict the location based on published or measured values of cartilage and alginate mechanical properties.

As an approximation, constitutive relationships of cartilage and alginate were simplified to those of bimodular elastic materials, possessing a different modulus in tension (+), E_+, than that in compression (-), E_-. The neutral axis location in an Euler-Bernoulli beam composed of a bimodular material subjected to pure bending has been previously derived as

$$d_{NA} = \frac{\sqrt{E_+}}{\sqrt{E_+} + \sqrt{E_-}} d \qquad (1)$$

where d_{NA} is the distance from the concave surface to the neutral axis and d is the beam thickness [17]. For cartilage samples, E_+ and E_- are equilibrium tensile and unconfined compressive moduli reported for bovine calf tissue with similar age, depth, and orientation as used here [3, 12]. Likewise, E_+ for 2% alginate of a similar preparation was obtained from the literature [30], while E_- was measured by equilibrium unconfined compression testing for lack of a suitable reference. The values for these parameters are shown in **Table 3.1**.

Data Analysis and Statistics

The effect of cartilage orientation on E_{xx} was determined using repeated measures ANOVA with orientation as a between-subjects factor and depth as a within-subjects factor. Planned comparisons were made at each depth between orientations using paired t-tests. The neutral axis, defined as the z-coordinate where $E_{xx}=0$, was determined by linear regression of E_{xx} on z for each sample. The neutral axis location was compared to the sample midline (half the thickness) by paired t-tests. Linear regressions of E_{zz} on z in the tensile and compressive regions were performed for cartilage. Assuming uniaxial stress, apparent Poisson's ratios in tension (ν_{+xz}) and compression (ν_{-xz}) were calculated as the negative ratio of the slope of E_{zz} (dE_{zz}/dz) to the slope of E_{xx} (dE_{xx}/dz) and compared by paired t-tests. Dilatation was calculated as $(1+E_{xx})(1+E_{yy})(1+E_{zz})$, where E_{yy} was estimated as stated in the results.

Effects of loading post-size on neutral axis location and dE_{xx}/dz were determined using repeated measures ANOVA with post-size as a within-subjects factor and post-hoc comparisons with Bonferroni correction. The slope, dE_{xx}/dz, was also linearly regressed on the inverse of the bending radius of curvature, and the slope of this regression was compared to the predicted value of 1 by t-test, with adjustment of the standard error for repeated measures [9].

Results are presented as means ± SEM, unless noted otherwise. Coefficients of determination (r^2) are reported for regressions. For all comparisons, a significance level, α, of 0.05 was used.

3.4 Results

Flexural Strains in Cartilage Versus Alginate

The first set of tests exposed similarities and differences in the flexural mechanics of cartilage and alginate. Representative strain maps (E_{xx}, E_{zz}, E_{xz}) within the ROI and superimposed on the reference image reveal general patterns for cartilage and alginate samples (**Fig. 3.2**). For both specimen types, the longitudinal normal strain, E_{xx}, demonstrated a gradient from compression on the concave side to tension on the convex side. An opposing gradient was produced in the transverse normal strain, E_{zz}, exhibiting a Poisson's effect. Shear strains, E_{xz}, were small throughout, as expected for materials in pure bending, and were generally less than the error (approximately ±1%) of this experimental technique [13].

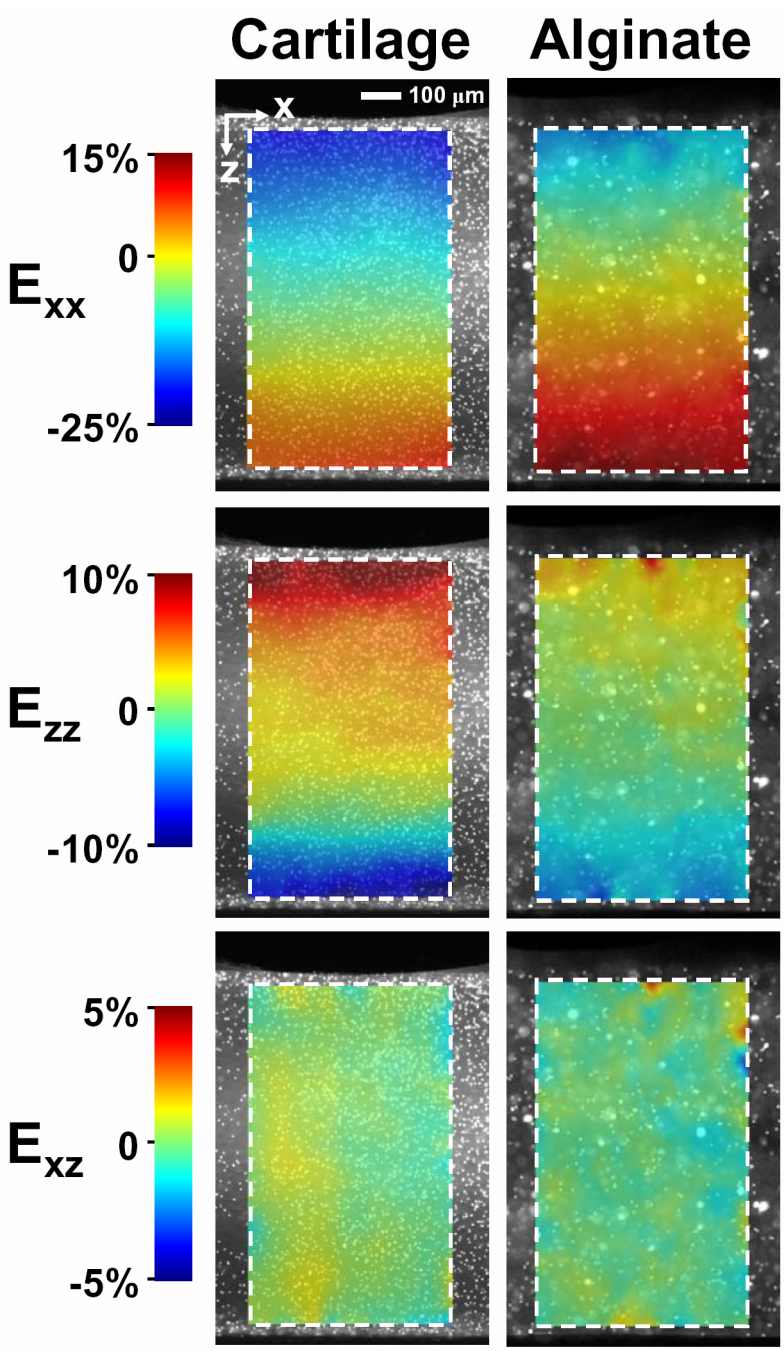

Figure 3.2: Lagrangian strain maps within the ROI of representative cartilage and alginate specimens bent around the small diameter loading post. Maps are superimposed on the reference images.

Quantification and comparison of strain patterns were achieved by analyzing profiles through the thickness (along the z-axis). Bending of cartilage towards or away from the superficial-most tissue was not found to be a statistically significant factor in determining the profile of E_{xx} ($p=0.25$). Planned comparisons further revealed that at all depths there was no significant difference between the two orientations. Consequently, data were pooled along with those from an additional animal. Together, the averaged cartilage strain profiles reveal a marked asymmetry of strains during flexure (**Fig. 3.3, A**). E_{xx} varied nearly linearly with z ($r^2>0.97$) from approximately -20% to 7%. The neutral axis location was determined to be 0.75 ± 0.02 mm from the concave surface, which was significantly different than the midline (0.50 ± 0.01 mm, $p<0.001$). In contrast, alginate specimens demonstrated a highly symmetrical strain state during flexure (**Fig. 3.3, B**). E_{xx} was also highly linear ($r^2>0.97$), but varied from approximately -15% on the concave side to 14% on the convex side. The alginate neutral axis was located at 0.53±0.02 mm and was not different than the midline (0.52 ± 0.02 mm, $p=0.48$).

Further analysis of cartilage revealed strong linearity of E_{zz} both on the tensile and compressive sides of the tissue ($r^2=0.91 \pm 0.03$ and $r^2=0.95 \pm 0.01$, respectively). The apparent Poisson's ratio in tension was greater than that in compression ($\nu_{+xz}=0.78 \pm 0.11$ vs. $\nu_{-xz}=0.32 \pm 0.03$, $p<0.01$). Estimating dilatation in the bent cartilage samples was accomplished by inferring the behavior in the y-direction. The normal strain, $E_{yy,}$ was calculated from E_{xx} by assuming $\nu_{-xy}=0.14$ as previously published [12] and $\nu_{+xy} = \nu_{+xz} = 0.78$, as measured in this study. Dilatation varied through the thickness with values approaching zero near the neutral axis and negative throughout the remaining tissue (**Fig. 3.4**). The volume loss increased with distance

from the neutral axis to reach a maximum of -12% at the concave (compressive) surface and -4% at the convex (tensile) surface.

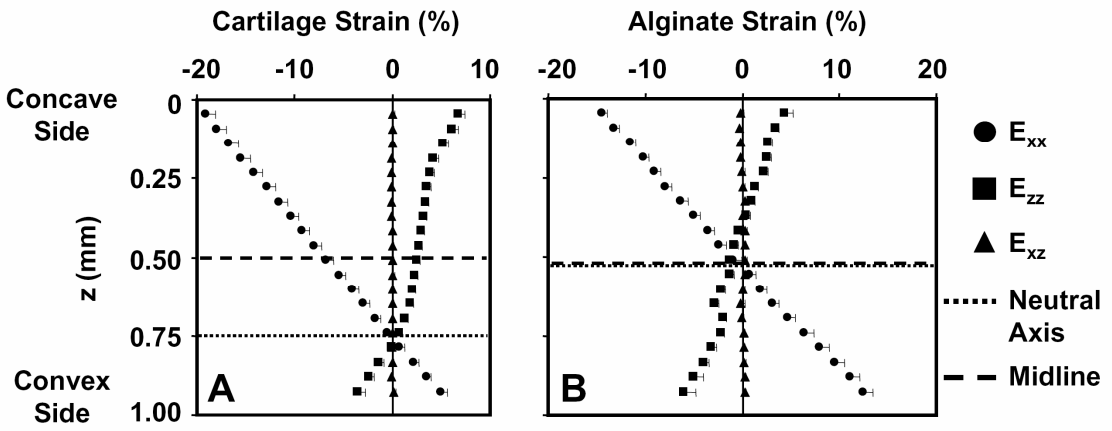

Figure 3.3: Strain profiles through the thickness of (**A**) cartilage and (**B**) alginate specimens from the concave surface (z=0) to the convex surface (z≈1). Location of the neutral axes, where E_{xx}=0, and sample midlines are indicated by dotted and dashed lines, respectively. Mean ± SEM; n=12 for cartilage and n=9 for alginate.

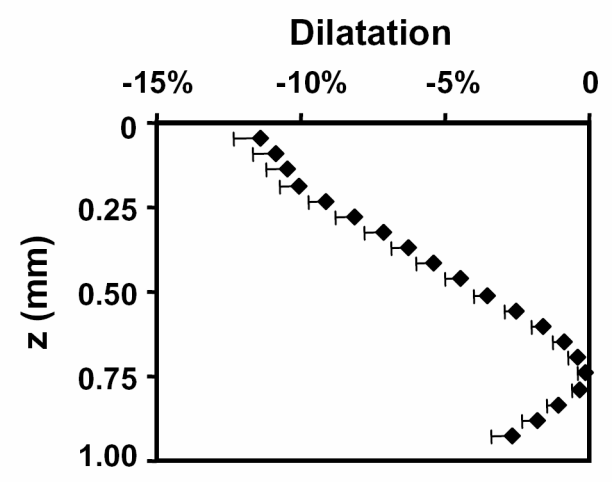

Figure 3.4: Estimated dilatation profile through the thickness of cartilage samples. Assumptions included $\nu_{-xy} = 0.14$ [12], and $\nu_{+xy} = \nu_{+xz} = 0.78$, as measured in this study. Mean ± SEM; n=12.

Effects of Magnitude of Bending on Cartilage Flexural Strains

A relationship between the magnitude of bending and the cartilage flexural strains was determined by varying the size of the loading post. Decreasing the loading post-size induced greater strains in the cartilage and increased the slope of the longitudinal strain profile (dE_{xx}/dz) with each being greater than the previous ($p<0.001$) (**Fig. 3.5**). However, the neutral axis location was not significantly affected, being 0.75 ± 0.01, 0.77 ± 0.01, and 0.77 ± 0.01 mm with the large, medium and small posts, respectively. The strain distributions induced by the small loading post were consistent with those found in the previous set of tests, even though these cartilage samples were preconditioned by two cycles of increasing flexural deformation.

The slope, dE_{xx}/dz, and the radius of curvature were further examined by linear regression ($r^2=0.88$, **Fig. 3.6**). Here, the bending radius of curvature was defined as the radius of the loading post plus the distance to the neutral axis, and then plotted as the inverse. The slope of this regression (0.93 ± 0.04) was not significantly different than unity, the value predicted by Euler-Bernoulli beam theory for materials in pure bending [5].

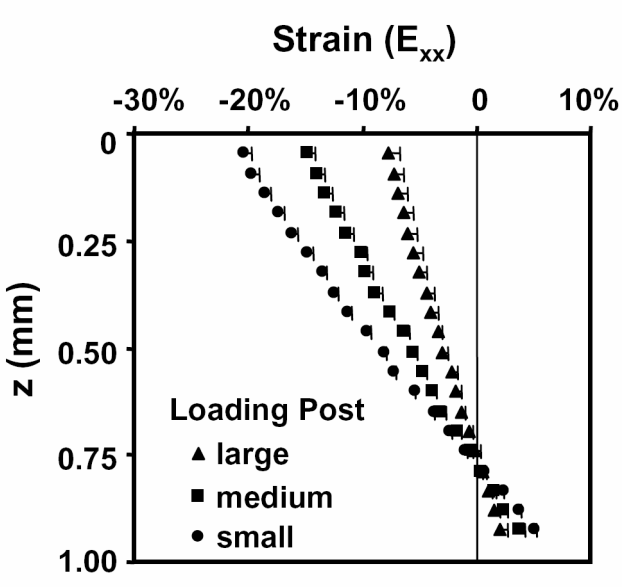

Figure 3.5: Effect of loading post size (and consequently radius of curvature) on longitudinal strain profiles (E_{xx}) of cartilage specimens. Mean ± SEM; n=7.

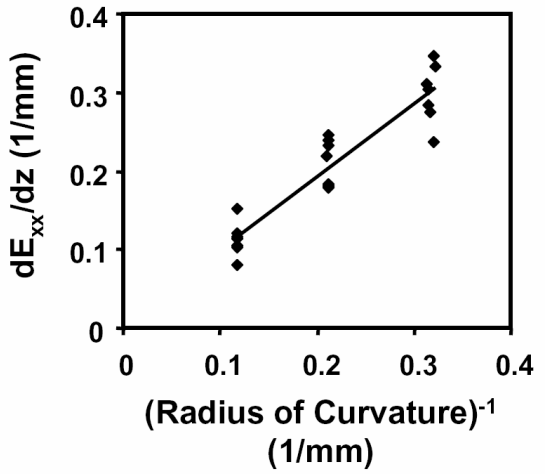

Figure 3.6: Relationship between the inverse of the radius of curvature at the neutral axis and the slope of the longitudinal strain profile (dE_{xx}/dz) for cartilage specimens.

Bimodular Model Predictions

Mean values of E_+ and E_- for calf articular cartilage and alginate (**Table 3.1**) were substituted into Equation (1) to predict the neutral axis location in samples with the same average thicknesses as those used in the experiment. The bimodular model predicted that the cartilage neutral axis would be 0.71 mm from the concave surface (**Table 3.1**). On the other hand, the alginate neutral axis was predicted to be more centrally located at 0.61 mm.

Table 3.1: Predicted neutral axis locations for cartilage and alginate modeled as bimodular elastic materials in pure bending versus the experimentally measured locations. Mechanical property input parameters (equilibrium tensile moduli, E_+, and unconfined compression moduli, E_-) were measured or obtained from [3, 12, 30]. Mean ± SEM.

Material	Tensile Modulus, E_+	Compressive Modulus, E_-	Modeled Neutral Axis	Measured Neutral Axis
cartilage	3.0 ± 1.0 MPa	0.5 ± 0.2 MPa	0.71 mm	0.75 ± 0.02 mm
alginate	4.1 ± 0.4 kPa	1.9 ± 0.1 kPa	0.61 mm	0.53 ± 0.02 mm

3.5 Discussion

The results of the micromechanical strain analysis support the hypothesis that tension-compression nonlinearity plays an important role in determining the flexural biomechanics of cartilage. The observed asymmetry in the longitudinal normal strain, E_{xx}, with the neutral axis being closer to the tensile surface, is consistent with the known material properties of cartilage (i.e. stiffer in tension than compression) and the necessary force balance within each sample. In contrast to the strain asymmetry of cartilage, alginate, a hydrogel with similar tensile and compressive moduli, exhibited a nearly symmetrical strain state.

Further support for the effects of T-C nonlinearity was provided by modeling cartilage and alginate as bimodular elastic materials in pure bending. The use of a model of pure beam bending was justified by several features consistent with the experimental flexure test, including uniform circular deformation, linear longitudinal strains, minimal shear strains, and a relationship between the bending radius of curvature and the slope of the longitudinal strain profile equal to ~1. The neutral axis locations predicted by the model were similar to those measured experimentally, suggesting that the bimodular simplification of T-C nonlinearity is a useful first approximation for the materials in these tests.

Articular cartilage exhibits depth-dependent inhomogeneity of tensile and compressive properties which could influence flexural mechanics depending on the sample preparation and orientation of bending [18, 25]. In this study, the superficial tissue including the articular surface (~0.5 mm) was removed from the cartilage to aid in preparation of uniformly flat strips and also to avoid a region where highly varying properties exist [2, 19]. Significant effects of inhomogeneity on flexural strains were excluded by testing paired samples in opposing orientations. However, the potential

effects of inhomogeneity on bending mechanics may be an important consideration for other sources or preparations of cartilaginous tissues.

Testing cartilage in flexure enables simultaneous observation of mechanical behavior over a wide range of tensile and compressive strains. Quantification of the apparent Poisson's ratio, ν_{xz}, of cartilage in both compression and tension was possible in a single test. The measured value of ν_{-xz} (0.32 ± 0.03) is similar to values (0.22-0.25 ± 0.05) previously obtained from unconfined compression of calf cartilage in the anterior-posterior and medial-lateral directions [12, 28]. Likewise, the measured ν_{+xz} (0.78 ± 0.11) is also consistent with published values of Poisson's ratios in tension (~0.5-2) for bovine and human articular cartilage [7, 8, 10, 34]. Calculation of these Poisson's ratios assumes uniaxial loading in the ROI without significant contact pressure from the loading post, which would otherwise act to decrease E_{zz}, near the concave surface, and correspondingly decrease ν_{-xz}. Since neither a shallowing of the profile of E_{zz} near the concave surface nor a comparably low ν_{-xz} was observed, the assumption of negligible contact pressure appears justified.

The range of tensile and compressive strains imposed on the samples can also be controlled during bending by varying the size of the loading post. Thus, modulating the post-size could provide information about nonlinear stress-strain behavior, with a shift in the neutral axis location indicating a relative change in the compressive and tensile moduli over the difference in the ranges of strain. There were no significant differences between the cartilage neutral axis locations using the three loading post-sizes to support previous reports of compressive stress-softening. The bending experiments may not have been sufficiently sensitive to detect subtle shifts of the neutral axis produced by such phenomenon, which may be small in magnitude [12] or limited to a narrow range of compressive strains (~0-5%) [6]. However, additional

flexure tests, particularly if done with multiple deformation states and in other planes (e.g. x-y, y-z), may have further utility in validating constitutive models of nonlinear and anisotropic cartilage behavior.

The techniques developed in this study may have applications in research involving other types of cartilage and soft tissues. For instance, quantification of the failure strain in flexure of engineered cartilage may be a useful functional measure for therapies targeting ear and nose reconstruction where bending is expected. Previous investigation of flexural failure in engineered auricular cartilage has been limited to marking lines on the tissue surface and qualitatively observing displacements [16]. By tracking ink microdots sprayed on the surface of arterial segments, a process similar to that presented here albeit at a coarser resolution, flexural strains have been measured to determine the mechanical properties of arterial wall layers [35]. Flexural strains have also been examined in comparisons of native and bioprosthetic aortic valve leaflets by analysis of banding patterns produced by polarized light microscopy [27]. Previous validation of the strain analysis algorithm used in the current study found maximum errors of ~1% strain for large deformations [13], making it an attractive technique for these types of applications.

The results of this study help elucidate the equilibrium distribution of strain within cartilage during simple flexure. Since the deformation applied during these tests mimicked that used previously for inducing alterations in cartilage explant shape, the findings are directly relevant to understanding the reshaping process [31]. Specifically, these results identify regions of tissue predominantly loaded in tension or compression and non-uniform volumetric changes which may differentially mediate cartilage shape change during *in vitro* culture. The characterization of the biomechanical state of these explants may facilitate further examination of the

mechanisms of cartilage reshaping as this technology is developed for bioengineering shaped chondral tissues.

3.6 Acknowledgments

Chapter 3, in full, is reproduced from *Journal of Biomechanics*, volume 42, number 3, 2009 with permission from Elsevier, Inc. The dissertation author was the primary author and thanks co-authors Kenneth R. Gratz and Robert L. Sah. This work was supported in part by grants from NIH, NSF, and HHMI through the HHMI Professors Program (to UCSD in support of RLS). Individual support was received through a NSF Graduate Research Fellowship (to GMW). The author thanks Dr. Albert Chen and Mr. Man Nguyen for technical assistance during this project.

3.7 References

1. Akizuki S, Mow VC, Muller F, Pita JC, Howell DS, Manicourt DH: Tensile properties of human knee joint cartilage: I. influence of ionic conditions, weight bearing, and fibrillation on the tensile modulus. *J Orthop Res* 4:379-92, 1986.

2. Asanbaeva A. Cartilage growth and remodeling: modulation of growth phenotype and tensile integrity. PhD Thesis. La Jolla: University of California, San Diego; 2006.

3. Asanbaeva A, Tam J, Schumacher BL, Klisch SM, Masuda K, Sah RL: Articular cartilage tensile integrity: Modulation by matrix depletion is maturation-dependent. *Arch Biochem Biophys* 474:175-82, 2008.

4. Bae WC, Lewis CW, Levenston ME, Sah RL: Indentation testing of human articular cartilage: effects of probe tip geometry and indentation depth on intra-tissue strain. *J Biomech* 39:1039-47, 2006.

5. Beer F, Johnston E, DeWolf J. Mechanics of Materials. 4th ed. New York: McGraw Hill; 2006.

6. Chahine NO, Wang CC, Hung CT, Ateshian GA: Anisotropic strain-dependent material properties of bovine articular cartilage in the transitional range from tension to compression. *J Biomech* 37:1251-61, 2004.

7. Chang DG, Lottman LM, Chen AC, Schinagl RM, Albrecht DR, Pedowitz RA, Brossman J, Frank LR, Sah RL: The depth-dependent, multi-axial properties of aged human patellar cartilage in tension. *Trans Orthop Res Soc* 24:644, 1999.

8. Charlebois M, McKee MD, Buschmann MD: Nonlinear tensile properties of bovine articular cartilage and their variation with age and depth. *J Biomech Eng* 126:129-37, 2004.

9. Donner A: Linear regression analysis with repeated measurements. *Journal of Chronic Diseases* 37:441-8, 1984.

10. Elliott DM, Narmoneva DA, Setton LA: Direct measurement of the Poisson's ratio of human patella cartilage in tension. *J Biomech Eng* 124:223-8, 2002.

11. Farhadi J, Fulco I, Miot S, Wirz D, Haug M, Dickinson SC, Hollander AP, Daniels AU, Pierer G, Heberer M, Martin I: Precultivation of engineered human nasal cartilage enhances the mechanical properties relevant for use in facial reconstructive surgery. *Ann Surg* 244:978-85; 2006.

12. Ficklin T, Thomas G, Barthel JC, Asanbaeva A, Thonar EJ-MA, Masuda K, Chen AC, Sah RL, Davol A, Klisch SM: Articular cartilage mechanical and biochemical property relations before and after in vivo growth. *J Biomech* 40:3607-14, 2007.

13. Gratz KR, Wong BL, Bae WC, Sah RL: The effects of focal articular defects on intra-tissue strains in the surrounding and opposing cartilage. *Biorheology* 45:193-207, 2008.

14. Grellmann W, Berghaus A, Haberland EJ, Jamali Y, Holweg K, Reincke K, Bierogel C: Determination of strength and deformation behavior of human cartilage for the definition of significant parameters. *J Biomed Mater Res A* 78:168-74, 2006.

15. Guilak F, Sah RL, Setton LA: Physical regulation of cartilage metabolism. In: *Basic Orthopaedic Biomechanics,* ed. by VC Mow, Hayes WC, Raven Press, New York, 1997, 179-207.

16. Jian-Wei X, Randolph MA, Peretti GM, Nazzal JA, Roses RE, Morse KR, Yaremchuk MJ: Producing a flexible tissue-engineered cartilage framework using expanded polytetrafluoroethylene membrane as a pseudoperichondrium. *Plast Reconstr Surg* 116:577-89, 2005.

17. Jones R: Apparent flexural modulus and strength of multimodulus materials. *Journal of Composite Materials* 10:342-54, 1976.

18. Kempson GE, Freeman MAR, Swanson SAV: Tensile properties of articular cartilage. *Nature* 220:1127-8, 1968.

19. Klein TJ, Chaudhry M, Bae WC, Sah RL: Depth-dependent biomechanical and biochemical properties of fetal, newborn, and tissue-engineered articular cartilage. *J Biomech* 40:182-90, 2007.

20. Laasanen M, Toyras J, Korhonen R, Rieppo J, Saarakkala S, Nieminen M, Hirvonen J, Jurvelin JS: Biomechanical properties of knee articular cartilage. *Biorheology* 40:133-40, 2003.

21. Lambert RK, Baile EM, Moreno R, Bert J, Pare PD: A method for estimating the Young's modulus of complete tracheal cartilage rings. *J Appl Physiol* 70:1152-9, 1991.

22. LeRoux MA, Guilak F, Setton LA: Compressive and shear properties of alginate gel: effects of sodium ions and alginate concentration. *J Biomed Mater Res* 47:46-53, 1999.

23. Mow VC, Kuei SC, Lai WM, Armstrong CG: Biphasic creep and stress relaxation of articular cartilage in compression: theory and experiment. *J Biomech Eng* 102:73-84, 1980.

24. Roy R, Kohles SS, Zaporajan V, Peretti GM, Randolph MA, Xu JW, Bonassar LJ: Analysis of bending behavior of native and engineered auricular and costal cartilage. *J Biomed Mater Res* 68A:597-602, 2004.

25. Schinagl RM, Gurskis D, Chen AC, Sah RL: Depth-dependent confined compression modulus of full-thickness bovine articular cartilage. *J Orthop Res* 15:499-506, 1997.

26. Soltz MA, Ateshian GA: A conewise linear elasticity mixture model for the analysis of tension-compression nonlinearity in articular cartilage. *J Biomech Eng* 122:576-86, 2000.

27. Vesely I, Boughner D: Analysis of the bending behaviour of porcine xenograft leaflets and of neutral aortic valve material: bending stiffness, neutral axis and shear measurements. *J Biomech* 22:655-71, 1989.

28. Wang CC, Chahine NO, Hung CT, Ateshian GA: Optical determination of anisotropic material properties of bovine articular cartilage in compression. *J Biomech* 36:339-53, 2003.

29. Wang CC, Deng JM, Ateshian GA, Hung CT: An automated approach for direct measurement of two-dimensional strain distributions within articular cartilage under unconfined compression. *J Biomech Eng* 124:557-67, 2002.

30. Williams GM, Klein TJ, Sah RL: Cell density alters matrix accumulation in two distinct fractions and the mechanical integrity of alginate-chondrocyte constructs. *Acta Biomaterialia* 1:625-33, 2005.

31. Williams GM, Lin JW, Sah RL: Cartilage reshaping via in vitro mechanical loading. *Tissue Eng* 13:2903-11, 2007.

32. Williamson AK, Chen AC, Masuda K, Thonar EJ-MA, Sah RL: Tensile mechanical properties of bovine articular cartilage: variations with growth and relationships to collagen network components. *J Orthop Res* 21:872-80, 2003.

33. Williamson AK, Chen AC, Sah RL: Compressive properties and function-composition relationships of developing bovine articular cartilage. *J Orthop Res* 19:1113-21, 2001.

34. Woo SL-Y, Lubock P, Gomez MA, Jemmott GF, Kuei SC, Akeson WH: Large deformation nonhomogeneous and directional properties of articular cartilage in uniaxial tension. *J Biomech* 12:437-46, 1979.

35. Yu Q, Zhou J, Fung YC: Neutral axis location in bending and Young's modulus of different layers of arterial wall. *Am J Physiol* 265:H52-60, 1993.

CHAPTER 4

IN VITRO MODULATION OF CARTILAGE SHAPE PLASTICITY BY BIOCHEMICAL REGULATION OF MATRIX REMODELING

4.1 Abstract

With consideration of the need for cartilage grafts in orthopedic and craniofacial surgery, explants of immature cartilage have recently been molded *in vitro* and *in vivo* to achieve desired shapes. Nonsurgical correction of cartilage deformities and malformations often use mechanical stimuli to alter the shapes of cartilaginous structures and further demonstrate the malleability of cartilage. Largely through anecdotal evidence, the plasticity of cartilage shape is believed to diminish with maturation, coincident with changing matrix composition. The objectives of this study were to characterize the shape plasticity of articular cartilage from immature and mature bovines and test whether shape plasticity can be modulated by altering proteoglycan (PG) and collagen (COL) remodeling *in vitro*. Cartilage explants were cultured in the presence of either β-D-xyloside to suppress glycosaminoglycan (GAG) accumulation or β-aminopropionitrile (BAPN) to inhibit lysyl oxidase-mediated collagen crosslinking and then assessed for altered size, matrix composition, and shape plasticity. The results indicate that culture with β-D-xyloside and BAPN

differentially regulate cartilage growth, composition, and shape plasticity. There was an inverse association between shape plasticity and the amount of COL relative to GAG in the cartilage matrix. The findings provide quantitative measures of articular cartilage shape plasticity at immature and mature stages of development and are consistent with the concept of diminishing shape plasticity with maturation. The ability to modulate cartilage size, composition and shape plasticity by varying *in vitro* biochemical conditions may be a useful tool in the development of shaped cartilage grafts for orthopedic and craniofacial therapies.

4.2 Introduction

In the fields of orthopaedic and craniofacial surgery, cartilage grafts of desired shapes and sizes are therapeutically useful for replacing or augmenting tissues compromised by injury, disease, or malformation. Focal articular cartilage lesions may be treated by autologous or allogeneic osteochondral grafts with careful attention to matching the normal joint contours and to filling the defect [7, 13]. Likewise for surgical reconstruction of the ear or nose, grafts of costal, auricular, or septal cartilage are routinely shaped through skillful carving, suturing, and scoring [25]. Emerging technologies in cartilage tissue engineering may address some of biomedical need for cartilage grafts, but tools and techniques are required to ensure that cartilage constructs can be created with desired shapes [28]. Recently, it was proposed that cartilage grafts could be contoured using mechanical stimuli *in vitro*, and static flexural deformation was shown to induce change in the shape of immature articular cartilage explants during short (<1 week) cultures [30]. Extending this concept to an *in vivo* application, a resorbable template was used to guide the reshaping of autologous costal cartilage grafts following subcutaneous implantation in rabbits [19]. These studies demonstrate the plasticity of cartilage shape, defined as the ability to change free-swelling conformation through mechanically guided remodeling.

The application of mechanical stimuli to alter the forms of developing cartilaginous structures is a technique which as has long been used by some clinicians to nonsurgically correct malformations and deformities. Examples include the treatment of hip dysplasia through external harnessing [11], of club foot by manipulation and casting [6], of cleft palate by nasoalveolar molding [12], and of ear deformity by splinting [27]. Among these procedures, a commonly practiced philosophy is that outcomes are better when the corrections are attempted early during

neonatal life. However, the mechanisms by which these procedures produce corrections in cartilage shape and their dependence on maturation remain somewhat speculative. In a study of club foot correction, changes in the shape of cartilage anlagen were observed immediately following manipulation and were maintained upon cast removal a week later leading the authors to hypothesize that cartilage matrix collagens (COL) and proteoglycans (PG) remodel to accommodate these structural changes [6]. Similarly, the high shape plasticity of auricular and nasal cartilage in early neonates has been hypothesized to result from an estrogen-induced abundance of hyaluronic acid and PG in the tissues, which facilitate remodeling during mechanical correction [12, 16, 27].

During *in vivo* growth and maturation, changes occur in the predominant components of articular cartilage including an increase in COL concentration and a maintenance or slight decrease in PG concentration [31, 32]. In turn, this change in matrix composition alters functional properties as indicated by increasing compressive and tensile stiffness with maturation [31, 32]. *In vitro* growth studies of immature articular cartilage have also shown that regulation of cartilage matrix metabolism and remodeling can modulate matrix composition and functional properties. The results of such studies suggest that a balance of PG and COL remodeling is a key determinant of *in vitro* volumetric growth, cartilage composition, and tensile integrity [3, 4]. However, it is undetermined how cartilage shape plasticity may be affected by similar *in vitro* modulation of matrix composition.

Specific biochemical agents can be used in cartilage explant culture to selectively alter PG and COL remodeling. β-D-xyloside acts as an exogenous substrate for the initiation of free chondroitin sulfate synthesis, the major glycosaminoglycan (GAG) of cartilage aggregating PG [17]. When added to cultures of chondrogenic

cells, β-D-xyloside competes with PG core protein for chondroitin sulfate synthesis [22]. Consequently, the newly synthesized PG incorporated into the matrix is significantly depleted of GAG, while soluble GAG chains synthesized on β-D-xyloside readily diffuse from the tissue [15]. In addition, COL remodeling can be perturbed using β-aminopropionitrile (BAPN), an inhibitor of lysyl oxidase-mediated COL crosslinking [24]. In cartilage explant cultures, BAPN inhibits the formation of difunctional COL crosslinks and consequently impairs the chemical stabilization of the COL network [1, 3, 8].

This study was conducted to help elucidate the relationship between cartilage composition and shape plasticity and to further the development of techniques for manipulating the shape of cartilage grafts. Specifically, this study tests the hypothesis that the shape plasticity of immature and mature articular cartilage may be modulated *in vitro* by altering the balance of PG and COL remodeling.

4.3 Materials and Methods

Experimental Design

Articular cartilage explants from calf and young adult bovines were analyzed fresh on day 0 (d0) or after being cultured for 14 days (d14) in the presence of BAPN or a β-D-xyloside, *p*-nitrophenyl-β-D-xylopyranoside (PNPX). Some explants were analyzed for changes in tissue size and matrix composition. Other explants were assessed for shape plasticity by application of flexural deformation during additional culture.

Sample Preparation and Culture

Samples were prepared from bovine stifle joints obtained from an abattoir as previously described [30]. Articular cartilage blocks were harvested from the patellofemoral grooves of two calves (1-3 weeks old) and two young adults (1-2 years old). The superficial ~0.3 mm of cartilage including the curvilinear articular surface was removed using a vibrating microtome and discarded. An adjacent flat slice of cartilage was then removed and punched into strips measuring ~10 mm x 2 mm. Cartilage strips, ~1 mm thick, were divided at intervals along the length to produce three site-matched explants for analysis of growth and matrix composition. The different growth rates among conditions (see results) necessitated that cartilage strips intended for shape plasticity analysis be cut to different initial thicknesses (~0.6-1 mm for calf and ~1 mm for adult) to target a uniform ~1 mm thickness among all conditions at the time flexure was applied. Each explant was weighed and measured for thickness using a non-contacting laser micrometer before and after culture.

Cartilage explants were cultured for 14 days in non-tissue culture treated plates to limit cell outgrowth. Explants were kept in ~70x tissue volume of basal medium with 20% fetal bovine serum (FBS) and either 0.2 mM BAPN or 1 mM PNPX. Basal medium consisted of Dulbecco's Modified Eagle's Medium supplemented with 100 μg/ml ascorbate, 0.1 mM nonessential amino acids, 0.4 mM L-proline, 2 mM L-glutamine, 10 mM HEPES, 100 U/ml penicillin, 100 μg/ml streptomycin, and 0.25 μg/ml amphotericin B. Cultures were placed in standard incubators with 5% CO_2 atmosphere at 37°C, and the medium was changed every other day. Samples of spent medium were saved for biochemical analysis.

Biochemical Analysis

The site-matched explants, consisting of one sample from each of the d0 control, d14 BAPN, and d14 PNPX groups, were lyophilized and weighed dry to determine water content as a percent of final wet weight. Samples were then digested with a solution of proteinase K (Roche Diagnostics, Indianapolis, IN) for analysis of cartilage matrix and chondrocyte content. Alternatively, some samples were extracted with a solution of 4 M guanidine, 50 mM sodium acetate, 10 mM dithiothreitol, and PIs at 20x tissue volume for 24 hours at 4°C. Samples were rinsed once in PBS+PIs for 1 hour and the rinse solution was added to the extract. Extracts were dialyzed against water (molecular weight cutoff = 2000) and then the extracts and residual extracted tissue were digested with proteinase K. Digests were assayed for sulfated GAG [9] and hydroxyproline [33]. Collagen content was determined from hydroxyproline using a ratio of 7.25 g COL/ g hydroxyproline [14, 18]. Matrix constituents in the tissue were normalized to initial tissue wet weight (WW_i) to indicate constituent content and to the final wet weight (WW_f) to indicate constituent concentration at the end of culture. Spent medium samples were pooled for each sample and assayed for GAG released by the explants during culture. The released GAG data were also normalized to either WW_i or WW_f.

Shape Plasticity Analysis

Assessment of cartilage shape plasticity was based on a previous study examining mechanically-induced changes in cartilage shape via culture of cartilage strips subjected to static flexure [30]. Prior to shape analysis, cartilage strips cultured in medium with BAPN or PNPX were thoroughly washed (6 times over 2 hours) in

basal medium to remove residual treatment agents. Using custom bioreactors, fresh and cultured cartilage strips were subjected to static flexural deformations and further cultured with basal medium and 2% FBS for 4 days (calf) or 8 days (adult). These loading durations were determined from pilot studies and differed in order to provide better sensitivity of measured cartilage shape plasticity.

Specimen shape was documented by digital photography in the free-swelling state prior to the application of flexure (initial shape) and at culture termination while loaded (imposed shape) and following 2 hours of stress relaxation (relaxed shape) by free-swelling in phosphate-buffered saline (PBS) with protease inhibitors (PIs) at 4°C (**Fig. 4.1**). Specimen shape was quantified as an opening angle (γ) using Image J (NIH, Bethesda, MD), and the shape retention [%], a measure of cartilage shape plasticity, was calculated as $((\gamma_{initial} - \gamma_{relaxed})/ (\gamma_{initial} - \gamma_{imposed}))\cdot 100$ [30].

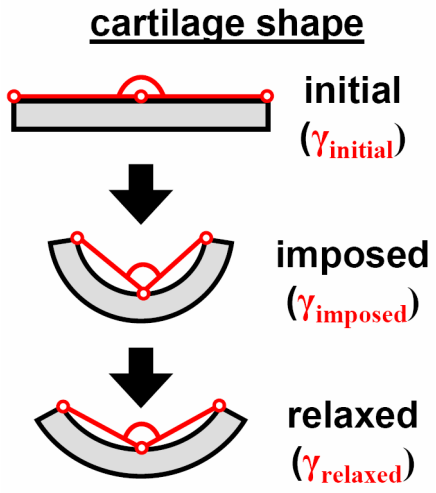

Figure 4.1: Shape plasticity was determined as the retention of a mechanically imposed deformation by cartilage explants. Specimen shape was quantified as an opening angle (indicated in red) at three different stages: initial ($\gamma_{initial}$) measured prior to the deformation application, imposed ($\gamma_{imposed}$) measured at culture termination, and relaxed ($\gamma_{relaxed}$) measured after unloading and stress relaxation.

Statistical Analysis

Data are presented as means ± SE. For each tissue maturity level (calf and adult), data were analyzed by ANOVA for the effect of culture condition on biochemical composition, shape retention, and changes in size. For composition and size data, site of matched explants was treated as a random factor; whereas, animal was treated as a random factor for shape data. Tukey post-hoc analysis was used to make individual comparisons between d0, d14 BAPN, and d14 PNPX groups. The significance criterion, α, was set at 0.05 for all tests.

4.4 Results

Growth of Cultured Cartilage Explants

Growth of calf articular cartilage during 14 days of culture was significant and dependent on culture condition, while little growth of adult cartilage was measured in either condition (**Fig. 4.2**). Culture with BAPN induced larger increases in calf cartilage wet weight (+70% vs. +35%, $p<0.001$) and thickness (+67% vs. +39%, $p<0.001$) than PNPX. Similar magnitudes of change in the wet weights and thicknesses of calf samples indicated that growth was primarily attributable to expansion in the thickness direction, corresponding to the articular surface-normal direction. In the adult cartilage cultures, PNPX treatment did not produce significant changes in either wet weight or thickness ($p=0.09$ and 0.43, respectively); whereas, BAPN treatment produced small but significant increases in wet weight (+7%, $p<0.001$) and thickness (+3%, $p<0.05$).

To account for the different magnitudes of growth between treatments, cartilage strips used for shape plasticity analysis were cut to slightly different initial

thicknesses (~0.6-1.00 mm). At the time flexural deformations were applied, the thickness of cartilage strips was found to be similar between conditions for calf and adult samples. This was an important consideration to ensure that samples received similar mechanical deformations, since sample thickness has been shown to be an important determinant of the strain distributions resulting from flexure [29].

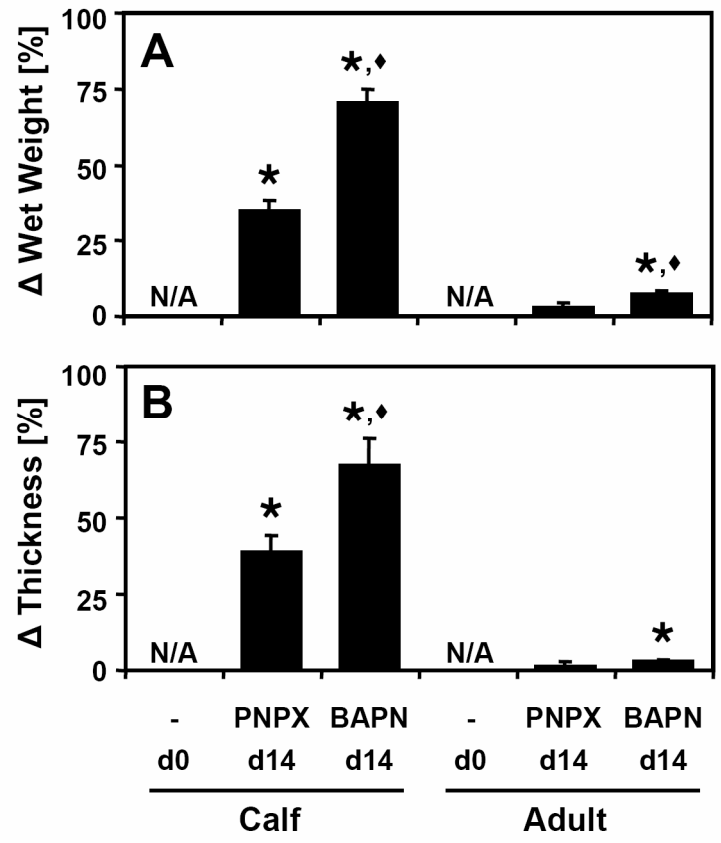

Figure 4.2: Change in (**A**) wet weight and (**B**) thickness for calf and adult articular cartilage explants cultured for 14 days with PNPX or BAPN. For each maturity level, ★ indicates $p<0.05$ versus zero (i.e. no change), and ♦ indicates $p<0.05$ for BAPN vs. PNPX. Mean ± SE; n=10.

Effects of PNPX and BAPN on Cartilage Matrix Composition

The remodeling of cartilage matrix during culture was differentially regulated by treatment with PNPX and BAPN (**Fig. 4.3**). The water content of calf cartilage was increased during culture with PNPX (+1.7%, $p<0.01$) and with BAPN (+3.6%, $p<0.001$) and was significantly higher in the BAPN group compared to PNPX ($p<0.005$). Total COL content in calf cartilage was increased during culture with PNPX (+14%, $p<0.001$) and with BAPN (+16%, $p<0.001$) but did not differ between the two treatments. Accounting for changes in tissue wet weight during culture, final COL concentration in the calf cartilage decreased during culture with PNPX (-16%, $p<0.01$) and with BAPN (+31%, $p<0.001$) and was lower in the BAPN treatment group ($p<0.05$). GAG content in the calf tissue was also increased during culture with PNPX (+43%, $p<0.001$) and with BAPN (+80%, $p<0.001$) and was higher in the BAPN-treated samples ($p<0.001$). The final GAG concentration in calf explants was not affected by culture condition ($p=0.49$). Reflecting the changes in cartilage matrix constituents, the ratio of COL to GAG in calf cartilage was lowered from d0 with PNPX treatment (1.6 ± 0.2 vs. 1.3 ± 0.1, $p<0.01$) and reduced even further with BAPN treatment (1.1 ± 0.1, $p<0.001$ vs. d0, $p<0.05$ vs. PNPX).

In many measures, the dynamics of matrix composition were affected differently in adult cartilage. Culture condition had no effect on the hydration ($p=0.32$), COL content ($p=0.22$), or COL concentration ($p=0.05$) of adult cartilage explants. However, GAG content of adult cartilage was decreased during culture with PNPX (-20%, $p<0.01$) but increased with BAPN (+14%, $p<0.05$). The final concentration of GAG in the tissue was also decreased with PNPX (-22%, $p<0.01$) but not significantly altered by BAPN ($p=0.33$). Both GAG content and concentration were higher in the adult BAPN-treated samples than in those cultured with PNPX

($p<0.001$). Consequently, the ratio of COL to GAG was lower in the BAPN condition versus PNPX (4.4 ± 0.3 vs. 6.7 ± 1.1, $p<0.05$), but did not significantly deviate from that of d0 adult samples with either culture condition (5.3 ± 0.6, $p>0.24$).

Additional biochemical analyses were performed as checks on the efficacy of culture treatments. The percent of tissue COL which was extractable under dissociative conditions was examined (**Fig. 4.3C**). For both calf and adult cartilage, extractable COL was higher in the BAPN-treated samples than in either PNPX-treated or d0 samples ($p<0.05$, for all). Additionally, spent culture medium was examined for GAG released from cartilage explants (**Fig. 4.4**). Calf and adult cartilage cultured with PNPX released greater amounts of GAG into the medium than with BAPN treatment ($p<0.001$, for all). When normalized to the initial wet weight of explants and culture duration, calf cartilage released GAG at rates of 2.8 mg/[g WW_i*day] with PNPX and 1.0 mg/[g WW_i*day] with BAPN. Similarly, adult cartilage released GAG at rates of 1.7 mg/[g WW_i*day] with PNPX and 1.0 mg/[g WW_i*day] with BAPN.

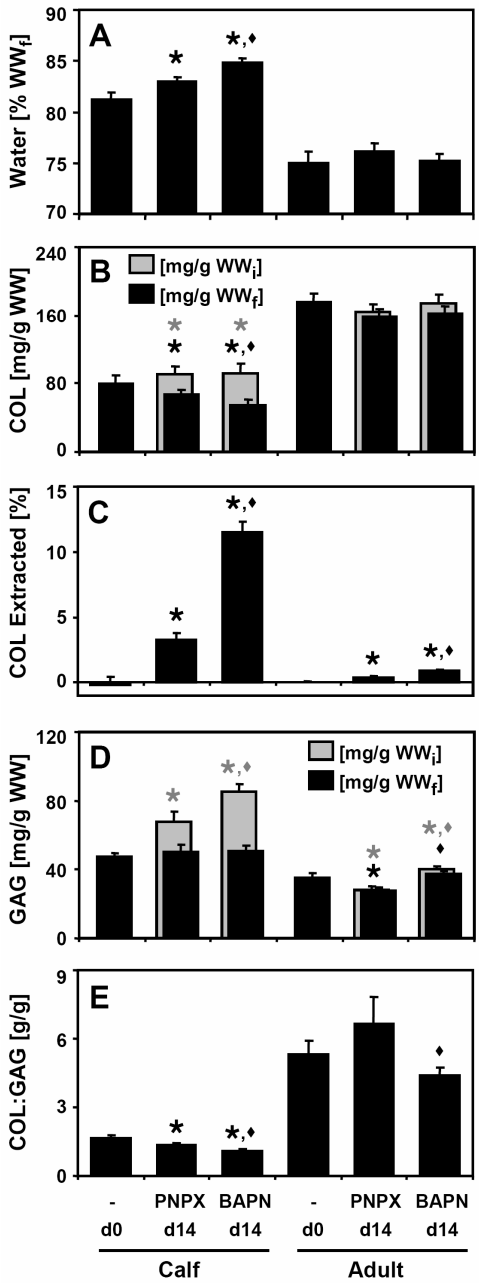

Figure 4.3: Effect of culture condition on cartilage matrix composition including (**A**) water, (**B**) total tissue COL, (**C**) the percent of total tissue COL extracted under dissociative conditions, (**D**) total tissue GAG, and (**E**) the ratio of tissue COL to GAG. Tissue COL and GAG are normalized to initial wet weight (WW_i, gray bars) to indicate constituent content or to final wet weight (WW_f, black bars) to indicate final concentration in the tissue (except for d0, where $WW_i = WW_f$). and are also presented. For each maturity level, ✱ indicates $p<0.05$ versus d0, and ♦ indicates $p<0.05$ for BAPN vs. PNPX. Mean ± SE; (**A, B, D, E**) n=10 and (**C**) n=4-5.

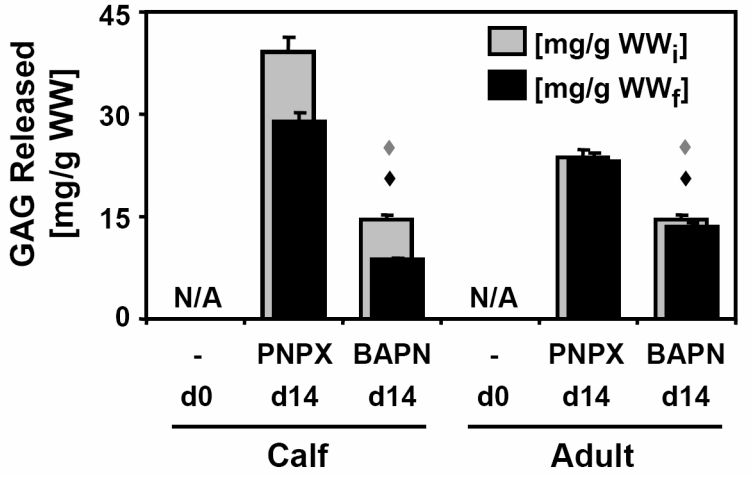

Figure 4.4: Effect of culture condition on the total GAG released into the medium by calf and adult cartilage explants. Data are normalized to initial tissue wet weight (WW_i, gray bars) or to final wet weight (WW_f, black bars). For each maturity level, ♦ indicates $p<0.05$ for BAPN vs. PNPX. Mean ± SE; n=10.

Effects on Cartilage Shape Plasticity

The retention of a mechanically imposed deformation by cartilage explants was used as a measure of shape plasticity and was found to differ with culture condition (**Fig. 4.5**). The shape retention of calf cartilage was increased by prior culture with BAPN compared to d0 samples (90 ± 2% vs. 69 ± 2%, $p<0.001$), but was maintained by culture with PNPX (74 ± 2%, $p=0.37$). BAPN-treated calf cartilage also had higher shape retention than samples cultured with PNPX ($p<0.001$). Similarly, the shape retention of adult cartilage was higher with BAPN treatment than with PNPX (54 ± 5% vs. 31 ± 8%, $p<0.01$). Culture of adult cartilage with PNPX tended to decrease shape retention versus that of d0 (42 ± 5%, $p=0.11$), and culture with BAPN tended to increase shape retention ($p=0.15$).

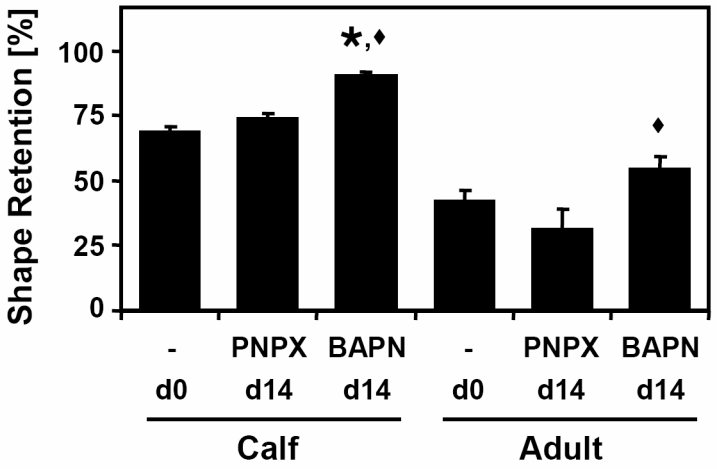

Figure 4.5: A measure of cartilage shape plasticity was determined as the percent of the mechanically-imposed shape which was retained following unloading. For each maturity level, ★ indicates $p<0.05$ versus d0, and ♦ indicates $p<0.05$ for BAPN vs. PNPX. Mean ± SE; n=9-10.

4.5 Discussion

The findings of this study provide a quantitative characterization of the shape plasticity of calf and adult bovine articular cartilage, based on the *in vitro* application of mechanical deformations. In addition, alteration of PG or COL remodeling differentially modulated the growth, matrix composition, and shape plasticity of cartilage explants. Changes in the concentration of COL relative to GAG (COL:GAG ratio) were inversely associated with trends in shape plasticity. This finding appears consistent with recent experimental and theoretical work which indicates that COL-GAG interactions may modulate cartilage mechanical properties during maturation [5, 26]. It has been postulated that a highly compliant matrix in immature cartilage may allow for tissue expansion during periods of growth [26]. Expanding on this concept, the results of this study suggest that the high shape plasticity of immature cartilage may facilitate tissue conformational changes during development.

Development of the experimental design required consideration of a number of factors which may influence the results and their interpretation. The dose of 0.2 mM BAPN was a choice supported by previous studies that found doses of BAPN of 0.1-0.25 mM in cultures of bovine articular cartilage inhibit crosslink formation with minimal cytotoxicity or alteration of PG synthesis and incorporation [1-3, 8]. In this and previous studies, a marked increase in extractable tissue COL with BAPN treatment was indicative of the efficacy of crosslink inhibition [2, 8]. A dose of 1 mM β-D-xyloside has been previously shown to produce near maximal stimulation of chondroitin sulfate synthesis in cultures of chick sternal chondrocytes and chondrogenic limb bud mesenchymal cells [15, 23]. It was also found that mesenchymal cells chronically cultured with 1 mM β-D-xyloside produce a matrix greatly depleted of GAG but only slightly depleted of COL, consistent with a small

decrease in total protein synthesis [15]. In this study, lower tissue GAG contents and higher rates of GAG release into the medium of PNPX-treated cultures are consistent with the formation of soluble, β-D-xyloside-initiated GAG chains at the expense of GAG chain synthesis on PG. Both treatment agents were subsequently washed from explants prior to the application of flexural deformations in order to evaluate shape plasticity under similar conditions.

Immature articular cartilage was observed to have a higher degree of shape plasticity than mature cartilage, though these findings were not directly compared via statistical analysis. The trend of decreased shape plasticity with increased cartilage maturation is consistent with the clinical wisdom of correcting cartilage deformities at an early age [11, 12, 27]. One reason for not comparing between the maturity levels was that shape plasticity deformations were applied over 4 days for calf cartilage and 8 days for adult cartilage in order to improve the sensitivity of the assessment for each group. Previously, it was found that the shape retention increased with loading time for calf cartilage explants [30], and this trend was also found with adult cartilage in preliminary tests. This suggests that shape retention results would be even more disparate between calf and adult cartilage if the assays had been conducted for the same duration.

Medium supplementation with 20% FBS was used to stimulate PG and COL anabolism above basal levels, as shown by previous studies [4, 20]. However, the effects of FBS on the composition of calf and adult cartilage have been shown to differ. Culture with 20% FBS stimulates calf cartilage to grow by accumulating GAG in excess of COL and also results in a reduction of compressive stiffness and tensile integrity [4, 10, 20]. On the other hand, 20% FBS is more homeostatic in adult cartilage culture with GAG, COL, and compressive stiffness being maintained [20,

21]. This maturation-dependent metabolic activity could explain some of the different trends observed in cartilage matrix composition between calf and adult cultures. For example, the reduced accumulation of GAG in calf PNPX-treated samples and loss of GAG in the corresponding adult samples are consistent with the differential effects of 20% FBS stimulation combined with suppression of GAG accumulation by β-D-xyloside.

Additional preliminary studies were conducted to distinguish the role of BAPN in altering cartilage shape plasticity. In light of the maturation dependent effects of FBS on cartilage PG and COL remodeling, a 20% FBS culture group was not considered a proper control group for the stated hypothesis; instead, fresh day 0 samples were used. However, pilot studies were conducted with 20% FBS control samples, and changes in explant size and matrix composition (i.e. content and concentration of COL and GAG) were very similar to samples cultured with the addition of BAPN, in accordance with the findings of others [2, 3]. Changes in shape plasticity were also nearly identical between 20% FBS control and BAPN-treated samples. Another experiment was conducted to test whether BAPN may increase cartilage shape plasticity through a build-up of COL crosslinking precursors which subsequently stabilize the imposed deformation following BAPN washout. BAPN was supplemented throughout the shape assessment, and no differences were observed versus washout or FBS control samples. Together, these findings indicate that the increase of shape plasticity in the d14 BAPN versus d0 samples is not solely the effect of BAPN but more likely that of a culture condition which promotes accumulation of PG and a weakening of the COL network.

The use of mechanical stimuli to alter cartilage shape is a potential tool for customizing cartilage grafts with applications to tissue engineering [19, 30]. The

results of this study further expand the understanding of mechanically-induced cartilage shape change and provide additional options for manipulating the process. While increasing cartilage shape plasticity may be useful for changing the shape of a graft, reducing shape plasticity may be desirable to set the shape prior to implantation. Changes in other functional properties, including the load-bearing properties, may be related to shape plasticity through the underlying dynamics of cartilage matrix composition. Since shape and biomechanical maturity may be among a number of important clinical requirements for a cartilage graft, these properties may need to be considered in a coordinated manner.

4.6 Acknowledgments

Chapter 4, in part, has been submitted for publication of the material as it may appear in *Matrix Biology*, 2009. The dissertation author was the primary author and thanks co-author Robert L. Sah. This work was supported in part by grants from NIH, NSF, and HHMI through the HHMI Professors Program (to UCSD in support of RLS). Individual support was received through a NIH Ruth L. Kirchstein Pre-Doctoral Fellowship (to GMW).

4.7 References

1. Ahsan T, Harwood FL, McGowan KB, Amiel D, Sah RL: Kinetics of collagen crosslinking in adult bovine articular cartilage. *Osteoarthritis Cartilage* 13:709-15, 2005.

2. Ahsan T, Lottman LM, Harwood FL, Amiel D, Sah RL: Integrative cartilage repair: inhibition by beta-aminoproprionitrile. *J Orthop Res* 17:850-7, 1999.

3. Asanbaeva A, Masuda K, Thonar EJ-MA, Klisch SM, Sah RL: Cartilage growth and remodeling: modulation of balance between proteoglycan and collagen in vitro with beta-aminopropionitrile. *Osteoarthritis Cartilage* 16:1-11, 2008.

4. Asanbaeva A, Masuda K, Thonar EJ-MA, Klisch SM, Sah RL: Regulation of immature cartilage growth by IGF-I, TGF-beta1, BMP-7, and PDGF-AB: role of metabolic balance between fixed charge and collagen network. *Biomech Model Mechanobiol* 7:263-76, 2008.

5. Asanbaeva A, Tam J, Schumacher BL, Klisch SM, Masuda K, Sah RL: Articular cartilage tensile integrity: Modulation by matrix depletion is maturation-dependent. *Arch Biochem Biophys* 474:175-82, 2008.

6. Brand RA, Siegler S, Pirani S, Morrison WB, Udupa JK: Cartilage anlagen adapt in response to static deformation. *Med Hypotheses* 66:653-9, 2006.

7. Bugbee WD: Osteochondral allograft transplantation. In: *Articular Cartilage Lesions: A Practical Guide to Assessment and Treatment,* ed. by BJ Cole, Malek MM, Springer, New York, 2004, 82-94.

8. DiMicco MA, Waters SN, Akeson WH, Sah RL: Integrative articular cartilage repair: dependence on developmental stage and collagen metabolism. *Osteoarthritis Cartilage* 10:218-25, 2002.

9. Farndale RW, Buttle DJ, Barrett AJ: Improved quantitation and discrimination of sulphated glycosaminoglycans by use of dimethylmethylene blue. *Biochim Biophys Acta* 883:173-7, 1986.

10. Ficklin T, Thomas G, Barthel JC, Asanbaeva A, Thonar EJ-MA, Masuda K, Chen AC, Sah RL, Davol A, Klisch SM: Articular cartilage mechanical and biochemical property relations before and after in vivo growth. *J Biomech* 40:3607-14, 2007.

11. Gabuzda GM, Renshaw TS: Reduction of congenital dislocation of the hip. *J Bone Joint Surg Am* 74:624-31, 1992.

12. Grayson BH, Maull D: Nasoalveolar molding for infants born with clefts of the lip, alveolus, and palate. *Clin Plast Surg* 31:149-58, vii, 2004.

13. Hangody L, Rathonyi GK, Duska Z, Vasarhelyi G, Fules P, Modis L: Autologous osteochondral mosaicplasty. *J Bone Joint Surg* 86-A, Supplement 1:65-72, 2004.

14. Herbage D, Bouillet J, Bernengo J-C: Biochemical and physicochemical characterization of pepsin-solubilized type-II collagen from bovine articular cartilage. *Biochem J* 161:303-12, 1977.

15. Lohmander LS, Hascall VC, Caplan AI: Effects of 4-methyl umbelliferyl-beta-D-xylopyranoside on chondrogenesis and proteoglycan synthesis in chick limb bud mesenchymal cell cultures. *J Biol Chem* 254:10551-61, 1979.

16. Matsuo K, Hirose T, Tomono T, Iwasawa M, Katohda S, Takahashi N, Koh B: Nonsurgical correction of congenital auricular deformities in the early neonate: a preliminary report. *Plast Reconstr Surg* 73:38-51, 1984.

17. Okayama M, Kimata K, Suzuki S: The influence of p-nitrophenyl beta-D-xyloside on the synthesis of proteochondroitin sulfate by slices of embryonic chick cartilage. *J Biochem* 74:1069-73, 1973.

18. Pal S, Tang L-H, Choi H, Habermann E, Rosenberg L, Roughley P, Poole AR: Structural changes during development in bovine fetal epiphyseal cartilage. *Collagen Rel Res* 1:151-76, 1981.

19. Pomahac B, Zuhaili B, Kudsi Y: Guided cartilage regeneration using resorbable template. *Eplasty* 8:e5, 2008.

20. Sah RL, Chen AC, Grodzinsky AJ, Trippel SB: Differential effects of bFGF and IGF-I on matrix metabolism in calf and adult bovine cartilage explants. *Arch Biochem Biophys* 308:137-47, 1994.

21. Sah RL, Trippel SB, Grodzinsky AJ: Differential effects of serum, insulin-like growth factor-I, and fibroblast growth factor-2 on the maintenance of cartilage physical properties during long-term culture. *J Orthop Res* 14:44-52, 1996.

22. Schwartz NB: Regulation of chondroitin sulfate synthesis. *J Biol Chem* 252:6316-21, 1977.

23. Schwartz NB, Galligani L, Ho PL, Dorfman A: Stimulation of synthesis of free chondroitin sulfate chains by beta-D-xylosides in cultured cells. *Proc Natl Acad Sci U S A* 71:4047-51, 1974.

24. Tang SS, Trackman PC, Kagan HM: Reaction of aortic lysyl oxidase with beta-aminopropionitrile. *J Biol Chem* 258:4331-8, 1983.

25. Tardy ME, Denneny J, 3rd, Fritsch MH: The versatile cartilage autograft in reconstruction of the nose and face. *Laryngoscope* 95:523-33, 1985.

26. Thomas GC, Asanbaeva A, Vena P, Sah RL, Klisch SM: A nonlinear constituent based viscoelastic model for articular cartilage and analysis of

tissue remodeling due to altered glycosaminoglycan-collagen interactions. *J Biomech Eng* 131:101002, 2009.

27. van Wijk MP, Breugem CC, Kon M: Non-surgical correction of congenital deformities of the auricle: a systematic review of the literature. *J Plast Reconstr Aesthet Surg* 62:727-36, 2009.

28. Williams GM, Chan EF, Temple-Wong MM, Bae WC, Masuda K, Bugbee WD, Sah RL: Shape, loading, and motion in the bioengineering design, fabrication, and testing of personalized synovial joints. *J Biomech* ePub:10.6.2009, 2009.

29. Williams GM, Gratz KR, Sah RL: Asymmetrical strain distributions and neutral axis location of cartilage in flexure. *J Biomech* 42:325-30, 2009.

30. Williams GM, Lin JW, Sah RL: Cartilage reshaping via in vitro mechanical loading. *Tissue Eng* 13:2903-11, 2007.

31. Williamson AK, Chen AC, Masuda K, Thonar EJ-MA, Sah RL: Tensile mechanical properties of bovine articular cartilage: variations with growth and relationships to collagen network components. *J Orthop Res* 21:872-80, 2003.

32. Williamson AK, Chen AC, Sah RL: Compressive properties and function-composition relationships of developing bovine articular cartilage. *J Orthop Res* 19:1113-21, 2001.

33. Woessner JF: The determination of hydroxyproline in tissue and protein samples containing small proportions of this imino acid. *Arch Biochem Biophys* 93:440-7, 1961.

CHAPTER 5

IGF-1 AND TGF-β1 DIFFERENTIALLY REGULATE IN VITRO GROWTH AND COMPRESSIVE PROPERTIES OF CALF ARTICULAR CARTILAGE

5.1 Abstract

Objective: To assess the effects of exogenous insulin-like growth factor 1 (IGF-1) and transforming growth factor beta 1 (TGF-β1) on geometric growth, biochemical composition, and compressive mechanical properties of cultured bovine calf articular cartilage, and to correlate biochemical and mechanical properties to help elucidate the mechanisms by which IGF-1 and TGF-β1 alter cartilage function.

Design: Bovine calf articular cartilage explants from superficial (S) and middle (M) layers were cultured for 12 days with IGF-1 or TGF-β1. Explants were analyzed for changes in size, for mechanical properties in confined (CC) and unconfined (UCC) compression, and for cartilage matrix and chondrocyte composition.

Results: Culture with IGF-1 resulted in substantially increased tissue volume, accumulation of glycosaminoglycan (GAG) and collagen (COL), softening in CC and UCC, and increased apparent Poisson's ratios. Culture with TGF-β1 produced little growth, but did promote maturational changes in the S layer, including increased concentrations of GAG, COL, and pyridinoline crosslinks (PYR) and stiffening in CC and UCC. Effects of TGF-β1 on M layer explants were more homeostatic. Across treatment groups, compressive moduli in CC and UCC were positively related to GAG and COL concentrations and negatively related to water content.

Conclusions: Anabolic growth factors IGF-1 and TGF-β1 differentially regulate the size and compressive mechanical properties of immature articular cartilage *in vitro*. Prescribing tissue growth, maturation, or homeostasis by controlling the *in vitro* biochemical environment may have applications in cartilage repair and tissue engineering.

5.2 Introduction

As articular cartilage grows and matures, it attains sufficient size and properties to function as a low-friction, wear-resistant bearing material within a joint. The bovine stifle joint provides a well-studied example of the changing biochemical composition and mechanical properties of articular cartilage during development. With progression from fetus to young adult, increasing collagen (COL) and pyridinoline crosslink (PYR) concentrations help stabilize the COL network [44, 45], providing the tissue with stiffness and strength in tension and shear [14, 32, 47]. Large aggregating proteoglycans (PG) impart a negative fixed charge density to the tissue via their glycosaminoglycan (GAG) side chains and exert a swelling pressure which provides resistance to compression [25, 32]. In contrast to COL, the concentration of GAG may be maintained or slightly decreased during maturation [44, 45]. The contributions of these matrix compositional dynamics to the mechanical function of the tissue are reflected in large increases in compressive aggregate modulus and equilibrium tensile modulus from fetus to adult [44, 45].

Insulin-like growth factor – 1 (IGF-1) and transforming growth factor – beta 1 (TGF-β1) appear to play important roles in the *in vivo* growth and maturation of articular cartilage. IGF-1 is present mostly in complexes in bovine calf and adult human articular cartilage at concentrations of 3-50 ng/g [22, 39], and in human synovial fluid at 30-50 ng/g [39]. Similarly, TGF-β1 is present in calf cartilage at ~65 ng/g [30], and its concentration decreases with maturation in rabbit synovial fluid from 113 pg/ml in young animals to 52 pg/ml in adults [43]. Articular chondrocytes *in situ* have been shown to express both IGF-1 [35] and TGF-β1 [2, 30] as well as their receptors [2, 42].

In vitro studies using cartilage explants have helped elucidate the roles of IGF-1 and TGF-β1 in regulating cartilage metabolism and cell fate. IGF-1 produces a strong anabolic response with dose-dependent increases in PG and COL synthesis in calf and adult bovine cartilage explants [37, 38]. IGF-1 has been identified as the primary component of serum responsible for stimulation of PG synthesis in cultured cartilage explants [27]. IGF-1 also reduces the rate of PG loss from adult, but not calf, explants and has no demonstrable effect on COL loss in either tissue [36]. Likewise, TGF-β1 increases PG synthesis by calf explants and slows the rate of PG loss [29, 31]. The increased biosynthesis of matrix components in these studies cannot be solely attributed to increased numbers of chondrocytes. While there are differing reports about whether IGF-1 maintains or slightly increases total DNA content [1, 36], TGF-β1 does not stimulate mitogenic activity in calf cartilage [1, 31]. In addition, both IGF-1 and TGF-β1 have potent anti-catabolic activity as demonstrated by their ability to protect cartilage against cytokine-induced collagenolysis [11-13] and to help restore PG synthesis following catabolic insult [28, 34].

With time in culture, growth factor-induced changes in cartilage metabolism may manifest as altered tissue composition, size, or mechanical properties. In calf cartilage explants stimulated by IGF-1, abundant deposition of newly synthesized GAG in excess of COL results in expansive growth characterized by large volumetric increases at the expense of reduced tensile stiffness and strength [1, 36]. On the other hand, calf explants stimulated with TGF-β1 increase only slightly in wet weight while maintaining GAG and COL content and tensile properties [1, 31]. However, the effects of IGF-1 or TGF-β1 on other functional properties of immature articular cartilage, including compressive moduli and Poisson's ratios, have not been determined.

With consideration of the broad interest in using anabolic factors to promote cartilage repair and tissue engineering, the objectives of this study are to 1) assess the effects of exogenous IGF-1 and TGF-β1 on geometric growth, biochemical composition, and compressive mechanical properties, including equilibrium confined and unconfined moduli and apparent Poisson's ratios, of cultured bovine calf articular cartilage and 2) correlate biochemical and mechanical properties to help elucidate the mechanisms by which IGF-1 and TGF-β1 alter cartilage function.

5.3 Materials and Methods

Sample Preparation and Culture

Articular cartilage blocks were harvested from the patellofemoral grooves of ten newborn (1-3 weeks) bovine calves. Day 0 (d0) control blocks were soaked for ~1 hour at 4°C in phosphate buffered saline (PBS) with protease inhibitors (+PIs: 2mM disodium ethylenediamine tetraacetate, 1mM phenylmethylsulfonyl fluoride, 5mM benzamidine hydrochloride, and 10mM N-ethylmaleimide) and stored at -70°C, while other blocks were immediately prepared for culture. Two samples, a superficial (S) slice with the intact articular surface (~0.8 mm thick) and an adjacent middle (M) zone slice (~0.6 mm thick), were taken from each block using a vibrating microtome. Samples were then trimmed to 6 mm x 6 mm. An orthogonal coordinate system was established where the 1-, 2-, and 3-directions corresponded to the medial-lateral, proximal-distal, and articular surface normal directions, respectively, and samples were notched to track orientation through culture. Initial thicknesses were measured

by a non-contacting laser micrometer (average of 3 points), and initial wet weights (WW_i) were obtained prior to culture.

The cartilage explants were cultured for 12 days (d12) in non-tissue culture treated plates with medium (DMEM supplemented with 100 μg/ml ascorbate, 0.01% bovine serum albumin, 0.1 mM nonessential amino acids, 0.4 mM L-proline, 2 mM l-glutamine, 10 mM HEPES, 100 U/ml penicillin, 100 μg/ml streptomycin, and 0.25 μg/ml amphotericin B) and either 50 ng/ml recombinant human (rh) IGF-1 or 10 ng/ml rhTGF-β1 (PeproTech, Rocky Hills, NJ) [1]. Plates were kept at 37°C in humidified 5% CO_2 – 95% air incubators. Medium (1.4 ml/explant) was changed every other day, and the plates were changed each week to limit cell outgrowth. Final thicknesses and wet weights (WW_f) were measured upon culture termination. Samples were then soaked in PBS+PIs at 4°C for 1 hr and stored at -70°C.

Compression Testing

For all mechanical tests, samples were thawed and tested in PBS+PIs at room temperature. Samples were sequentially tested in confined compression (CC) followed by unconfined compression (UCC) according to previously established protocols [4, 7, 45]. A pilot study indicated that properties measured during UCC testing were similar whether or not prior CC testing was performed. For CC testing, Ø4.8 mm disks were punched from cartilage slices, and their thicknesses were measured. Disks were placed in a confining ring between permeable platens in a materials testing machine (Dynastat, IMASS, Accord, MA). The test sequence consisted of consecutive, 400 s ramps to 15%, 30%, and 45% compressive strain (in the 3-direction). Preliminary tests indicated that samples cultured with IGF-1 did not fully recover following testing to 45%, and consequently were only tested to 30% if subsequent UCC testing was to be

performed. A stress relaxation period followed each ramp until samples reached equilibrium as determined with the criterion of a change in stress of <0.003 MPa over 180 s. At each static offset, stress relaxation was followed by oscillatory displacements with amplitudes decreasing from 1% to 0.3% and frequencies of 0.01 to 0.5 Hz. An equilibrium confined compression modulus (H_A) was determined at each strain offset as the total equilibrium stress divided by total equilibrium strain.

To facilitate comparisons with previous studies, the equilibrium confined compression modulus at the free-swelling thickness (H_{A0}) was also estimated, as done previously [4, 45], by a least-squares fit of the equilibrium stress-strain data to a finite deformation constitutive relationship, with d_1 = 0.9 [20]. The strain-dependent hydraulic permeability (k_p) was also estimated from the oscillatory load-displacement data, as done previously [4, 45]. To determine k_p at each offset, the dynamic stiffnesses were fit to the theoretical solution using the H_A value at that offset obtained from the previous fit [9]. From these estimates of k_p, the permeability at the free-swelling thickness (k_{p0}) and strain-dependence parameter (M) were fit according to $k_p=k_{p0}\cdot e^{M\varepsilon}$, where strain ($\varepsilon$) equals λ-1, and stretch (λ) equals the ratio of the compressed thickness to the free-swelling thickness [21].

Following CC testing, disks were allowed to re-swell in PBS+PIs at 4°C overnight, which was determined to be sufficient for them to recover to their pre-CC testing thickness. For subsequent UCC testing, Ø3.2 mm disks were punched from the larger disks, to reduce UCC relaxation times and ensure well-defined sample edges for photography. Samples were re-mounted in the materials testing machine between smooth, impermeable platens in an unconfined manner. An optical system of mirrors and prisms projected perpendicular lateral views of the disk to a digital camera, which allowed for measurements of dimensions in the 1- and 2-directions during axial

compression in the 3-direction. The test sequence consisted of consecutive, 400 s ramps to 15%, 30%, and 45% compressive strain. Each ramp was followed by stress relaxation to equilibrium, defined by the same criterion as for CC testing, at which point the lateral-view images were acquired. An equilibrium unconfined compression modulus (E) was determined at each strain offset as the total equilibrium stress divided by total equilibrium strain. Images were processed in MATLAB (Mathworks, Natick, MA) using a custom-written algorithm to determine lateral expansion [7], which was used to calculate apparent Poisson's ratios in compression (ν_{31} and ν_{32}) at each offset relative to zero strain state. Here, the term apparent Poisson's ratio is used to indicate the Poisson's ratio for large strains.

Biochemical Analyses

Tested and residual tissue portions from d0 control and d12 cultured samples were collected for biochemical analysis. The tissue was lyophilized and weighed to obtain a dry weight. Water content was calculated as the difference between the final wet and dry weights as a percentage of the final wet weight. The tissue was solubilized with a solution of 0.5 mg/ml proteinase K (Roche Diagnostics, Indianapolis, IN). Portions of the tissue digests were assessed for DNA [26], glycosaminoglycans (GAG) [6], hydroxyproline [46], and pyridinoline (PYR) crosslinks [41]. Cell and collagen (COL) contents were calculated using ratios of 7.7 pg DNA/cell [15] and 7.25 g COL/g hydroxyproline [10, 33]. Data were normalized to WW_i to indicate constituent content and to WW_f to indicate constituent concentration, though for d0 samples $WW_i = WW_f$. Biochemical data are representative of what remained in the tissue following the mechanical testing sequence. Pilot studies determined that a small portion of GAG was lost to solutions used during mechanical

testing, representing about 5% of total sample GAG in d12 IGF-1 samples and about half as much in other samples.

Statistical Analyses

Data are presented as means ± SE. For each layer (S and M), single-factor analysis of variance (ANOVA) was used to compare the change in structural parameters (thickness and wet weight) between culture conditions (d12 IGF-1 and d12 TGF-β1) and between each condition and no change (i.e. zero). For each layer and each strain level (where applicable), the effects of culture condition (d0, d12 IGF-1, and d12 TGF-β1) on biomechanical and biochemical properties were determined by ANOVA, with Tukey *post hoc* testing for comparisons between individual groups. The hydraulic permeability data were normalized by log transformation prior to statistical analysis. The significance level, α, was set at 0.05 for all tests.

Univariate and multivariate linear regression were used to analyze relationships between the cartilage mechanical properties (H_A, E, ν_{31}, and ν_{32}) at 30% compressive strain and biochemical properties (water, GAG, COL, PYR, cells [$\%WW_f$]) across treatment groups for each layer. Multivariate regression was performed via the forward selection procedure [40], by adding variables, in order of strongest partial correlation, until the incremental improvement in the relationship became nonsignificant. Coefficients of determination (r^2) and of multiple determination (R^2) are reported for significant relationships ($p<0.05$).

5.4 Results

Geometric Growth of Cartilage Explants

Calf articular cartilage incubated for 12 days in medium with 50 ng/ml IGF-1 or 10 ng/ml TGF-β1 exhibited stark differences in growth, as measured by changes in weight and dimensions relative to initial values. Culture with IGF-1 resulted in large increases (~50% to 70%) in wet weight of both S and M cartilage slices, which were significantly greater than those observed in the TGF-β1 groups ($p<0.001$, **Fig. 5.1A**). Changes in wet weight with IGF-1 were matched by similarly large magnitudes of expansion of sample thickness (**Fig. 5.1B**). Measures of dimensional changes were similar in the 1- and 2-directions, averaging <5% for IGF-1 samples and <2% for TGF-β1 samples (data not shown), and support the finding that IGF-1 primarily induced growth in the axial direction. Within the TGF-β1 groups, a small increase in wet weight (~4%) of M samples was the only measure of geometric growth which differed significantly from zero ($p<0.05$). Tissue water content was also differentially regulated by growth factor treatment, with the resulting water content being higher in the IGF-1 samples than in TGF-β1 samples for both S and M layers ($p<0.01$, **Fig. 5.1C**). Samples from the S layer treated with TGF-β1 were the only group to show a difference in water content versus d0 (-3.7%, $p<0.001$). The slight changes in water content of all groups indicate that changes in wet weight were primarily caused by changing tissue volume and not tissue density.

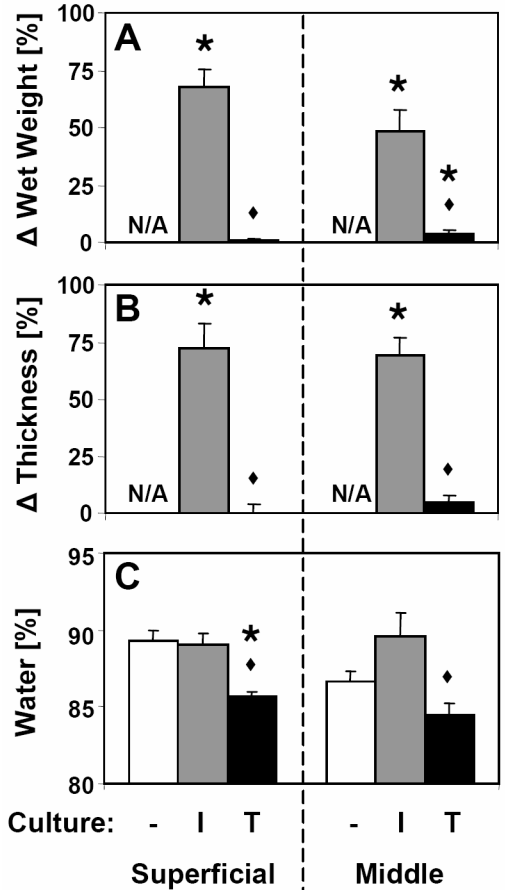

Figure 5.1: Change in (**A**) wet weight and (**B**) thickness for superficial and middle cartilage explants cultured for 12 days with IGF-1 (I, gray bars) or TGF-β1 (T, black bars). (**C**) Water content of day 0 (-, white bars) and cultured explants. For each tissue layer, ★ indicates $p<0.05$ versus zero (i.e. no change) for Δ wet weight and Δ thickness and versus d0 for water content. ♦ indicates $p<0.05$ versus d12 IGF-1. Mean ± SE; n=12-18.

Biomechanical Properties in Compression

Biomechanical properties of cartilage explants measured via CC testing were differentially affected by culture with IGF-1 and TGF-β1. The measured equilibrium confined compression modulus, H_A, (**Fig 2A**) was significantly reduced by culture with IGF-1 compared to d0 at 30% compressive strain in the S layer (-65%, $p<0.05$) and at all strains in the M layer (-61% to -74%, $p<0.05$), but was increased by culture with TGF-β1 at 30% and 45% strain in the S layer (103% and 108%, $p<0.01$). For all strain levels and layers, treatment with TGF-β1 resulted in greater H_A than IGF-1 treated samples ($p<0.05$). Similar differences were observed in the estimated confined compression modulus at the free-swelling strain, H_{A0}, (**Table 1**) with IGF-1 treated samples being less stiff in both layers ($p<0.05$) and TGF-β1 treated samples being stiffer in the S layer than d0 controls ($p<0.01$). The estimated hydraulic permeability at the free-swelling thickness, k_{p0}, and the permeability strain-dependence parameter, *M*, (**Table 1**) did not vary with culture condition for either layer ($p=0.67$ and 0.42 for S layer and $p=0.15$ and 0.57 for M layer).

Biomechanical properties obtained via UCC testing, including equilibrium unconfined compression modulus, E, and apparent Poisson's ratios, ν_{31} and ν_{32}, also varied with culture condition (**Fig. 2B-D**). Compared to d0, E was reduced by culture with IGF-1 for all strain levels and layers (-80% to -89%, $p<0.05$), but was increased by culture with TGF-β1 in the S layer (65% to 77%, $p<0.05$). Culture with TGF-β1 resulted in greater E than IGF-1 treated samples for all strain levels and layers ($p<0.05$). Apparent Poisson's ratios did not vary between directions for either the S layer ($p>0.34$) or M layer ($p>0.13$); however, culture condition was a significant factor ($p<0.05$), except for ν_{32} at 15% and 30% strain for S layer samples ($p=0.20$ and 0.10). In general, the apparent Poisson's ratios were increased from d0 by culture with

IGF-1 (198% for S layer and 97% for M layer, averaged across strain levels and directions), but were maintained by culture with TGF-β1.

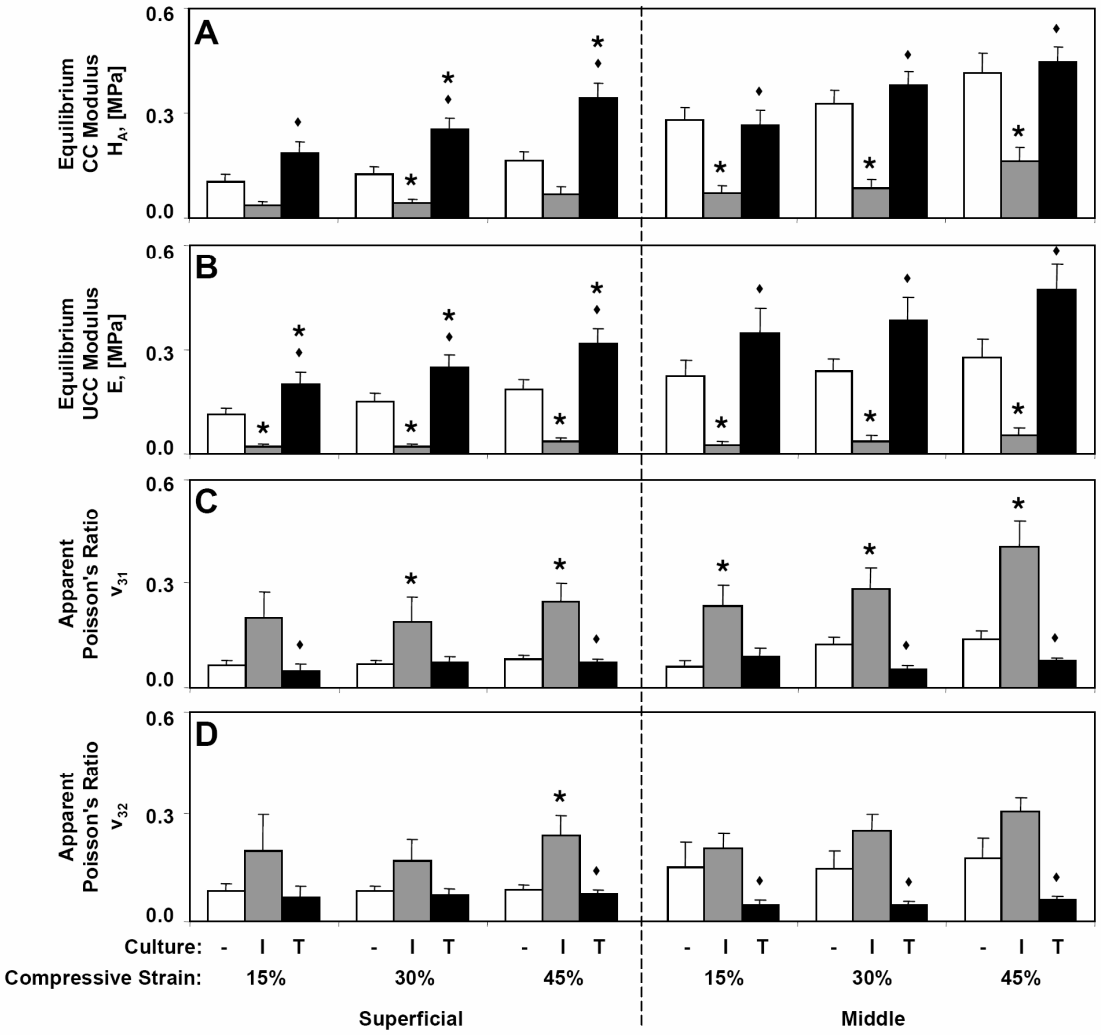

Figure 5.2: Compressive properties of superficial and middle cartilage explants at day 0 (-, white bars) or following 12 days culture with IGF-1 (I, gray bars) or TGF-β1 (T, black bars). (**A**) Equilibrium confined compression (CC) modulus, H_A, (**B**) equilibrium unconfined compression (UCC) modulus, E, and apparent Poisson's ratios, (**C**) ν_{31}, and (**D**) ν_{32} were measured at three compressive offset strains of 15, 30, and 45%. For each strain level and tissue layer, ✶ indicates $p<0.05$ versus d0, and ♦ indicates $p<0.05$ versus d12 IGF-1. Mean ± SE; n=6-15.

Table 5.1: Equilibrium confined compression modulus, H_A [MPa], and hydraulic permeability, k_p [$m^2/(Pa \cdot s)$], were estimated at the free-swelling thickness. The permeability strain-dependence parameter, *M*, was also determined. For each tissue layer, ✱ indicates $p<0.05$ versus d0, and ♦ indicates $p<0.05$ versus d12 IGF-1. Mean ± SE; n=9-15.

	d0		d12 IGF-1		d12 TGF-β1	
	Superficial	Middle	Superficial	Middle	Superficial	Middle
H_{A0}	0.096 ± 0.014	0.233 ± 0.031	0.033 ± 0.008✱	0.068 ± 0.017✱	0.188 ± 0.024✱,♦	0.253 ± 0.024♦
$\log_{10} k_{p0}$	-14.49 ± 0.19	-14.98 ± 0.13	-14.57 ± 0.18	-14.57 ± 0.28	-14.34 ± 0.19	-14.51 ± 0.16
M	8.6 ± 1.3	6.8 ± 0.6	7.4 ± 0.9	7.7 ± 1.4	9.1 ± 0.8	8.2 ± 0.7

Biochemical Composition

Cartilage matrix and chondrocyte content varied with culture condition (**Fig 5.3A, C, E, G**). In the S layer, GAG and COL contents were increased following treatment with IGF-1 (62%, $p<0.05$ and 50%, $p<0.01$, respectively) and with TGF-β1 (27%, $p<0.05$ and 40%, $p<0.01$). PYR crosslink content was also increased by culture with TGF-β1 (72%, $p<0.05$), but not with IGF-1 ($p=0.31$). However, when PYR was normalized to COL (**Fig. 5.4**), there were no differences in the extent of COL crosslinking for either layer ($p=0.60$ for S and $p=0.19$ for M). Changes in cartilage matrix content were less pronounced in M layer explants. Cell contents did not differ from d0 in either culture condition ($p>0.25$), but TGF-β1 treated samples had slightly fewer cells than IGF-1 treated samples for both layers ($p<0.05$).

After accounting for changes in wet weight during culture, the final concentrations of matrix components and chondrocytes also varied according to culture condition (**Fig 5.3B, D, F, H**). GAG, COL, and PYR concentrations in samples cultured with IGF-1 were similar to those of d0 samples, except for a reduction of GAG concentration in M layer samples (-31%, $p<0.01$). Increases in GAG (27%, $p<0.01$), COL (40%, $p<0.001$), and PYR (72%, $p<0.05$) concentrations were observed in S layer samples cultured with TGF-β1 compared to d0. Final concentrations of GAG, COL, and PYR were higher in TGF-β1 treated samples than in IGF-1 treated samples for both layers ($p<0.05$). Cell concentration decreased moderately following culture with IGF-1 (-33%, $p<0.01$ for S layer and -24%, $p<0.05$ for M layer) and slightly following culture with TGF-β1 for M layer explants (-12%, $p<0.05$).

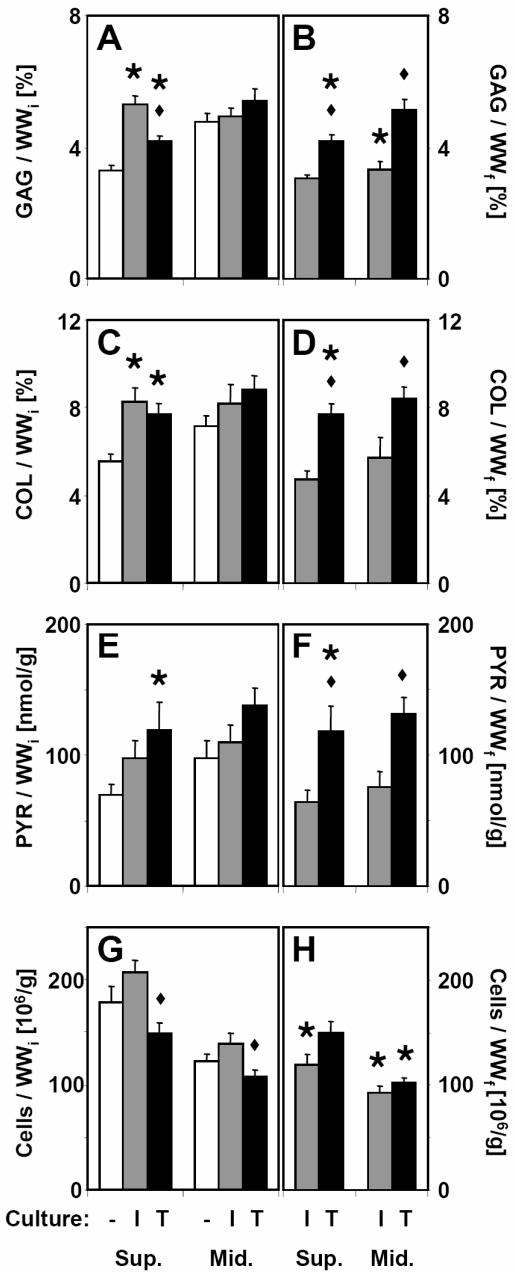

Figure 5.3: (**A, B**) Glycosaminoglycan, (**C, D**) collagen, (**E, F**) pyridinoline crosslinks, and (**G, H**) cellularity of superficial and middle cartilage explants analyzed on day 0 (-, white bars) or following 12 days culture with IGF-1 (I, gray bars) or TGF-β1 (T, black bars). Data are normalized to (**A, C, E, G**) initial wet weight (WW_i) to indicate constituent content or (**B, D, F, H**) final wet weight (WW_f) to indicate constituent concentration. For d0 samples, $WW_i = WW_f$, and the data is presented once. For each tissue layer, ✶ indicates $p<0.05$ versus d0, and ♦ indicates $p<0.05$ versus d12 IGF-1. Mean ± SE; n=11-18.

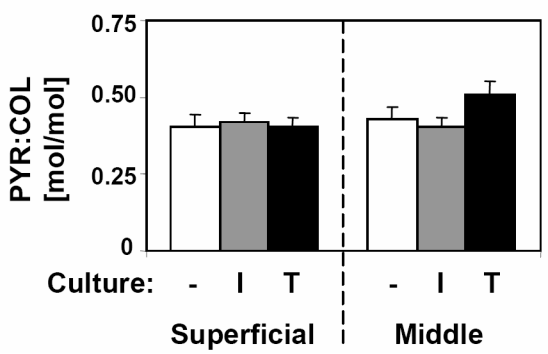

Figure 5.4: The ratio of pyridinoline crosslinks to collagen molecules for superficial and middle cartilage explants analyzed on day 0 (-, white bars) or following 12 days culture with IGF-1 (I, gray bars) or TGF-β1 (T, black bars). Mean ± SE; n=7-15.

Composition-Function Correlative Analyses

Univariate regression analysis indicated significant relationships between certain cartilage biomechanical properties and matrix constituents (**Fig. 5.5**). H_A at 30% compressive strain was negatively related to water (r^2=0.24 for S, r^2=0.37 for M), and positively related to GAG (r^2=0.52 for S, r^2=0.37 for M) and COL concentrations (r^2=0.54 for S, r^2=0.21 for M). Similarly, E at 30% strain was negatively related to water (r^2=0.26 for S, r^2=0.34 for M), and positively related to GAG (r^2=0.55 for S, r^2=0.46 for M), COL (r^2=0.54 for S, r^2=0.22 for M), and also PYR concentrations (r^2=0.23 for M). Poisson's ratios at 30% strain were weakly related to matrix constituents, with ν_{31} negatively related to GAG (r^2=0.37 for M) and ν_{32} negatively related to GAG (r^2=0.43 for M) and COL (r^2=0.22 for S, r^2=0.20 for M). There were no significant relationships between the mechanical properties and cell concentration.

For some compressive moduli, multiple regression analysis significantly improved the explanation of variability over the univariate analysis. $H_{A\text{-}.30}$ was related to GAG and COL in the S layer with regression coefficients of 0.0618 and 0.0283, respectively, and a constant of -0.2477 (R^2=0.63), and to GAG and water in the M layer with regression coefficients of 0.0518 and -0.0164, respectively, and a constant of 1.4678 (R^2=0.48). Similarly, $E_{-.30}$ was related to GAG and COL in the S layer by coefficients of 0.0744 and 0.0289, respectively, and a constant of -0.2987 (R^2=0.70); however, the univariate regression of $E_{-.30}$ on GAG in the M layer with a coefficient of 0.1056 and constant of -0.2460 (r^2=0.46) was not improved by the addition of other variables.

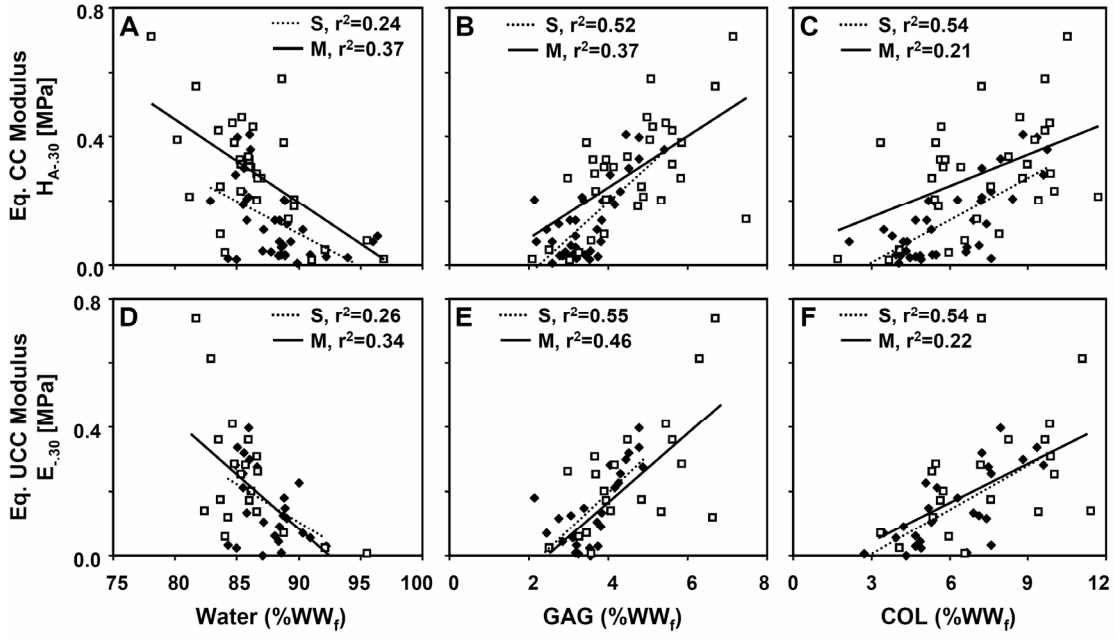

Figure 5.5: Regression of (**A-C**) equilibrium CC modulus and (**D-F**) equilibrium UCC modulus at 30% offset strain on matrix constituent concentrations (% final WW), including (**A, D**) water, (**B, E**) GAG, and (**C, F**) COL. Data points and relationships are for d0 and cultured cartilage explants from the S layer (◆, dotted line) and the M layer (□, solid line). Coefficients of determination (r^2) are indicated for significant relationships ($p<0.05$).

5.5 Discussion

The findings of this study indicate that *in vitro* growth and remodeling of immature articular cartilage explants, as assessed by changing size, matrix and cell content, and mechanical properties in compression, are differentially regulated by the anabolic growth factors IGF-1 and TGF-β1. While IGF-1 induces large increases in cartilage volume, primarily by growth in the axial direction, TGF-β1 generally maintains explant size. These findings are consistent with those of a previous study, where it was proposed that *in vitro* cartilage growth can result from deposition of PG in excess of COL [1]. The resulting imbalance in PG swelling pressure and the restraint provided by the COL network can produce volumetric expansion of the tissue [18, 24]. In the S-layer cultures with IGF-1 where increases in tissue weight tended to be largest, the increase in GAG content exceeded that of COL (on a percentage basis). The reverse occurred in S-layer cultures with TGF-β1 where COL increased more than GAG. Many of the effects of IGF-1 and TGF-β1 on the biochemical composition of cartilage explants agree with previous studies [1, 31, 36]. The changing biochemical composition corresponded to altered functional properties too. Culture with IGF-1 was marked by cartilage softening and increased Poisson's ratios, whereas, culture with TGF-β1 was more homeostatic and even maturational in the S layer where moduli were increased.

Consideration was given to a number of factors in the development of this experimental design which may limit the interpretation of these findings. Immature articular cartilage from bovine calf patellofemoral grooves was chosen as the tissue source, since this tissue has been examined in previous characterization studies of *in vivo* maturation and *in vitro* growth [1, 7, 45]. Moreover, cartilage explants from two depths, a superficial layer containing the intact articular surface and a middle/growth

layer, were used in this study similar to previous work [1]. Comparing the layers was not a primary goal of this study, since depth-dependent compressive properties from both CC and UCC testing have been previously reported for fresh calf articular cartilage [3, 16]. Nevertheless, the data from the two layers may facilitate comparisons of these results to other studies and also be useful for future theoretical work. Accordingly, the biochemical and mechanical properties of the d0 control cartilage from this study are in general agreement with those preceding studies. The selection of growth factor concentrations was an additional important choice in the experimental design. For calf articular cartilage, the stimulatory effects of IGF-1 on DNA, GAG, and hydroxyproline synthesis and deposition saturate between 30-300 ng/ml [36], while the stimulation of GAG synthesis by TGF-β1 saturates between 5-20 ng/ml [31]. Thus the concentrations used in this study (50 ng/ml IGF-1 and 10 ng/ml TGF-β1) represent near maximal stimulation of calf cartilage metabolism and were capable of producing measurable changes in cartilage composition and function within the chosen 12 day culture duration.

The effects of IGF-1 and TGF-β1 on immature cartilage compressive properties in CC and UCC are novel findings, though not wholly unanticipated. The expansive growth which characterizes culture with IGF-1 coincides with a functional impairment of mechanical properties, as measured by softening in compression as found here as well as softening and reduction in strength in tension as reported previously [1]. The increased Poisson's ratios of cartilage cultured with IGF-1 may also be indicative of a loss of tensile integrity and a reduced ability of the COL network to restrain PG swelling and lateral expansion during UCC testing. The changes in H_A, E, ν_{31}, and ν_{32} and maintenance of k_{p0} and *M* during culture with IGF-1 also resemble those that occur during the culture of calf articular cartilage with 20%

fetal bovine serum [7]. This observation is consistent with reports that IGF-1 is the primary component of serum responsible for stimulating cartilage PG synthesis [27] and that serum and IGF-1 produce similar changes in cartilage composition and function [1]. On the other hand, culture with TGF-β1 was more homeostatic with some functional improvement in the S layer indicated by increased compressive moduli and matrix constituent concentrations. Relationships between mechanical properties, particularly H_A and E, and cartilage matrix constituent concentrations became more evident when explored by regression analysis. Positive relationships between compressive moduli and concentrations of GAG and COL and negative relationships between moduli and water content recapitulate those of articular cartilage examined at various developmental stages from fetus to young adult [45] or following *in vitro* growth with FBS supplemented medium [7].

The compressive properties measured in this study complement an earlier study which measured changes in tensile properties of calf explants cultured with IGF-1 or TGF-β1 [1]. Measures of cartilage composition and tensile properties from this earlier study of explant growth have helped refine and validate a cartilage growth mixture (CGM) model [1, 17]. CGM models have been developed to describe the evolving biochemical and mechanical properties of cartilage during growth and remodeling [18, 19]. These models consider the cartilage matrix as a set of elastic constituents (e.g. PG and COL) that can independently grow and remodel and are made compatible by mechanical deformations. Thus, comprehensive biochemical, structural, and mechanical data from *in vitro* growth studies such as this may further enhance CGM model parameters and the accuracy of simulations.

Due to an ability to elicit strong anabolic responses, IGF-1 and TGF-β1 have been investigated in numerous studies for their potential to promote cartilage repair or

enhance the formation of engineered cartilage constructs [5, 8, 23]. A translational goal of this work and related CGM modeling is to help elucidate specific conditions for manipulating the growth, maturation, or homeostasis of cartilaginous tissues. The identification of such conditions may ultimately aid the development of cartilage repair techniques or the fabrication and storage of transplantable cartilaginous grafts of desired sizes and properties.

5.6 Acknowledgments

Chapter 5, in part, has been submitted for publication of the material as it may appear in *Osteoarthritis and Cartilage*, 2009. The dissertation author was the primary author and thanks co-authors Kristin J. Dills, Christian R. Flores, Michael E. Stender, Kevin M. Stewart, Lauren M. Nelson, Albert C. Chen, Koichi Masuda, Scott J. Hazelwood, Robert L. Sah, and Stephen M. Klisch. This work was supported in part by grants from NIH (SJH, RLS, SMK), NSF (RLS, SMK), HHMI through the HHMI Professors Program (to UCSD in support of RLS), and the Donald E. Bently Center for Engineering Innovation (SMK). Individual support was received through a NSF Graduate Research Fellowship and a NIH Ruth L. Kirchstein Pre-Doctoral Fellowship (to GMW).

5.7 References

1. Asanbaeva A, Masuda K, Thonar EJ-MA, Klisch SM, Sah RL: Regulation of immature cartilage growth by IGF-I, TGF-beta1, BMP-7, and PDGF-AB: role of metabolic balance between fixed charge and collagen network. *Biomech Model Mechanobiol* 7:263-76, 2008.

2. Blaney Davidson EN, Scharstuhl A, Vitters EL, van der Kraan PM, van den Berg WB: Reduced transforming growth factor-beta signaling in cartilage of old mice: role in impaired repair capacity. *Arthritis Res Ther* 7:R1338-47, 2005.

3. Chahine NO, Wang CC, Hung CT, Ateshian GA: Anisotropic strain-dependent material properties of bovine articular cartilage in the transitional range from tension to compression. *J Biomech* 37:1251-61, 2004.

4. Chen AC, Bae WC, Schinagl RM, Sah RL: Depth- and strain-dependent mechanical and electromechanical properties of full-thickness bovine articular cartilage in confined compression. *J Biomech* 34:1-12, 2001.

5. Elisseeff J, McIntosh W, Fu K, Blunk BT, Langer R: Controlled-release of IGF-I and TGF-beta1 in a photopolymerizing hydrogel for cartilage tissue engineering. *J Orthop Res* 19:1098-104, 2001.

6. Farndale RW, Buttle DJ, Barrett AJ: Improved quantitation and discrimination of sulphated glycosaminoglycans by use of dimethylmethylene blue. *Biochim Biophys Acta* 883:173-7, 1986.

7. Ficklin T, Thomas G, Barthel JC, Asanbaeva A, Thonar EJ-MA, Masuda K, Chen AC, Sah RL, Davol A, Klisch SM: Articular cartilage mechanical and biochemical property relations before and after in vivo growth. *J Biomech* 40:3607-14, 2007.

8. Fortier LA, Lust G, Mohammed HO, Nixon AJ: Coordinate upregulation of cartilage matrix synthesis in fibrin cultures supplemented with exogenous insulin-like growth factor-I. *J Orthop Res* 17:467-74, 1999.

9. Frank EH, Grodzinsky AJ: Cartilage electromechanics-II. A continuum model of cartilage electrokinetics and correlation with experiments. *J Biomech* 20:629-39, 1987.

10. Herbage D, Bouillet J, Bernengo J-C: Biochemical and physicochemical characterization of pepsin-solubilized type-II collagen from bovine articular cartilage. *Biochem J* 161:303-12, 1977.

11. Hui W, Cawston T, Rowan AD: Transforming growth factor beta 1 and insulin-like growth factor 1 block collagen degradation induced by oncostatin M in combination with tumour necrosis factor alpha from bovine cartilage. *Ann Rheum Dis* 62:172-4, 2003.

12. Hui W, Rowan AD, Cawston T: Transforming growth factor beta1 blocks the release of collagen fragments from boving nasal cartilage stimulated by oncostatin M in combination with IL-1alpha. *Cytokine* 12:765-9, 2000.

13. Hui W, Rowan AD, Cawston T: Insulin-like growth factor 1 blocks collagen release and down regulates matrix metalloproteinase-1, -3, -8, and -13 mRNA expression in bovine nasal cartilage stimulated with oncostatin M in combination with interleukin 1alpha. *Ann Rheum Dis* 60:254-61, 2001.

14. Kempson GE, Muir H, Pollard C, Tuke M: The tensile properties of the cartilage of human femoral condyles related to the content of collagen and glycosaminoglycans. *Biochim Biophys Acta* 297:456-72, 1973.

15. Kim YJ, Sah RLY, Doong JYH, Grodzinsky AJ: Fluorometric assay of DNA in cartilage explants using Hoechst 33258. *Anal Biochem* 174:168-76, 1988.

16. Klein TJ, Chaudhry M, Bae WC, Sah RL: Depth-dependent biomechanical and biochemical properties of fetal, newborn, and tissue-engineered articular cartilage. *J Biomech* 40:182-90, 2007.

17. Klisch SM, Asanbaeva A, Oungoulian SR, Masuda K, Thonar EJ-MA, Davol A, Sah RL: A cartilage growth mixture model with collagen remodeling: validation protocols. *J Biomech Eng* 130:031006, 2008.

18. Klisch SM, Chen SS, Sah RL, Hoger A: A growth mixture theory for cartilage with applications to growth-related experiments on cartilage explants. *J Biomech Eng* 125:169-79, 2003.

19. Klisch SM, Sah RL, Hoger A: A cartilage growth mixture model for infinitesimal strains: solutions of boundary-value problems related to in vitro growth experiments. *Biomech Model Mechanobiol* 3:209-23, 2005.

20. Kwan MK, Hacker SA, Woo SL-Y, Wayne JS: The effect of storage on the biomechanical behavior of articular cartilage-a large strain study. *J Biomech Eng* 114:149-53, 1992.

21. Lai WM, Mow VC, Roth V: Effects of nonlinear strain-dependent permeability and rate of compression on the stress behavior of articular cartilage. *J Biomech Eng* 103:61-6, 1981.

22. Luyten FP, Hascall VC, Nissley SP, Morales TI, Reddi AH: Insulin-like growth factors maintain steady-state metabolism of proteoglycans in bovine articular cartilage explants. *Arch Biochem Biophys* 267:416-25, 1988.

23. Madry H, Zurakowski D, Trippel SB: Overexpression of human insulin-like growth factor-I promotes new tissue formation in an ex vivo model of articular chondrocyte transplantation. *Gene Ther* 8:1443-9, 2001.

24. Maroudas A: Balance between swelling pressure and collagen tension in normal and degenerate cartilage. *Nature* 260:808-9, 1976.

25. Maroudas A, Katz EP, Wachtel EJ, Mizrahi J, Soudry M: Physico-chemical properties and functional behavior of normal and osteoarthritic human cartilage. In: *Articular Cartilage Biochemistry,* ed. by K Kuettner, Schleyerbach R, Hascall VC, Raven Press, New York, 1986.

26. McGowan KB, Kurtis MS, Lottman LM, Watson D, Sah RL: Biochemical quantification of DNA in human articular and septal cartilage using PicoGreen and Hoechst 33258. *Osteoarthritis Cartilage* 10:580-7, 2002.

27. McQuillan DJ, Handley CJ, Campbell MA, Bolis S, Milway VE, Herington AC: Stimulation of proteoglycan biosynthesis by serum and insulin-like growth factor-I in cultured bovine articular cartilage. *Biochem J* 240:423-30, 1986.

28. Morales TI: Transforming growth factor-beta and insulin-like growth factor-1 restore proteoglycan metabolism of bovine articular cartilage after depletion by retinoic acid. *Arch Biochem Biophys* 315:190-8, 1994.

29. Morales TI, Hascall VC: Transforming growth factor-β1 stimulates synthesis of proteoglycan aggregates in calf articular organ cultures. *Arch Biochem Biophys* 286:99-106, 1991.

30. Morales TI, Joyce ME, Soble ME, Danielpour D, Roberts AB: Transforming growth factor-β in calf articular cartilage organ cultures: synthesis and distribution. *Arch Biochem Biophys* 288:397-405, 1991.

31. Morales TI, Roberts AB: Transforming growth factor-β regulates the metabolism of proteoglycans in bovine cartilage organ cultures. *J Biol Chem* 263:12828-31, 1988.

32. Mow VC, Gu WY, Chen FH: Structure and Function of Articular Cartilage and Meniscus. In: *Basic Orthopaedic Biomechanics and Mechano-Biology,* ed. by VC Mow, Huiskes R, Lippincott Williams & Wilkins, Philadelphia, 2005, 720.

33. Pal S, Tang L-H, Choi H, Habermann E, Rosenberg L, Roughley P, Poole AR: Structural changes during development in bovine fetal epiphyseal cartilage. *Collagen Rel Res* 1:151-76, 1981.

34. Rayan V, Hardingham T: The recover of articular cartilage in explant culture from interleukin-1α: effects on proteoglycan synthesis and degradation. *Matrix Biol* 14:263-71, 1994.

35. Reinecke M, Schmid AC, Heyberger-Meyer B, Hunziker EB, Zapf J: Effect of growth hormone and insulin-like growth factor I (IGF-I) on the expression of IGF-I messenger ribonucleic acid and peptide in rat tibial growth plate and articular chondrocytes in vivo. *Endocrinology* 141:2847-53, 2000.

36. Sah RL, Chen AC, Grodzinsky AJ, Trippel SB: Differential effects of bFGF and IGF-I on matrix metabolism in calf and adult bovine cartilage explants. *Arch Biochem Biophys* 308:137-47, 1994.

37. Sah RL, Trippel SB, Grodzinsky AJ: Differential effects of serum, insulin-like growth factor-I, and fibroblast growth factor-2 on the maintenance of cartilage physical properties during long-term culture. *J Orthop Res* 14:44-52, 1996.

38. Schalkwijk J, Joosten LAB, van den Berg WB, van Wyk JJ, van de Putte LBA: Insulin-like growth factor stimulation of chondrocyte proteoglycan synthesis by human synovial fluid. *Arthritis Rheum* 32:66-71, 1989.

39. Schneiderman R, Rosenberg N, Hiss J, Lee P, Liu F, Hintz RL, Maroudas A: Concentration and size distribution of insulin-like growth factor-I in human normal and osteoarthritic synovial fluid and cartilage. *Arch Biochem Biophys* 324:173-88, 1995.

40. Sokal RR, Rohlf FJ. Biometry. 3rd ed. New York: WH Freeman and Co.; 1995.

41. Uebelhart D, Thonar EJ-MA, Pietryla DW, Williams JW: Elevation in urinary levels of pyridinium cross-links of collagen following chymopapin-induced degradation of articular cartilage in the rabbit knee provides evidence of metabolic changes in bone. *Osteoarthritis Cartilage* 1:185-92, 1993.

42. Verschure PJ, van Marle J, Joosten LA, van den Berg WB: Chondrocyte IGF-1 receptor expression and responsiveness to IGF-1 stimulation in mouse articular cartilage during various phases of experimentally induced arthritis. *Ann Rheum Dis* 54:645-53, 1995.

43. Wei X, Messner K: Age- and injury-dependent concentrations of transforming growth factor-beta 1 and proteoglycan fragments in rabbit knee joint fluid. *Osteoarthritis Cartilage* 6:10-8, 1998.

44. Williamson AK, Chen AC, Masuda K, Thonar EJ-MA, Sah RL: Tensile mechanical properties of bovine articular cartilage: variations with growth and relationships to collagen network components. *J Orthop Res* 21:872-80, 2003.

45. Williamson AK, Chen AC, Sah RL: Compressive properties and function-composition relationships of developing bovine articular cartilage. *J Orthop Res* 19:1113-21, 2001.

46. Woessner JF: The determination of hydroxyproline in tissue and protein samples containing small proportions of this imino acid. *Arch Biochem Biophys* 93:440-7, 1961.

47. Zhu W, Mow VC, Koob TJ, Eyre DR: Viscoelastic shear properties of articular cartilage and the effects of glycosidase treatment. *J Orthop Res* 11:771-81, 1993.

CHAPTER 6

CONCLUSIONS

The studies presented in the preceding chapters were conducted 1) to establish whether flexural deformations can aid in the contouring of cartilage by inducing changes in tissue shape through matrix remodeling, 2) to characterize more thoroughly the biomechanical behavior of cartilage in flexure, and 3) to determine how biochemical regulation of matrix metabolism and remodeling modulates cartilage shape plasticity, volume, and maturity. The primary findings of these studies are summarized below and then discussed with suggestions for future research directions.

6.1 Summary of Findings

The application of static flexure to articular cartilage explants during short-term (<1 week) culture induced changes in the macroscopic, free-swelling configuration of the tissue, such that specific contours were reproducibly obtained (**Chapter 2 & 4**). The duration of deformation was a significant factor in determining the degree to which the imposed deformation was retained by the cartilage explant after unloading. However, for calf cartilage, a near-maximal response was achieved in only 4-6 days. Compared to calf, the response of cartilage from adult bovines was substantially less, indicating a dependence of cartilage shape plasticity upon

maturational stage. During the course of reshaping, chondrocyte viability was preserved, demonstrating that the flexural stimulus was non-injurious. Moreover, changes in tissue size and composition during culture with flexure generally mimicked those of non-loaded control cultures.

The process of altering the shape of cartilage explants was largely independent of active chondrocyte-mediated matrix synthesis or remodeling (**Chapter 2 & 4, App. B**). Inhibition of chondrocyte protein synthesis with cycloheximide only yielded a small reduction in the reshaping response. Mechanically induced shape change was not a result of collagen network stabilization through the formation of new difunctional crosslinks, as indicated by use of the inhibitor β-aminopropionitrile (BAPN). It also did not appear to be mediated by catabolic activity within the matrix, as determined by broad-spectrum inhibition of matrix-metalloproteinases and other proteases. However, the reshaping process was markedly inhibited by reducing the temperature from 37°C to 4°C for the duration of the culture.

The flexural stimulus used in these studies was characterized through a novel application of micromechanical analysis (**Chapter 3**). A linear gradient of longitudinal normal strain from ~20% compressive strain at the concave surface to ~7% tensile strain at the convex surface was measured in cartilage explants, and the neutral axis was located about three-quarters of the sample thickness from the concave surface. Empirical comparison of cartilage strains with those in samples of alginate, a material chosen for similar moduli in tension and compression, and theoretical modeling of the tissue as a bimodular material in pure bending indicated that the tension-compression nonlinearity was a key determinant of the asymmetry of strains.

Perturbing proteoglycan and collagen remodeling with medium supplemented with fetal bovine serum and either BAPN or β-D-xyloside differentially modulated

cartilage explant size, matrix composition, and shape plasticity (**Chapter 4**). Calf cartilage treated with β-D-xyloside exhibited reduced accumulation of glycosaminoglycans (GAG) and volumetric growth compared to samples treated with BAPN. Shape plasticity was significantly increased with BAPN treatment but was maintained with β-D-xyloside. In cultures of adult cartilage, these treatments produced little growth, but composition did differ between. Consistent with the lower metabolism of adult cartilage, β-D-xyloside resulted in a net loss of GAG, while BAPN treatment maintained GAG. Like calf cartilage, adult cartilage treated with BAPN had higher shape plasticity than those treated with β-D-xyloside. Overall, there was a strong inverse association between changing matrix composition, reflected in the COL:GAG ratio, and cartilage shape plasticity.

Finally, anabolic growth factors, insulin-like growth factor – 1 (IGF-1) and transforming growth factor – beta1 (TGF-β1), could differentially regulate calf cartilage size, composition, and mechanical properties in confined and unconfined compression (**Chapter 5**). IGF-1 promoted expansive growth of cartilage, generally marked by accumulation of GAG in excess of collagen, but also impaired the compressive properties by reducing stiffness and increasing Poisson's ratios. On the other hand TGF-β1 produced little growth and was more homeostatic and even slightly maturational in superficial (S) slices in terms of composition and compressive properties. TGF-β1 promoted a more balanced accumulation of GAG, collagen, and pyridinoline crosslinks and increased compressive stiffness in S slices. In general, regression analysis found that matrix constituent concentrations were positively related to compressive moduli and negatively related to Poisson's ratios.

6.2 Discussion and Future Directions

6.2.a Choice of Stimuli/Treatments

Early in the formulation of this dissertation, consideration was given to the various types of mechanical stimuli that could be investigated with regards to eliciting changes in cartilage shape. Tensile, compressive, and flexural deformations applied statically or dynamically were among the options. Previous studies have shown that *in situ* or *in vitro* tensile distraction can be used effectively to lengthen arteries [5], small intestine [10, 12], and tendon [4, 6, 18]. Static and dynamic compression can regulate the thickness of growing calf articular cartilage *in vitro* [9], and ongoing research continues to explore how compression modulates the aspect ratio (thickness/radius) of explants. However, a 2-dimensional static flexural deformation, which produced a gradient of compressive and tensile strains within the tissue, was ultimately chosen for this work. One advantage of flexure was that local cartilage strains could be kept within non-injurious levels while producing large and easily measured displacements in explant shape. Additionally, flexural deformations could be chosen with curvatures similar to those present in anatomical features such as an articular surface or fold of an ear. Future studies might focus on producing shapes of a more anatomical nature as a further translational step. Certainly, understanding the kinematics of such 3-dimensional deformations would be more challenging than the 2-dimensional analysis presented in this dissertation.

The dynamic application of a shaping stimulus could also be examined, since this might be more favorable than a static stimulus for maintaining or promoting chondrocyte metabolism. Knowing that a large portion of the cartilage explant was under some amount of static compression in flexure and that static compression can inhibit proteoglycan synthesis and incorporation in a dose-dependent manner [14], it is

likely that matrix metabolism was mildly inhibited by the flexural stimulus used in this dissertation. Differences were not apparent in the matrix composition between loaded and non-loaded control samples, but this finding may reflect that culture durations were too short for metabolic changes to appear as altered tissue composition. Dynamic stimuli which promote matrix synthesis could be useful during longer cultures or when it is desirable to manipulate shape and matrix composition concurrently.

Several biochemical agents and growth factors were also chosen for these studies to regulate chondrocyte metabolism of matrix molecules or to perturb the post-translational modification and assembly of matrix. While β-D-xyloside and BAPN were used to alter proteoglycan and collagen remodeling and, consequently, matrix composition, other methods of directly modulating matrix composition could be further investigated. Matrix components such as chondroitin sulfate and hyaluronan could be enzymatically degraded with high specificity. Alternatively, dissociative conditions, such as 4M guanidine-HCl, could be used to extract non-covalently bound matrix components such as aggrecan. The growth factors, IGF-1 and TGF-β1, were selected for a number of reasons, including their use in a similar *in vitro* growth study where tensile properties were measured [2] and more broadly in other cartilage repair and tissue engineering studies. However, these growth factors are not unique in their ability to regulate the size and maturity of articular cartilage [2, 13, 15]. Admittedly, the use of IGF-1 and TGF-β1 at near maximally stimulating doses was a somewhat narrow and arbitrary selection, but their use helped elucidate relationships between matrix composition and functional properties which may be widely relevant among *in vitro* growth conditions.

6.2.b Furthering a Mechanistic Understanding

While several experiments were conducted to investigate potential mechanisms of mechanically-induced reshaping of cartilage, no specific process was identified with certainty as the primary mediator. Chondrocyte synthesis of matrix molecules and other proteins was found to contribute only slightly to the overall shape response, suggesting that the tissue does not grow into the imposed shape, but rather that existing components remodel to accommodate the altered conformation. A strong temperature-dependent effect of reshaping potentially indicated roles for either cell-independent biochemical reactions within the matrix or a biophysical remodeling of matrix. Additional experiments examined biochemical reactions which could alter the internal stress-state of the tissue, including stabilization through lysyl oxidase-mediated collagen crosslink formation and catabolic cleavage of matrix molecules. Using inhibitors of these processes did not alter the ability to reshape the tissue. It is possible that stabilization of cartilage shape could occur through the maturation of existing difunctional collagen crosslinks to trifunctional pyridinoline crosslinks, though the characteristic time constant for mature crosslink formation (~7-30 days, [1]) is considerably longer than the time necessary to achieve significant changes in immature cartilage shape (2-6 days). Future studies may be able to block the process of crosslink maturation through borohydride reduction to support or refute this mechanism more conclusively.

An attractive working hypothesis for future experiments is that cartilage reshaping occurs through a biophysical remodeling of matrix and is mediated by specific interactions between matrix components. This mechanism would be compatible with the temperature- and maturation-dependence of cartilage reshaping, as well as the inverse association observed between matrix composition (collage:GAG

ratio) and shape plasticity. Polymer entanglement and non-covalent bonding of various matrix constituents could be interesting targets for investigation. Previous experimental and theoretical studies have indicated that interactions between GAG collagen mediate the tensile properties of articular cartilage during maturation [3, 16]. Using similar experimental treatments, a preliminary study was carried out with cartilage in flexure at 4°C to determine if dissociation of matrix components followed by re-association could reproduce the positive reshaping response of cartilage at 37°C. However, the results were fairly inconclusive, since proteoglycan and other matrix molecules were partially depleted from the tissue, despite trying to saturate the dissociative solution with matrix prior to treatment. Previous studies have found that small peptide inhibitors of non-covalent decorin-fibronectin bonding facilitate the lengthening of tendons by collagen fiber sliding during tensile distraction [4, 6, 18]. Similar approaches might be used to perturb specific matrix interactions in cartilage and obviate the use of broadly dissociative conditions.

6.2.c Translational Considerations

As an additional avenue for future studies, the techniques developed in this dissertation may be adapted to other more clinically-relevant tissues including various types of engineered constructs or even native cartilage from sources currently used in chondral grafting. Clinical reports of the successful reattachment and healing of loose articular cartilage fragments support the concept of using engineered, shaped chondral grafts to treat articular lesions [7, 8]. However, transplantation of osteochondral grafts is a more commonly practiced treatment for articular lesions and offers benefits in graft fixation and enhanced bone-to-bone healing. Ongoing research into tissue interface engineering may assist in integrating mechanically shaped chondral tissue to

native subchondral bone or to an osseous substrate to form an osteochondral graft [19]. For many craniofacial applications, shaped chondral grafts are implanted in ways that integration to bone is not a concern, but often these grafts must be sufficiently mature to provide structural support themselves. While shaping could be performed *in vitro* as in the preceding studies, grafts for craniofacial applications could also be shaped *in vivo* and possibly *in situ* as recently demonstrated by using resorbable templates to shape subcutaneous costal cartilage grafts [11].

While the overall motivation of this work was to contribute to understanding how the shape, size, and maturity of cartilage can be prescribed through selected biophysical and biochemical stimuli, many of the approaches used in these studies altered these properties concurrently rather than discretely. Common underlying mediators, e.g. matrix composition and structure, may not allow for completely independent manipulation of these properties. Further translation of this dissertation's experimental approaches to engineering chondral grafts may require carefully chosen stimuli to be applied in parallel or series. For example, ongoing experiments are exploring whether sequential application of growth factors can enlarge calf articular cartilage without impairing mechanical properties. Preliminary results indicate that initial treatment with IGF-1 induces growth and softening, while subsequent treatment with TGF-β1 maintains the enlarged size and partially rescues the mechanical properties [17]. With further development of a mechanistic understanding of how chondrocyte metabolism and matrix remodeling coordinately affect the shape, size, and maturity of cartilage, regimens of prescribed stimuli may be improved to produce chondral tissues with desired properties

6.3 References

1. Ahsan T, Harwood FL, McGowan KB, Amiel D, Sah RL: Kinetics of collagen crosslinking in adult bovine articular cartilage. *Osteoarthritis Cartilage* 13:709-15, 2005.

2. Asanbaeva A, Masuda K, Thonar EJ-MA, Klisch SM, Sah RL: Regulation of immature cartilage growth by IGF-I, TGF-beta1, BMP-7, and PDGF-AB: role of metabolic balance between fixed charge and collagen network. *Biomech Model Mechanobiol* 7:263-76, 2008.

3. Asanbaeva A, Tam J, Schumacher BL, Klisch SM, Masuda K, Sah RL: Articular cartilage tensile integrity: Modulation by matrix depletion is maturation-dependent. *Arch Biochem Biophys* 474:175-82, 2008.

4. Caprise PA, Lester GE, Weinhold P, Hill J, Dahners LE: The effect of NKISK on tendon in an in vivo model. *J Orthop Res* 19:858-61, 2001.

5. Clerin V, Nichol JW, Petko M, Myung RJ, Gaynor JW, Gooch KJ: Tissue engineering of arteries by directed remodeling of intact arterial segments. *Tissue Eng* 9:461-72, 2003.

6. Esther RJ, Creighton RA, Draeger RW, Weinhold PS, Dahners LE: Effect of NKISK on tendon lengthening: an in vivo model for various clinically applicable dosing regimens. *J Orthop Res* 26:971-6, 2008.

7. Kaplonyi G, Zimmerman I, Frenyo AD, Farkas T, Nemes G: The use of fibrin adhesive in the repair of chondral and osteochondral injuries. *Injury* 19:267-72, 1988.

8. Nakamura N, Horibe S, Iwahashi T, Kawano K, Shino K, Yoshikawa H: Healing of a chondral fragment of the knee in an adolescent after internal fixation. A case report. *J Bone Joint Surg Am* 86-A:2741-6, 2004.

9. Nugent GE, Schmidt TA, Schumacher BL, Voegtline MS, Bae WC, Jadin KD, Sah RL: Static and dynamic compression regulate cartilage metabolism of proteoglycan 4 (PRG4). *Biorheology* 43:191-200, 2006.

10. Park J, Puapong DP, Wu BM, Atkinson JB, Dunn JC: Enterogenesis by mechanical lengthening: morphology and function of the lengthened small intestine. *J Pediatr Surg* 39:1823-7, 2004.

11. Pomahac B, Zuhaili B, Kudsi Y: Guided cartilage regeneration using resorbable template. *Eplasty* 8:e5, 2008.

12. Printz H, Schlenzka R, Requadt P, Tscherny M, Wagner AC, Eissele R, Rothmund M, Arnold R, Goke B: Small bowel lengthening by mechanical distraction. *Digestion* 58:240-8, 1997.

13. Sah RL, Chen AC, Grodzinsky AJ, Trippel SB: Differential effects of bFGF and IGF-I on matrix metabolism in calf and adult bovine cartilage explants. *Arch Biochem Biophys* 308:137-47, 1994.

14. Sah RL, Kim YJ, Doong JH, Grodzinsky AJ, Plaas AHK, Sandy JD: Biosynthetic response of cartilage explants to dynamic compression. *J Orthop Res* 7:619-36, 1989.

15. Sah RL, Trippel SB, Grodzinsky AJ: Differential effects of serum, insulin-like growth factor-I, and fibroblast growth factor-2 on the maintenance of cartilage physical properties during long-term culture. *J Orthop Res* 14:44-52, 1996.

16. Thomas GC, Asanbaeva A, Vena P, Sah RL, Klisch SM: A nonlinear constituent based viscoelastic model for articular cartilage and analysis of tissue remodeling due to altered glycosaminoglycan-collagen interactions. *J Biomech Eng* 131:101002, 2009.

17. Van Donk J, Dills K, Williams GM, Smith SA, Chen AC, Raub CB, Hazelwood SJ, Klisch SM, Sah RL: Regulation of articular cartilage volume and compressive properties by sequential application of IGF-1 and TGF-beta 1 during in vitro growth. *Biomedical Engineering Society*, 2009.

18. Wood ML, Luthin WN, Lester GE, Dahners LE: Tendon creep is potentiated by NKISK and relaxin which produce collagen fiber sliding. *Iowa Orthop J* 23:75-9, 2003.

19. Yang PJ, Temenoff JS: Engineering Orthopedic Tissue Interfaces. *Tissue Eng Part B Rev*, 2009.

APPENDIX A

CELL DENSITY ALTERS MATRIX ACCUMULATION IN TWO DISTINCT FRACTIONS AND THE MECHANICAL INTEGRITY OF ALGINATE-CHONDROCYTE CONSTRUCTS

A.1 Abstract

Chondrocyte density in articular cartilage is known to change with the development and growth of the tissue and may play an important role in the formation of a functional extracellular matrix (ECM). The objective of this study was to determine how initial chondrocyte density in an alginate hydrogel affects the matrix composition, its distribution between the cell-associated (CM) and further removed matrix (FRM) fractions, and the tensile mechanical properties of the developing engineered cartilage. Alginate constructs containing primary bovine chondrocytes at densities of 0, 4, 16, and 64 million cells/ml were fabricated and cultured for 1 or 2 weeks, at which time structural, biochemical, and mechanical properties were analyzed. Both matrix content and distribution varied with the initial cell density. Increasing cell density resulted in an increasing content of collagen and sulfated-glycosaminoglycan (GAG) and an increasing proportion of these molecules localized

in the CM. While the equilibrium tensile modulus of cell-free alginate did not change with time in culture, the constructs with highest cell density were 116% stiffer than cell-free controls after two weeks of culture. The equilibrium tensile modulus was positively correlated with total collagen (r^2=0.47, $p<0.001$) and GAG content (r^2=0.68, $p<0.001$), and these relationships were enhanced when analyzing only those matrix molecules in the CM fraction (r^2=0.60 and r^2=0.72 for collagen and GAG respectively, each $p<0.001$). Overall, the results of this study indicate that initial cell density has a considerable effect on the developing composition, structure, and function of alginate-chondrocyte constructs.

A.2 Introduction

Articular cartilage functions as the load-bearing, low-friction, wear-resistant tissue lining the ends of bones in diarthrodial joints. These remarkable functions arise in part from the composition and structure of the highly hydrated cartilage extracellular matrix (ECM) consisting primarily of a collagen network which constrains the swelling pressure of proteoglycans. During the development and growth of articular cartilage, the attainment of these functional properties is concurrent with changes in biochemical content, tissue structure, and cellular organization [20, 40, 41]. All too frequently, the normal functions of adult articular cartilage are compromised by traumatic injury, age-related degeneration, or disease. Strategies for addressing these problems include cartilage tissue engineering, which may seek to recapitulate the natural growth processes to produce a biological replacement tissue [34]. Therefore, elucidating the principles underlying the formation of a functional extracellular matrix in articular cartilage is important for the understanding of cartilage development and repair.

The in vitro study of chondrocytes, the cells within articular cartilage, has been aided by methods of three-dimensional culture within hydrogels, such as alginate [5] and agarose [3, 15]. These commonly studied hydrogels enable chondrocytes to maintain their phenotype in cell culture and have proven useful for investigations of matrix metabolism. The matrix produced by chondrocytes encapsulated in alginate or agarose is similar in composition to the ECM of native articular cartilage and becomes entrapped in the surrounding hydrogel [2, 3, 17]. Moreover, this newly synthesized matrix exhibits many of the physicochemical properties associated with native articular cartilage [4]. As a result of these findings, there has been significant interest in using these hydrogels as scaffolds for the development of engineered cartilage in

vitro [1, 10, 19, 27, 43] and in vivo [5, 30, 33]. These materials allow chondrocytes to be organized into three-dimensional constructs and can serve as a medium through which biochemical and mechanical stimuli can be delivered to direct the development of the engineered cartilage [9]

The mechanism of alginate gelation provides a means to separate two distinct matrix fractions from alginate cultures. Alginate is a linear polysaccharide consisting of D-mannuronic and L-guluronic acid subunits that gels in the presence of divalent cations such as Ca^{2+} [13, 15]. The ionotropic gelation of alginate is readily reversible through the chelation of these cations. When alginate is solubilized in this manner, entrapped chondrocytes and the matrix bound around them, termed the cell-associated matrix (CM), can be separated from the soluble, further removed matrix (FRM) fraction by centrifugation [16]. The relative amounts of matrix in these two fractions may be an indicator of interactions between matrix molecules during the development of a cohesive ECM

The integrity of engineered cartilage is commonly assessed using compressive, tensile, and shear mechanical tests [6]. The compressive properties of alginate and alginate-chondrocyte constructs have been well characterized [19, 23, 30, 43], and, recently, the tensile properties of alginate have been analyzed [8, 39]. In native articular cartilage, tensile properties such as the equilibrium and dynamic moduli and the strength at failure show positive correlations with measures of the collagen content and cross-links [40]. Consequently, measuring the tensile mechanical properties of alginate-chondrocyte constructs may yield important information for the evolving composition-structure-function relationships for the tissue formed in this culture system.

The cellularity of native articular cartilage varies with both age and depth [20] and decreases from approximately 120 to 50 million cells/ml from the fetal to adult stages in deeper portions of bovine patellofemoral groove tissue. In hydrogel constructs, cell density has been shown to affect the bulk matrix content of collagen and sulfated-glycosaminoglycans (GAG) and the compressive mechanical properties [25, 26, 30]. In alginate, cell density and the resulting nutrient utilization can also contribute to cell death and characteristic viability profiles through the depth of the construct [19]. However, it remains unclear how cell density affects the composition of matrix in the CM and FRM of alginate cultures and how the amount and distribution of this matrix relates to the mechanical properties of the constructs.

To address the factors contributing to the formation of a functional cartilage matrix, this study focuses on the role of initial chondrocyte density in alginate culture. The objective of this study was to examine how the accumulation of matrix molecules in the CM and FRM and the mechanical integrity of the constructs in tension are coordinately affected by initial cell density.

A.3 Materials and Methods

Cartilage Harvest and Chondrocyte Isolation

Osteochondral cores were harvested from the patellofemoral groove and femoral condyles of 1-3 week old bovine calves. Cores were obtained from four animals and pooled into two groups, each containing cores from two animals. These two groups were collected at different times and used for separate cultures. Using a guide, the superficial ~0.5 mm of articular cartilage was removed with a scalpel and discarded. The remaining cartilage was minced and sequentially digested for 1 h with

0.2% pronase (Sigma-Aldrich, St. Louis, MO) and for 16 h with 0.02% collagenase P (Roche Diagnostics, Indianapolis, IN) [29] to isolate middle and growth zone chondrocytes.

Alginate Construct Formation and Culture

A 2% alginate (Keltone LVCR, Kelco, Chicago, IL) solution in 0.9% NaCl was prepared and sterilized by filtering through a 0.22 μm pore size polyethersulfone filter (Millipore, Billerica, MA). Following enzymatic digestion of the tissue, chondrocytes were washed in phosphate-buffered saline (PBS), and their concentration and viability were assessed with a hemocytometer and trypan blue dye exclusion. The chondrocytes were then resuspended in the 2% alginate solution at cell densities of 4, 16, and 64 million cells/ml. Chondrocyte-alginate suspensions were injected into a custom designed slab mold consisting of two Ca^{2+} permeable membranes (Whatman 5 filter paper, Whatman International Ltd., Maidstone, England) rigidly supported by stainless steel mesh and separated by a stainless-steel casting frame, similar to previously reported devices [32, 43]. The suspensions were gelled via Ca^{2+} diffusion, achieved by submerging the mold in 102 mM $CaCl_2$ in an excess volume of 0.9% NaCl for 10 min and then washing in 0.9% NaCl for 5 min. The chondrocyte-alginate slabs were removed from the mold and punched into circular constructs measuring 10 mm in diameter and 1.7 mm in thickness. Remaining portions of the slabs were weighed wet and frozen for later analysis of DNA content. Cell-free alginate constructs were formed similarly to serve as controls for subsequent measurements of structural and mechanical properties.

Constructs were cultured in a humidified incubator at 37°C and 5% CO_2 in DMEM/F-12 (Invitrogen, Carlsbad, CA) supplemented with 20% fetal bovine serum

(FBS), ascorbic acid (25 μg/ml), antimicrobials (100 U/ml penicillin, 100 μg/ml streptomycin, 0.25 μg/ml Fungizone), and amino acids (0.1 mM MEM non-essential amino acids, 0.4 mM L-proline, and 2 mM L-glutamine). Medium was changed every 2-3 days and the volume used (1 ml per million cells per day) was based on initial cell densities. Constructs were maintained in culture for either one or two weeks (n=6-9 constructs per cell density group per time point).

Mechanical Testing

Following culture, constructs were weighed wet, and their thickness was measured using a contact-sensing micrometer. A tapered tensile specimen, with a gauge region measuring 5 mm in length by 1.8 mm in width, was punched through the full thickness of the center of each construct. Specimens were inserted into clamps on a mechanical testing apparatus (E100, BioSynTech Ltd., Laval, Quebec, Canada) equipped with a 1 N load cell and kept hydrated throughout testing with Dulbecco's PBS containing calcium and magnesium. Each specimen was elongated at 0.5 mm/min to reach a tare load of 1 mN and then allowed to relax for 10 min to ensure equilibrium had been reached. Specimens were then elongated to 10% strain at a constant strain rate of 0.2% per second and allowed to relax to equilibrium for 20 min. From these data, an equilibrium tensile modulus was calculated for each construct. Tensile tests were also performed on cell-free alginate constructs on day 0 (n=7).

Biochemical Analysis

Qualitative histological analysis of selected samples with Alcian Blue or hematoxylin and eosin indicated that the ECM appeared nearly homogeneously distributed through the constructs, while, microscopically, matrix accumulation was

pronounced in the pericellular region. Consequently, a large remaining portion of each construct (approximately one third of the whole) was used for biochemical analysis since this portion should be representative of the whole and also not be altered by mechanical testing. These samples were weighed wet and nutated for 30 min at 4°C in five volumes of 55 mM sodium citrate in 0.9% NaCl to solubilize the alginate. Samples were centrifuged for 10 min at 100 g to separate the cells and their associated matrix (CM) from the soluble further removed matrix (FRM). These fractions were digested with proteinase K (Roche Diagnostics) and analyzed for DNA with PicoGreen® (Molecular Probes, Eugene, OR) [28], for hydroxyproline with dimethylaminobenzaldehyde (DMBA) [42], and for GAG with a modified dimethylmethylene blue (DMMB) assay [11]. Collagen content was calculated by assuming a collagen to hydroxyproline mass ratio of 7.25 [18, 31]. Day 0 samples were also solubilized, separated, digested and analyzed for DNA content.

Viability Testing

Two constructs of each cell density cultured for one or two weeks were randomly chosen for viability analysis. A full-thickness 2mm diameter core was removed from a location approximately 3mm from the edge of each construct. Cores were incubated at room temperature in 200μl PBS containing 40 μM calcein AM and 20 μM ethidium homodimer-1 (Molecular Probes) for 20 min to stain viable and non-viable cells, respectively, and then washed twice in PBS for 10 min each. Cores were sectioned in half to expose a full-thickness plane and imaged using fluorescent microscopy. Automated cell counts were made using a custom-written code in Matlab (The Mathworks Inc., Natick, MA), and these were validated with manual counting.

Statistical Analysis and Data Presentation

Data are presented as mean ± SEM. A two factor ANOVA (α=0.05) was used to determine the effects of initial cell density and culture time, and appropriate post-hoc comparisons were made with Tukey tests. Since percentages form binomial rather than normal distributions, arcsine transformation was applied to the matrix distribution data (i.e., % GAG and % collagen in the CM) to normalize these data [37]. However, since the transformation resulted in no changes in statistical trends, only untransformed data is presented for clarity. Additionally, a single factor ANOVA (α=0.05) was used to determine the effect of culture time on the mechanical properties of the cell-free control constructs.

Univariate and multivariate linear regression were used to analyze relationships between the constructs' mechanical properties and biochemical content. The analyses were performed on all data from chondrocyte-seeded constructs, and significant relationships were determined using a criterion of $p<0.05$ when assessing regression slopes. Coefficients of determination (r^2) and coefficients of multiple determination (R^2) are reported along with significant relationships.

All statistical analyses were performed using Systat 10.2.05 (Systat Software, Richmond, CA).

A.4 Results

Construct Growth and Physical Properties

Alginate-chondrocyte construct growth was macroscopically apparent. The higher cell density constructs were larger and more opaque following culture (**Fig. A.1**). Physical manipulation of these higher density constructs was also easier with

increasing time in culture. Quantitative measures of the construct structural properties, including thickness (**Fig. A.2A**) and wet weight (**Fig. A.2B**), confirmed visual observations. Thickness was significantly affected by initial cell density ($p<0.001$) and culture time ($p<0.05$) and was greatest for constructs initially seeded at 64 million cells/ml ($p<0.05$). After two weeks of culture, constructs seeded at 16 or 64 million cells/ml had wet weights which were greater than those of lower density constructs ($p<0.001$) and were increased from their respective values at one week ($p<0.01$). For the cell-free alginate disks, neither construct thickness nor wet weight were significantly changed from the initial value by subsequent culture. To characterize construct growth, an index of relative net cell proliferation was calculated as total DNA content after culture normalized to pre-culture values. Relative proliferation increased from one to two weeks for each of the cell-containing groups ($p<0.01$) and this effect was dependent upon initial cell density ($p<0.001$) and highest at two weeks for constructs seeded at 16 million cells/ml (**Fig. A.2C**). Cell viability was uniform through the thickness of the constructs and exceeded 96% for all densities following one and two weeks of culture. No differences in viability were observed between groups.

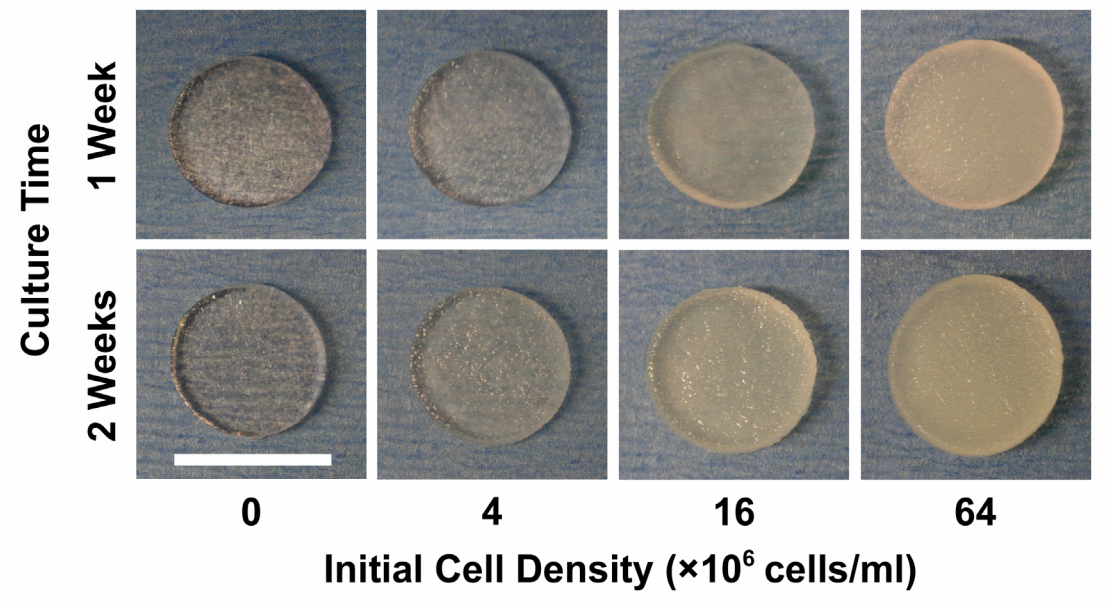

Figure A.1: Gross appearance of chondrocyte-seeded alginate constructs after 1 or 2 weeks of culture. Higher cell density constructs are visibly larger and more opaque. (bar = 10 mm)

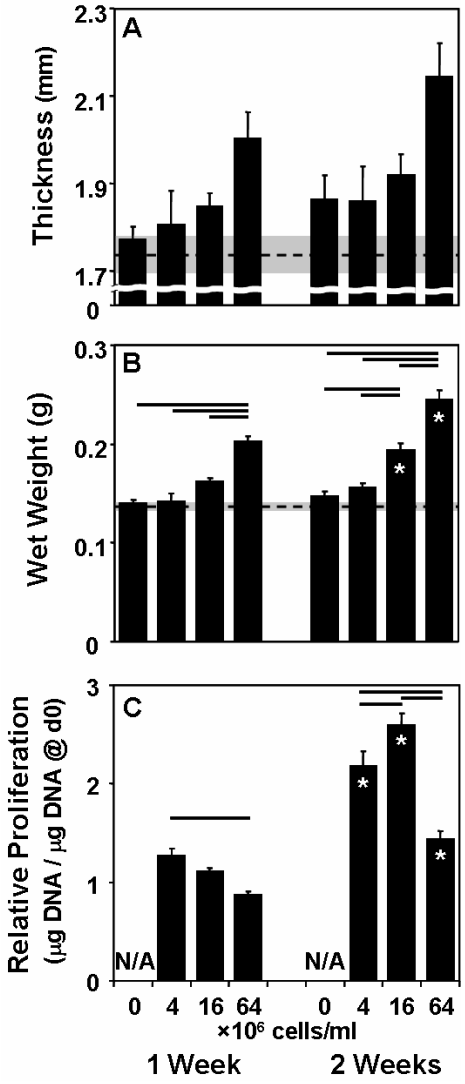

Figure A.2: Measurements of construct growth: thickness (**A**), wet weight (**B**), and proliferation (**C**) measured as total DNA content relative to that at day 0. Dotted line and gray bar represent the mean ± SEM of cell-free alginate disks on day 0. Bars (**—**) indicate a significant difference between cell density groups at the same time point ($p<0.05$). Stars (✲) indicate a significant difference compared to 1 week for the same cell density ($p<0.05$). (n=6-9)

Deposition and Distribution of Cartilage Matrix

Cartilage matrix content, calculated as total GAG or collagen as a percentage of wet weight, varied among the construct groups following culture. GAG content increased with increasing cell density at both time points ($p<0.001$) and increased from one to two weeks for each density ($p<0.01$, **Fig. A.3A**). Collagen content increased with increasing density at two weeks ($p<0.05$) and increased from one to two weeks for the two highest density groups ($p<0.01$, **Fig. A.3B**).

Matrix content was also normalized to the total DNA content of the samples (**Fig. A.3C, D**). The total amount of GAG was similar among the different density groups at both one and two week culture times, except for those constructs seeded at 4 million cells/ml and cultured for two weeks, which had significantly greater amounts of GAG ($p<0.001$). Collagen content was also similar for the two highest density groups, but slightly higher for constructs seeded at 4 million cells/ml ($p<0.01$). Among all constructs, collagen content increased from one to two weeks ($p<0.001$). At each culture time, collagen content in the CM was similar among constructs of different densities, but collagen content in the FRM decreased with increasing cell density ($p<0.05$).

The distribution of matrix molecules between the CM and FRM fractions was also dependent upon initial cell density, and the collagen distribution was dependent on time in culture. The percentage of GAG localized in the CM increased with increasing cell density ($p<0.01$) and exceeded 98% in the highest cell density constructs at two weeks (**Fig. A.3E**). Similarly, the percentage of collagen in the CM increased with increasing cell density ($p<0.05$) and also increased slightly with time in culture ($p<0.001$, **Fig. A.3F**).

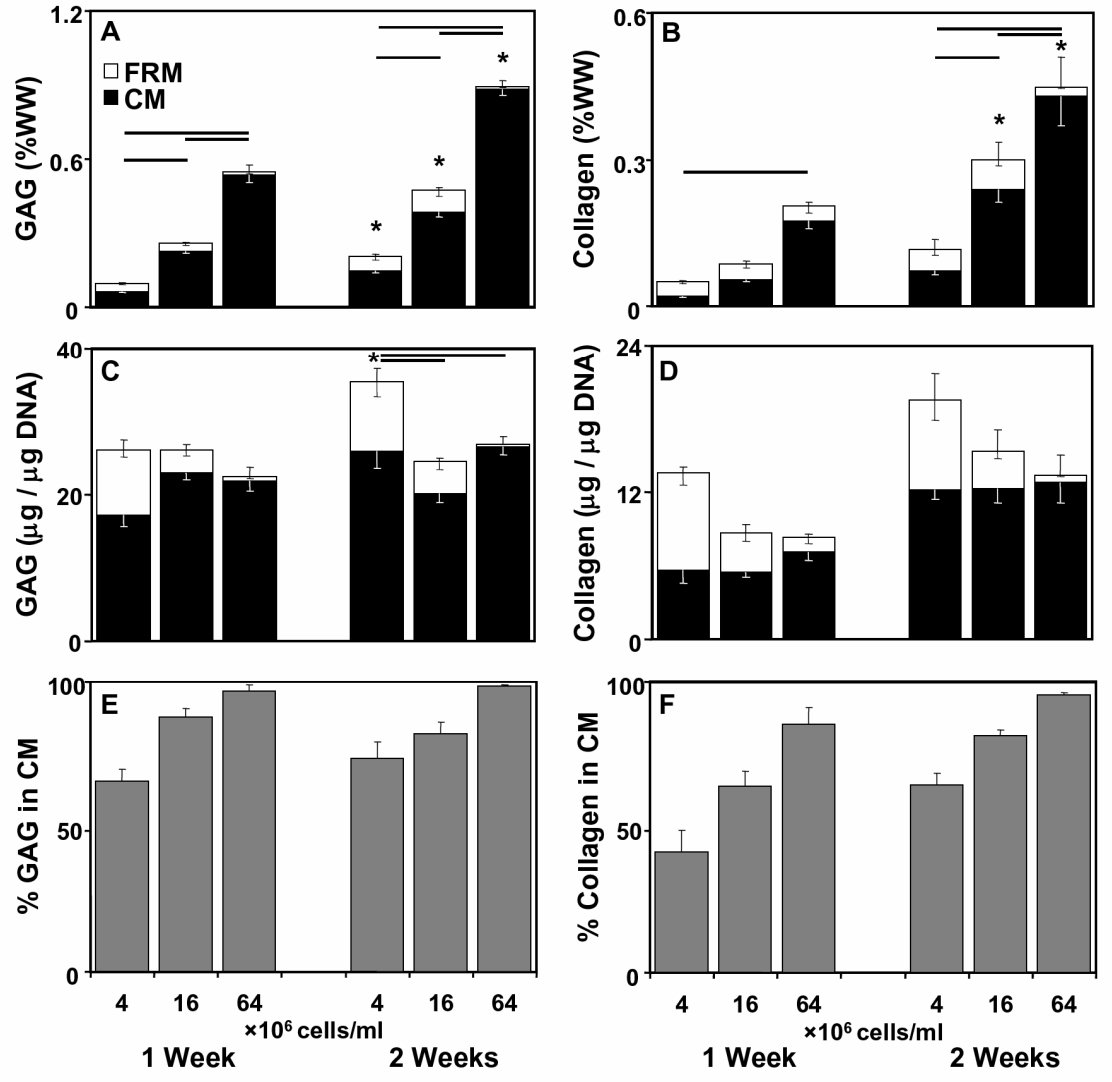

Figure A.3: GAG (**A,C**) and collagen (**B,D**) content normalized to wet weight (**A,B**) and DNA content (**C,D**) in the CM (black) and FRM (white). Percentage of GAG (**E**) and collagen (**F**) localized in the CM. Significant differences between total matrix content are indicated by bars (**–**) ($p<0.05$) for comparisons at the same time point and stars (**✶**) ($p<0.05$) for comparisons to the same density group at 1 week. (n=6-9)

Tensile Mechanical Properties

Mechanical testing of cell-free alginate constructs on day 0 revealed an initial equilibrium tensile modulus of 4.1 ± 0.4 kPa (n=7). Subsequent culture of cell-free alginate disks for either one or two weeks did not significantly change the modulus from this value (**Fig. A.4**). However, constructs initially seeded at 16 and 64 million cells/ml demonstrated moduli which were, respectively, 45% ($p<0.01$) and 116% ($p<0.001$) greater than cell-free controls after two weeks. The highest cell density constructs were significantly stiffer than all lower density constructs at two weeks ($p<0.001$) and 60% stiffer after two weeks of culture compared to one week ($p<0.001$). Equilibrium moduli of constructs seeded at 4 million cells/ml were not significantly different than cell-free controls at either culture time point.

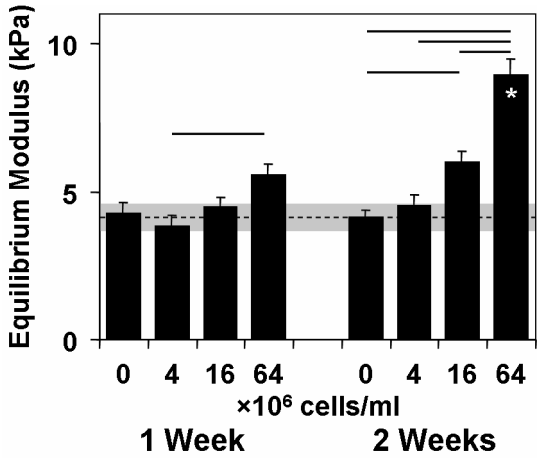

Figure A.4: Equilibrium tensile moduli of chondrocyte-seeded alginate constructs following 1 or 2 weeks of culture. Dotted line and gray bar represent the mean ± SEM of cell-free alginate disks on day 0. Bars (**—**) indicate a significant difference between cell density groups at the same time point ($p<0.05$). Stars (☆) indicate a significant difference compared to 1 week for the same cell density ($p<0.05$). (n=6-9)

Composition-Structure-Function Relationships

Measures of collagen and GAG content in these constructs were correlated to the equilibrium tensile modulus. Total collagen content as a percentage of wet weight was positively correlated to the equilibrium tensile modulus (r^2=0.47, p<0.001, **Fig. A.5A**), as was total GAG content as a percentage of wet weight (r^2=0.68, p<0.001, **Fig. A.5C**). Both of these relationships were improved when only the amounts of these molecules in the CM were considered (r^2=0.60 and r^2=0.72 for collagen and GAG respectively, each p<0.001, **Fig. A.5B, D**). Similarly, multivariate regression analysis indicated that the modulus was related to total collagen and GAG content (R^2=0.68, p<0.001) as well as collagen and GAG content in the CM (R^2=0.74, p<0.001). The collagen and GAG content in the FRM were negatively correlated with the equilibrium tensile modulus (data not shown), but these relationships were poorly fit to the data (r^2=0.16, p<0.01 for collagen; r^2=0.14, p<0.05 for GAG).

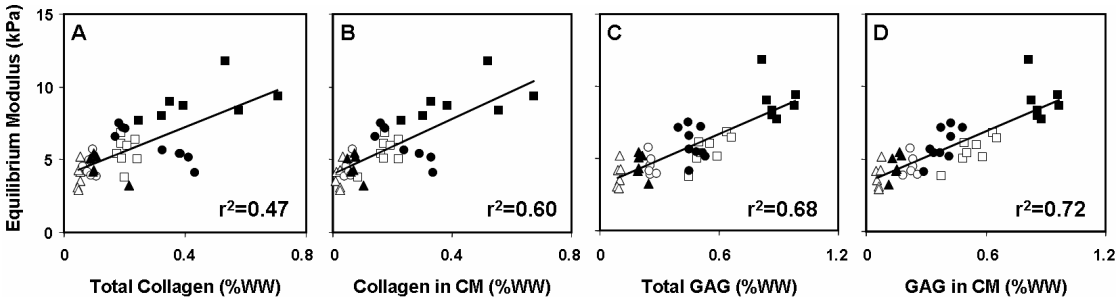

Figure A.5: Regression analysis between the equilibrium tensile modulus and measures of biochemical content (positive correlations, $p<0.001$). Data points are shown for constructs with initial cell densities of 4 (△,▲), 16 (○,●), and 64 (□,■) million cells/ml after 1 week (△,○,□) or 2 weeks (▲,●,■) of culture.

A.5 Discussion

The results of this study show that the initial cell density in alginate constructs plays a substantial role in determining the composition, structure, and function of the developing tissue. Cell density is a strong determinant of the growth characteristics of these constructs (**Fig. A.1, A.2**) and is likely an important design parameter for the creation of engineered cartilage suitable for therapeutic applications. The biochemical analysis of the constructs clarifies the effects of initial cell density on matrix content and its distribution between the CM and FRM fractions. Within the ranges studied here, higher cell density and longer culture duration were generally associated with increased GAG and collagen content (**Fig. A.3A, B**) and a greater proportion of these molecules localized in the CM (**Fig. A.3E, F**). This latter finding may indicate that constructs of higher cell density are initially capable of forming a more extensive collagen network which can entrap a larger proportion of proteoglycans. In addition, the increasing mechanical integrity in the constructs of higher cell density (**Fig. A.4**) provides evidence that the newly assembled cartilage matrix in these tissues is mechanically functional.

Significant relationships were revealed between measures of matrix accumulation and the mechanical behavior of the constructs in tension, and these help distinguish the functional roles of matrix in the CM and FRM. While the total collagen and GAG contents were positively correlated with the equilibrium tensile modulus (**Fig. A.5A, C**), these relationships were improved, especially for collagen, by only considering the fraction of matrix in the CM (**Fig. A.5B, D**). A possible explanation for this result is that while the soluble FRM likely consists of unbound and degraded matrix constituents, the CM is primarily composed of those molecules which are bound around the chondrocytes and contribute to the formation of a functional ECM.

This finding also highlights the complexity of composition-structure-function relationships, where mechanical properties may depend not only on the amount of matrix present, but also on the spatial distribution and interactions of the matrix components.

The highest initial cell density chosen for this study (64 million cells/ml) corresponds to that of bovine articular cartilage at an intermediate stage of growth between calf (1-3 weeks) and adult (1 year) [20]. The two lower cell densities (4 and 16 million cells/ml) represent sub-physiologic densities, but are within the range of values used previously in cartilage tissue engineering studies [10, 19, 26, 30, 33, 43]. These cell densities changed with time and may have varied spatially through the constructs, as subsequent culture resulted in both cell proliferation and construct growth. Estimates determined from the DNA content and wet weight data indicate that the spatially averaged cell density increased for the two lowest density groups and decreased for the highest density group. A choice was also made to use full-thickness specimens taken through the center of each construct for mechanical testing. Though this provided a measurement of the tensile behavior of an entire construct, such methods would not be able to detect any possible heterogeneity in the mechanical properties through the thickness of a construct. The potential of producing depth-dependent properties in engineered tissues is of interest [22] since the compressive and tensile properties of native articular cartilage vary with depth from the surface [21, 35].

Differences in cell density can directly impact the availability of nutrients throughout the construct and alter chondrocyte biosynthetic function. Previous studies have raised concerns about insufficiencies or differences in nutrient availability which may arise from varying cell densities in hydrogel constructs [19, 25, 26]. The limited

nutrient availability in constructs of high cell density was responsible for reduced matrix synthesis and, in extreme cases, chondrocyte death. However, the present investigation appeared to minimize such problems by providing a set and sufficient ratio of media to the number of initial cells and by choosing the construct geometry to have relatively short diffusion distances. Evidence for adequate nutrition includes the uniformly high chondrocyte viability through the thickness of the constructs. In addition, the apparent homogeneity of matrix within the samples and the similar biochemical content normalized to DNA content among samples of varying cell density indicate that biosynthetic function was not adversely affected by nutrient limitation.

The effect of cell density on diffusion phenomena within the developing tissue may potentially account for the observed trends in matrix accumulation in the CM and FRM. The intercellular distances determined by cell density will dictate the diffusion of soluble factors and matrix molecules between chondrocytes [7, 12]. As the transport characteristics of soluble factors vary with cell density, cell-cell signaling and, consequently, matrix metabolism may be altered. Similarly, variations in the diffusion of matrix molecules may affect the distribution of matrix between the CM and FRM fractions. In lower density cultures, matrix molecules are able to diffuse to a position farther from any neighboring cell; whereas, in higher density cultures, matrix molecules will have a closer proximity to the cells, where they are more likely to be incorporated into the CM.

To our knowledge, this study includes the first reported values of the tensile behavior of alginate-chondrocyte constructs. Mechanical tensile testing has typically been bypassed as a tool for studying hydrogel-based engineered cartilage in favor of compressive testing. However, this study shows that tensile testing can help delineate

the composition-structure-function relationships of these constructs. An understanding of these relationships may be important for the effective design and assessment of engineered cartilage. In this study, equilibrium tensile moduli were determined for the alginate-chondrocyte constructs, and this data provides a sensitive measure of the mechanical integrity of the specimens. Though failure properties were not ascertained, they could provide a more complete picture of the tensile behavior and composition-structure-function relationships of the constructs and warrant further study.

In the present study, no significant change was noted in the equilibrium tensile modulus of cell-free alginate from gelation on day 0 through two weeks of culture. This finding differs from that of Drury et al. who found that the tangent tensile modulus of alginate increased following incubation, with most of the change occurring during the first week [8]. This difference may be attributable to differences in alginate composition, gelation conditions, and culture environment, all of which have been shown to variously affect the mechanical properties of the hydrogel [8, 23, 24, 43]. In fact, other studies have reported decreases in the compressive stiffness of alginate with culture [23, 43], indicating the sensitivity of alginate's mechanical integrity to a variety of factors.

The extent of maturation of the functional properties of cartilage constructs in vitro will likely affect their load-bearing and integrative capabilities in therapeutic applications in vivo [36]. The equilibrium tensile modulus of native cartilage increases from ~1 MPa in superficial fetal bovine tissue to ~4MPa in superficial adult tissue [40]. In comparison, the tensile stiffness exhibited by these alginate-chondrocyte constructs is inferior to that of native cartilage, even at the fetal stage. However, the mechanical properties of these constructs could likely be modulated and even enhanced by lengthening the culture period, modifying the hydrogel properties, or

providing additional biochemical and biomechanical stimuli [14, 34, 38]. A more thorough analysis of these factors may provide additional insight into the mechanisms governing the formation and development of functional matrix in engineered cartilage.

A.6 Acknowledgments

Appendix A, in full, is reproduced from *Acta Biomaterialia*, volume 1, number 6, 2005 with permission from Elsevier, Inc. The dissertation author was the primary author and thanks co-authors Travis J. Klein and Robert L. Sah. This work was supported in part by grants from NASA, NIH, and NSF. Individual support was received through a NSF Graduate Research Fellowship (to GMW). The author thanks Dr. Albert Chen and Mr. Van Wong for training and assistance and Dr. Won Bae for generously providing the automated viability analysis code.

A.7 References

1. Awad HA, Wickham MQ, Leddy HA, Gimble JM, Guilak F: Chondrogenic differentiation of adipose-derived adult stem cells in agarose, alginate, and gelatin scaffolds. *Biomaterials* 25:3211-22, 2004.

2. Aydelotte MB, Schleyerbach, R., Zeck, B.J., Kuettner, K.E.: Articular chondrocytes cultured in agarose gel for study of chondrocytic chondrolysis. In: *Articular Cartilage Biochemistry,* ed. by KE Kuettner, Schleyerback, R., Hascall, V.C., Raven Press, New York, 1986, 235-56.

3. Benya PD, Shaffer JD: Dedifferentiated chondrocytes reexpress the differentiated collagen phenotype when cultured in agarose gels. *Cell* 30:215-24, 1982.

4. Buschmann MD, Gluzband YA, Grodzinsky AJ, Kimura JH, Hunziker EB: Chondrocytes in agarose culture synthesize a mechanically functional extracellular matrix. *J Orthop Res* 10:745-58, 1992.

5. Chang SC, Rowley JA, Tobias G, Genes NG, Roy AK, Mooney DJ, Vacanti CA, Bonassar LJ: Injection molding of chondrocyte/alginate constructs in the shape of facial implants. *J Biomed Mater Res* 55:503-11, 2001.

6. Chen AC, Klisch SM, Bae WC, Temple MM, McGowan KB, Gratz KR, Schumacher BL, Sah RL: Mechanical characterization of native and tissue-engineered cartilage. In: *Cartilage and Osteoarthritis,* ed. by M Sabatini, DeCeuninck F, Pastoureau P, Humana Press, Totowa, NJ, 2004, 157-90.

7. DiMicco MA, Sah RL: Dependence of cartilage matrix composition on biosynthesis, diffusion, and reaction. *Transport in Porous Media* 50:57-73, 2003.

8. Drury JL, Dennis RG, Mooney DJ: The tensile properties of alginate hydrogels. *Biomaterials* 25:3187-99, 2004.

9. Drury JL, Mooney DJ: Hydrogels for tissue engineering: scaffold design variables and applications. *Biomaterials* 24:4337-51, 2003.

10. Elisseeff JH, Lee A, Kleinman HK, Yamada Y: Biological response of chondrocytes to hydrogels. *Ann N Y Acad Sci* 961:118-22, 2002.

11. Enobakhare BO, Bader DL, Lee DA: Quantification of sulfated glycosaminoglycans in chondrocyte/alginate cultures, by use of 1,9-dimethylmethylene blue. *Anal Biochem* 243:189-91, 1996.

12. Francis K, Palsson BO: Effective intercellular communication distances are determined by relative time constants for cyto/chemokine secretion and diffusion. *Proc Natl Acad Sci USA* 94:12258-62, 1997.

13. Grant GT, Morris, E.R., Rees, D.A., Smith, P.J.C., Thom, D.: Biological interactions between polysaccharides and divalent cations: the egg-box model. *FEBS Letters* 32:195-98, 1973.

14. Guilak F, Butler DL, Goldstein SA: Functional tissue engineering: the role of biomechanics in articular cartilage repair. *Clin Orthop Rel Res*:S295-305., 2001.

15. Guo JF, Jourdian GW, MacCallum DK: Culture and growth characteristics of chondrocytes encapsulated in alginate beads. *Connect Tissue Res* 19:277-97, 1989.

16. Häuselmann HJ, Aydelotte MB, Schumacher BL, Kuettner KE, Gitelis SH, Thonar EJ-MA: Synthesis and turnover of proteoglycans by human and bovine adult articular chondrocytes cultured in alginate beads. *Matrix* 12:116-29, 1992.

17. Häuselmann HJ, Fernandes RJ, Mok SS, Schmid TM, Block JA, Aydelotte MB, Kuettner KE, Thonar EJ: Phenotypic stability of bovine articular chondrocytes after long-term culture in alginate beads. *J Cell Sci* 107:17-27, 1994.

18. Herbage D, Bouillet J, Bernengo J-C: Biochemical and physicochemical characterization of pepsin-solubilized type-II collagen from bovine articular cartilage. *Biochem J* 161:303-12, 1977.

19. Heywood HK, Sembi PK, Lee DA, Bader DL: Cellular utilization determines viability and matrix distribution profiles in chondrocyte-seeded alginate constructs. *Tissue Eng* 10:1467-79, 2004.

20. Jadin KD, Wong BL, Bae WC, Li KW, Williamson AK, Schumacher BL, Price JH, Sah RL: Depth-varying density and organization of chondrocyte in immature and mature bovine articular cartilage assessed by 3-D imaging and analysis. *J Histochem Cytochem* 53:1109-19, 2005.

21. Kempson GE, Freeman MAR, Swanson SAV: Tensile properties of articular cartilage. *Nature* 220:1127-8, 1968.

22. Klein TJ, Schumacher BL, Schmidt TA, Li KW, Voegtline MS, Masuda K, Thonar EJ-MA, Sah RL: Tissue engineering of stratified articular cartilage from chondrocyte subpopulations. *Osteoarthritis Cartilage* 11:595-602, 2003.

23. LeRoux MA, Guilak F, Setton LA: Compressive and shear properties of alginate gel: effects of sodium ions and alginate concentration. *J Biomed Mater Res* 47:46-53, 1999.

24. Martinsen A, Skjak-Braek G, Smidsrod O: Alginate as immobilization material: I. correlation between chemical and physical properties of alginate gel beads. *Biotechnol Bioeng* 33:79-89, 1989.

25. Mauck RL, Nicoll SB, Seyhan SL, Ateshian GA, Hung CT: Synergistic action of growth factors and dynamic loading for articular cartilage tissue engineering. *Tissue Eng* 9:597-611, 2003.

26. Mauck RL, Seyhan SL, Ateshian GA, Hung CT: Influence of seeding density and dynamic deformational loading on the developing structure/function relationships of chondrocyte-seeded agarose hydrogels. *Ann Biomed Eng* 30:1046-56, 2002.

27. Mauck RL, Soltz MA, Wang CC, Wong DD, Chao PH, Valhmu WB, Hung CT, Ateshian GA: Functional tissue engineering of articular cartilage through dynamic loading of chondrocyte-seeded agarose gels. *J Biomech Eng* 122:252-60, 2000.

28. McGowan KB, Kurtis MS, Lottman LM, Watson D, Sah RL: Biochemical quantification of DNA in human articular and septal cartilage using PicoGreen and Hoechst 33258. *Osteoarthritis Cartilage* 10:580-7, 2002.

29. Mok SS, Masuda K, Häuselmann HJ, Aydelotte MB, Thonar EJ: Aggrecan synthesized by mature bovine chondrocytes suspended in alginate. Identification of two distinct metabolic matrix pools. *J Biol Chem* 269:33021-7, 1994.

30. Paige KT, Cima LG, Yaremchuk MJ, Schloo BL, Vacanti JP, Vacanti CA: De novo cartilage generation using calcium alginate-chondrocyte constructs. *Plast Reconstr Surg* 97:168-78, 1996.

31. Pal S, Tang L-H, Choi H, Habermann E, Rosenberg L, Roughley P, Poole AR: Structural changes during development in bovine fetal epiphyseal cartilage. *Collagen Rel Res* 1:151-76, 1981.

32. Ragan PM, Chin VI, Hung HH, Masuda K, Thonar EJ, Arner EC, Grodzinsky AJ, Sandy JD: Chondrocyte extracellular matrix synthesis and turnover are influenced by static compression in a new alginate disk culture system. *Arch Biochem Biophys* 383:256-64, 2000.

33. Rahfoth B, Weisser J, Sternkopf F, Aigner T, von der Mark K, Brauer R: Transplantation of allograft chondrocytes embedded in agarose gel into cartilage defects of rabbits. *Osteoarthritis Cartilage* 6:50-65, 1998.

34. Sah RL, Klein TJ, Schmidt TA, Albrecht DR, Bae WC, Nugent GE, McGowan KB, Temple MM, Jadin KD, Schumacher BL, Chen AC, Sandy JD: Articular cartilage repair, regeneration, and replacement. In: *Arthritis and Allied Conditions: A Textbook of Rheumatology,* ed. by WJ Koopman, Lippincott Williams & Wilkins, Philadelphia, 2004, 2277-301.

35. Schinagl RM, Gurskis D, Chen AC, Sah RL: Depth-dependent confined compression modulus of full-thickness bovine articular cartilage. *J Orthop Res* 15:499-506, 1997.

36. Schreiber RE, Ilten-Kirby BM, Dunkelman NS, Symons KT, Rekettye LM, Willoughby J, Ratcliffe A: Repair of osteochondral defects with allogeneic tissue engineered cartilage implants. *Clin Orthop Rel Res* 367S:382-95, 1999.

37. Sokal RR, Rohlf FJ. Biometry. 3rd ed. New York: WH Freeman and Co.; 1995.

38. van der Kraan PM, Buma P, van Kuppevelt T, van den Berg WB: Interaction of chondrocytes, extracellular matrix and growth factors: relevance for articular cartilage tissue engineering. *Osteoarthritis Cartilage* 10:631-7, 2002.

39. Wang L, Shelton RM, Cooper PR, Lawson M, Triffitt JT, Barralet JE: Evaluation of sodium alginate for bone marrow cell tissue engineering. *Biomaterials* 24:3475-81, 2003.

40. Williamson AK, Chen AC, Masuda K, Thonar EJ-MA, Sah RL: Tensile mechanical properties of bovine articular cartilage: variations with growth and relationships to collagen network components. *J Orthop Res* 21:872-80, 2003.

41. Williamson AK, Chen AC, Sah RL: Compressive properties and function-composition relationships of developing bovine articular cartilage. *J Orthop Res* 19:1113-21, 2001.

42. Woessner JF: The determination of hydroxyproline in tissue and protein samples containing small proportions of this imino acid. *Arch Biochem Biophys* 93:440-7, 1961.

43. Wong M, Siegrist M, Wang X, Hunziker E: Development of mechanically stable alginate/chondrocyte constructs: effects of guluronic acid content and matrix synthesis. *J Orthop Res* 19:493-9., 2001.

APPENDIX B

CARTILAGE RESHAPING WITH INHIBITION OF MATRIX CATABOLISM

B.1 Introduction

This appendix serves as a supplement to Chapter 2, where certain inhibitors of chondrocyte and cartilage matrix metabolism were examined for effects on mechanically-induced cartilage reshaping. Inhibition of chondrocyte protein synthesis with cycloheximide slightly inhibited the overall reshaping response, whereas a reduced temperature of 4°C strongly attenuated any reshaping. These findings suggested that calf cartilage did not grow into the imposed shape via matrix synthesis and accumulation. Instead, the findings indicated a temperature-dependent mechanism, possibly a biochemical or biophysical remodeling of the extracellular matrix. Endogenous proteases present in cartilage, including matrix metalloproteinases (MMPs) and aggrecanases, could potentially be involved in remodeling the extracellular matrix during mechanically induced reshaping. The pilot study presented in this appendix extended upon the investigations of Chapter 2 by using inhibitors of cartilage matrix catabolism. A broad-spectrum hydroxymate MMP inhibitor, (GM6001 a.k.a. Ilomastat) was used to inhibit MMP activity, as done in previous cartilage explant studies [2, 4]. A more broadly acting protease inhibitor

cocktail for cell cultures (P1860) was also used in order to test the hypothesis that catabolic enzymatic processes within the extracellular matrix partially mediate mechanically-induced reshaping of calf articular cartilage

B.2 Materials and Methods

Dose Response of GM6001 Against APMA-Activated MMPs

A dose response study was conducted to examine the ability of GM6001 to inhibit glycosaminoglycan (GAG) release in cartilage explants cultured with aminophenylmercuric acetate (APMA) to activate latent MMPs [1]. Cartilage blocks were harvested from the patellofemoral groove of two 1-3 week old calves. A ~1 mm thick slice of middle zone tissue (n=5 per animal) was obtained and punched into 5 site-matched 2.5 mm disks. All samples were incubated overnight in medium consisting of DMEM+ with 20% FBS and 100 μg/ml ascorbate. The following day site-matched samples were divided among the 5 experimental groups: control (n=10), or APMA with 0, 0.1, 1, or 10 μM GM6001 (n=10, each). The explants were washed in DMEM+ to remove FBS components and wet weights were found. Samples in the control group were cultured in 0.25ml DMEM+ with 0.4% DMSO and 100 μg/ml cycloheximide. Samples in the experimental groups were cultured in 0.25ml DMEM+ with 0.4% DMSO, 100 μg/ml cycloheximide, 1 mM APMA, and either 0, 0.1, 1.0, or 10 μM of GM6001. Cycloheximide was included in all cultures to inhibit chondrocyte synthesis and release of GAG and to prevent any adverse chondrocyte response to the inhibitors.

Culture was terminated after two days. Tissues digested with proteinase K and spent culture medium were analyzed for GAG [3]. GAG released into the medium was

normalized to initial cartilage wet weight and then to that of the site-matched control disk.

Mechanical Reshaping with Inhibitors of Matrix Catabolism

Cartilage reshaping was performed according to the methods of Chapter 2 for inhibition of cartilage matrix metabolism. Cartilage strips (n=2 per group) were treated with 100 μg/ml cycloheximide and either no protease inhibitor as a control, 10 μM GM6001, or a 1/200x dilution of P1860 (Sigma Aldrich, St. Louis, MO) according to manufacturer recommendations. Shape retention was analyzed following 6 days of deformation.

Statistical Analysis and Data Presentation

Data are presented as mean ± SE. ANOVA was used to determine the effects of GM6001 concentration on GAG release with site as a random factor and the effects of inhibitor on cartilage shape retention. Tukey post-hoc tests were used for individual comparisons, and the significance criterion (α) was 0.05.

B.3 Results

Dose Response of GM6001 Against APMA-Activated MMPs

Control explants without APMA activation released 2.8 ± 0.1% of total tissue GAG during 2 days of culture. The induction of matrix degradation and release of GAG into the medium by APMA was fairly inconsistent, leading to large variation between site-matched sets of explants. Nevertheless, GM6001 produced a dose-dependent inhibition of GAG release ($p<0.05$, **Fig. B.1**). At a concentration of 10 μM,

GM6001 inhibited GAG release to levels similar to those of control samples ($p=0.99$). Consequently, this concentration was further used during reshaping studies.

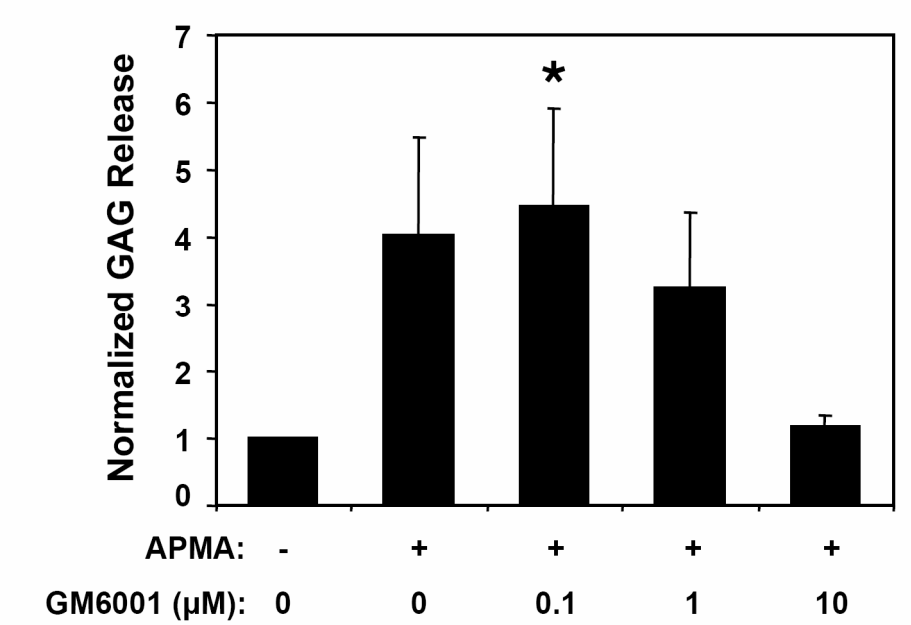

Figure B.1: Dose response of GM6001 on GAG released into the medium when cartilage MMPs were activated with APMA. Data are normalized to tissue wet weight and then to the non-activated, site-matched control (no APMA, no GM6001). ✶= $p<0.05$ versus non-activated control. Mean ± SE, n=10.

Mechanical Reshaping with Inhibitors of Matrix Catabolism

Addition of the MMP inhibitor, GM6001, or the protease inhibitor cocktail, P1860, to the culture medium during mechanically-induced reshaping did not significantly affect the retention of the imposed shape ($p=0.55$, **Fig. B.2**).

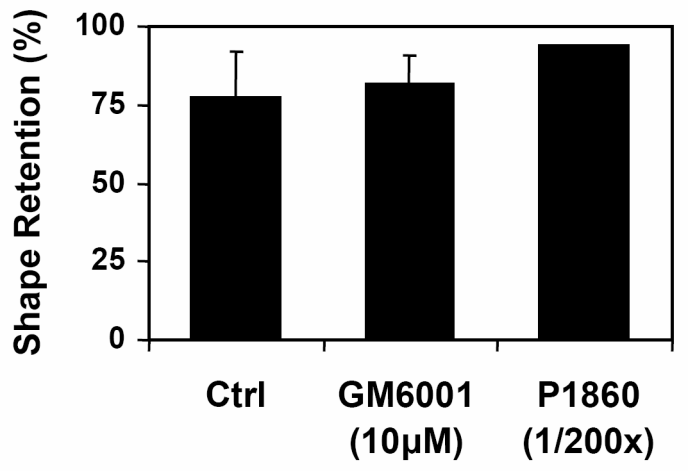

Figure B.2: Effect of MMP inhibitor (GM6001) and protease inhibitor cocktail (P1860) on the shape retention of calf cartilage. Mean ± SE, n=2.

B.4 Discussion

The results from the shaping pilot study did not provide any evidence that catabolic activity by either MMPs or other proteases partially mediates the mechanically-induced reshaping of calf articular cartilage. Shape retention values were high in both the GM6001 and P1860 groups and were consistent with the controls in this study and the cycloheximide-treated samples reported in Chapter 2.

B.5 Acknowledgments

The dissertation author was the primary author of Appendix B and thanks co-author Robert L. Sah. This work was supported in part by grants from NIH, NSF, and HHMI through the HHMI Professors Program (to UCSD in support of RLS). Individual support was received through a NSF Graduate Research Fellowship (to GMW).

B.6 References

1. Bonassar LJ, Stinn JL, Paguio CG, Frank EH, Moore VL, Lark MW, Sandy JD, Hollander AP, Poole AR, Grodzinsky AJ: Activation and inhibition of endogenous matrix metalloproteinases in articular cartilage: effects on composition and biophysical properties. *Arch Biochem Biophys* 333:359-67, 1996.

2. DiMicco MA, Patwari P, Siparsky PN, Kumar S, Pratta MA, Lark MW, Kim YJ, Grodzinsky AJ: Mechanisms and kinetics of glycosaminoglycan release following in vitro cartilage injury. *Arthritis Rheum* 50:840-8, 2004.

3. Farndale RW, Buttle DJ, Barrett AJ: Improved quantitation and discrimination of sulphated glycosaminoglycans by use of dimethylmethylene blue. *Biochim Biophys Acta* 883:173-7, 1986.

4. Naqvi T, Duong TT, Hashem G, Shiga M, Zhang Q, Kapila S: Relaxin's induction of metalloproteinases is associated with the loss of collagen and glycosaminoglycans in synovial joint fibrocartilaginous explants. *Arthritis Res Ther* 7:R1-11, 2005.